Design of a 170 m span bridge over the fjord Thorskafjordur in Iceland

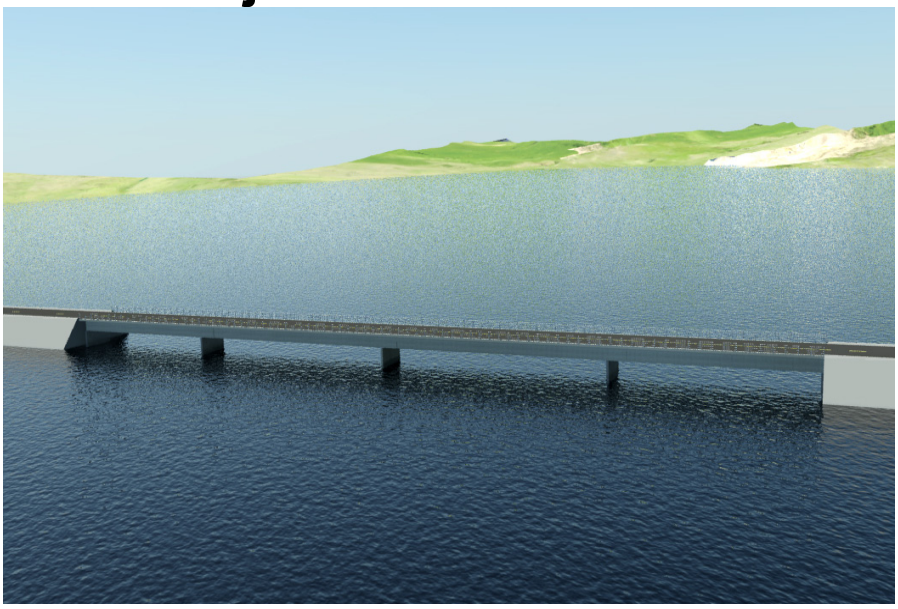

Jóhannes Helgi Jóhannesson

Avdelningen för Konstruktionsteknik
Lunds Tekniska Högskola
Lunds Universitet, 2010

Rapport TVBK - 5185

Avdelningen för Konstruktionsteknik
Lunds Tekniska Högskola
Box 118
221 00 LUND

Department of Structural Engineering
Lund Institute of Technology
Box 118
S-221 00 LUND
Sweden

Design of a 170 m long bridge over the fjord Þorskafjörður in Iceland

Dimensionering av 170 m lång bro över fjorden Þorskafjörður på Island

Jóhannes Helgi Jóhannesson

2010

Abstract

Determining the structural type of a bridge is often a difficult task. The purpose of this thesis is to preliminary design three bridge alternatives. The bridge shall cross the fjord Þorskafjörður in Iceland. The goal is to determine the most favorable option. That decision will be based on economy, construction and aesthetics. Following that a more detailed design of the superstructure is performed for the chosen alternative. All calculations are performed according to Eurocode.

Keywords: concrete girder bridge; arch bridge; cable-stayed bridge; concrete; reinforcement; prestress

Rapport TVBK-5185
ISSN 0349-4969
ISRN: LUTVDG/TVBK-10/5185+92p

Examensarbete
Supervisor: Dr. Fredrik Carlsson
Examinator: Prof. Sven Thelandersson
October 2010

Foreword

This thesis was written under the administration of the Division of Structural Engineering at the University of Lund. It was written during the period September 2009 - September 2010 under the supervision of Dr. Fredrik Carlsson.

I especially want to thank my supervisor, Dr. Fredrik Carlsson, for all his help with making this thesis become real. I also want to thank Einar Hafliðason, the head of the bridge division of the Icelandic Road Administration, for the help with finding a subject for this thesis and for giving me necessary information regarding this subject. For the cost of various structural materials I would like to thank Oskar Bruneby, a site manager at Peab, for his contribution. In addition I would like to thank a good friend from Iceland, Ástþór Ingvason, for making 3D animations of the three bridge alternatives presented in this thesis. Finally, I want to thank my friends at LTH: Bzav Abdulkarim, Daniel Honfi, Ívar Björnsson and Valdimar Örn Helgason for all their help and last but not least other friends and family for their moral support.

Lund, October 2010
Jóhannes Helgi Jóhannesson

Table of Contents

1 Introduction

1.1 Background

The motivation for writing this thesis is an interest in bridges that the author has acquired during his studies in structural engineering. Many people consider bridges to be state of the art of all civil structures. That can be for many reasons; f. ex. bridges sometimes cross a difficult passing or because of their aesthetic aspects.

During the time the subject for this thesis was under consideration the author decided to contact the bridge division of the Icelandic Road Administration (ICERA). Einar Hafliðason, the head of the bridge division of ICERA, was contacted and he was more than willing to help. He came up with a few options to look into which were all considered. Following that, a decision was made and a bridge that is to be constructed to cross the fjord Þorskafjörður in Iceland was chosen as a subject for this thesis.

1.2 Objectives

The main purpose for a bridge over the fjord Þorskafjörður is to shorten the distance of the route on the way to the northwestern part of Iceland. With this bridge the route will shorten of about 10 km. Another purpose is to increase traffic security by eliminating all one-lane bridges on this 10 km sector.

The main objective of this thesis is divided into two parts. First, a preliminary design of three bridge alternatives is made. A rough cost estimation and an estimation of quantity of materials is made based on the preliminary design for these three alternatives. Secondly, a more detailed design is made of the most appropriate bridge type. The choice of a bridge type is based on the conclusions from the first part. These conclusions will primarily be based on economy, aesthetics and construction method.

1.3 Outline of the thesis

Chapter 2 consists of a general discussion about aesthetics, advantages and disadvantages and other aspects for the three bridge types that are chosen to be analyzed.

Chapter 3 displays the bridge location and describes the boundary conditions and geometry at the construction site. It also includes information about why this bridge is to be built.

Chapter 4 includes preliminary design and cost estimations of the three chosen bridge alternatives with respect to the quantity of materials needed for each type. That chapter also includes conclusions of the preliminary design, that is, which type of bridge is chosen for a more detailed design with respect to the limits that are set.

Chapter 5 includes more detailed structural analysis for the superstructure of the chosen bridge alternative.

2 Bridge types

There are many areas of concern that need to be focused on when designing a bridge. There are four main subjects considered in this thesis. They can be listed in order of priority as:

1. Safety
2. Serviceability
3. Economy
4. Aesthetics

These issues and their order of priority may though be criticized and are merely the authors´ preference.

Safety and serviceability are achieved through systematic application of scientific and engineering principles and thus depend on the analytical skills of the engineer. Economy and aesthetics are achieved through nonscientific means and depend almost entirely on the creativity of the engineer.

In this thesis three bridge types are investigated as options for the project and a choice is established based on the four aforementioned areas of concern. These three bridge types are; a concrete beam bridge (post tensioned), an arch bridge and a cable-stayed bridge. The choice of these alternatives is based on the author´s interest.

2.1 Concrete bridge

Concrete slab- or girder bridges are by far the most common of all bridge types nowadays. Prestressed concrete bridges are an attractive alternative for long-span bridges and are considered by many as one of the simplest forms for a bridge with respect to its structural mode of action. A typical cross-section for this type of bridge can be seen in figure 2-1.

Figure 2-1: A typical cross-section for a concrete girder bridge.

These types of cross-sections with prestress reinforcement in the girders are usually used for spans longer than ca. 25 m. They are economically compatible and can easily be designed in the manner that they integrate to the surroundings on site. They are also easy to construct compared to many other alternatives. Nevertheless, the author considers them not as the state-of the-art bridges in the same sense as the two types that are considered in the next chapters. An example of a concrete beam bridge with two girders can be seen in figure 2-2.

Figure 2-2: An example of a prestressed girder bridge.

2.2 Arch bridge

Arches have been used throughout the ages as structural elements. A perfect arch, theoretically, is one in which only compressive forces act at the centroid of each element of the arch. The shape of the perfect arch can be thought of as the inverse of a hanging chain between abutments. It is practically impossible to have a perfect arch bridge except for one loading condition while it is usually subjected to multiple loadings.

For many people, an arch is considered to be one of the most competitive options from the aesthetic perspective and a pleasure for a motorist to drive over. With the appropriate lighting arches can also be very attractive during night.

The arch type that is chosen in this paper is a zero hinged steel arch, figure 2-3, which implies no rotation possible at supports. The deck will be located at an elevation between the supports of the arch itself and the crown of the arch, so called half-through arch. Good foundation conditions are required since an arch can be sensitive to settlements and a zero-hinged arch has high reaction forces at foundation; horizontal, vertical and bending.

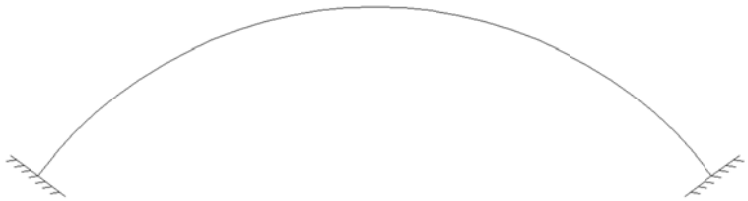

Figure 2-3: A model of a zero hinge arch.

Arches can span up to about 550 m and in the case of slender structures of steel, various instability risks such as the risk for torsional buckling of the arches, must be taken into consideration.

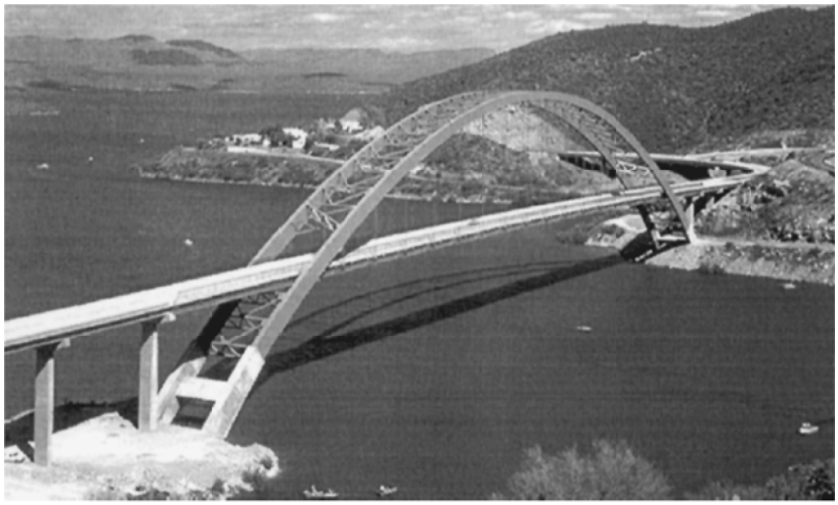

Figure 2-4: A typical arch bridge with the deck hanging on ties connected to the arch.

2.3 Cable-stayed bridge

The concept of a cable-stayed bridge is simple although the loading mechanism is not so easy to predict. A bridge carries mainly vertical loads acting on the girder. The stay cables provide intermediate supports for the girder so that it can span a long distance. The basic structural form of a cable-stayed bridge is a series of overlapping triangles that connect the deck to the pylons. The deck, the cables and the pylon are under predominant axial forces, with the cables under tension and both the pylon and the deck under compression. Axially loaded members are generally more efficient than flexural members. This contributes to the economy of a cable-stayed bridge. They also have less steel consumption but on the other hand larger stress variations can occur and their structural behavior is complex.

Nowadays, cable-stayed bridges are the most common bridge type for long-span bridges and can span up to around 1000 m and come in various forms because of economy and aesthetics. They are beautiful structures that appeal to most people. The towers, or pylons, are the most visible elements of a cable-stayed bridge and therefore contribute the most from an aesthetic point of view. A clean and simple configuration is preferable with free standing towers. Under special circumstances they can also serve as tourist attractions, for example when lighting is a part of the design which enhances the beauty and visibility of the bridge at night. An example of a cable-stayed bridge can be seen in figure 2-5.

Figure 2-5: A cable-stayed bridge with two pylons on each side.

3 The actual project – geometry and boundary conditions

The position of this bridge is in the north-western part of Iceland passing a fjord called Þorskafjörður.

Currently there is a road that goes along the fjord and at the end of the fjord there is a bridge that crosses a river with only one lane. The purpose of the new bridge is therefore to have two lanes, one in each direction, to increase traffic safety, efficiency and to shorten the route of about 10 km by crossing the fjord.

In figure 3-1 the position of the fjord can be seen. The figure displays the northwestern part of Iceland. The light gray line where the arrow points is the current road.

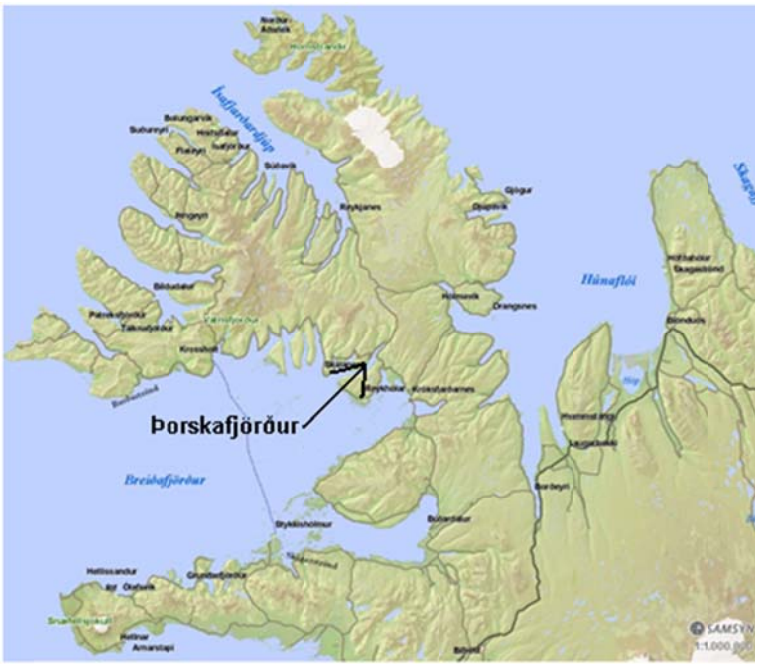

Figure 3-1: Position of the fjord on the north-western coast of Iceland.

As was mentioned, the bridge will have two traffic lanes for normal vehicle traffic, one in each direction. The required length of the bridge, 170 m, is mainly due to ecological reasons. The necessary area of water opening needs to be of minimum 560 m^2 so that full water changes will be acquired. For full water changes the water flow is assumed to be 2.5 m/sec.

The rest of the distance required to cross the fjord will be achieved by a road, on a rock filling on both sides of the bridge. Therefore the bridge will be positioned in the middle of the fjord. The width of the fjord where the bridge is to be positioned is around 1 km.

The largest possible depth of sea level is around 6.35 m and the smallest possible depth of sea level is around 1.65 m from the sea bed. The average sea level is 4 m from the sea bed. Hence, the total maximum difference between highest and lowest sea level is 4.7 m. It can be assumed that the minimum water opening would be reduced by a few meters because of piers and abutments. Guiding rock fillings will be at each end abutments and erosion protection will be at all supports. The alignment of the planned road line that will be considered is displayed in figure 3-2.

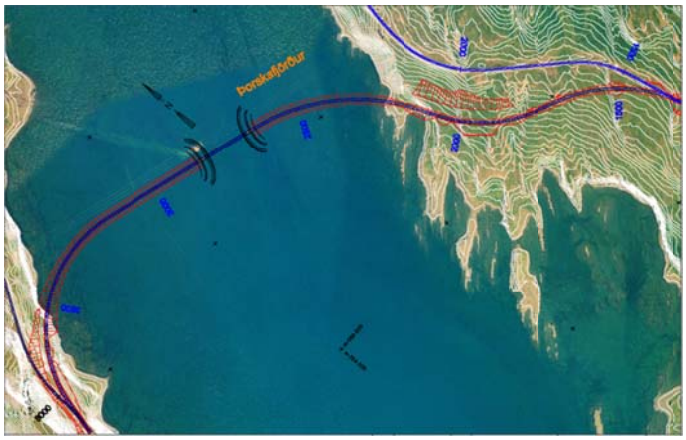

Figure 3-2: The road line where the bridge will be constructed.

The soil at the sea bed consists of sediment layers. The sediment layers are cohesive materials so all fundaments will be founded on cohesive piles.

A section of the fjord is displayed in figure 3-3. Note that the height is scaled 10 times the width.

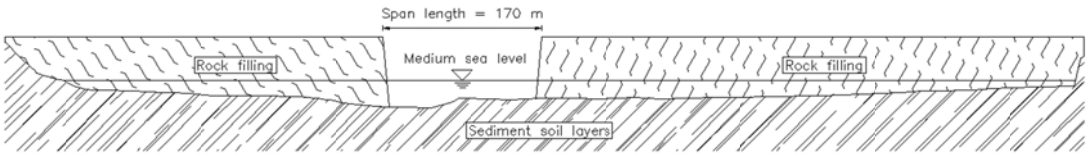

Figure 3-3: A cross section of the fjord, the height is scaled up of the factor 10.

The fjord is not located in an earthquake zone and the peak value for surface acceleration, a_g, is defined as <2% g in this area, see figure 3-4. According to Eurocode 8 for structures with a_g not greater than 4% g the provisions of Eurocode 8 can be neglected. The different earthquake zones in Iceland are displayed in figure 3-4.

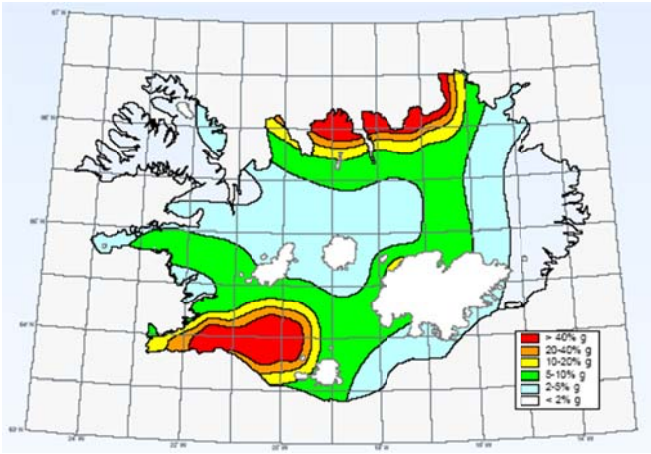

Figure 3-4: Maximum values of surface acceleration. (Earthquake Engineering Research Centre, University of Iceland).

4 Preliminary design

4.1 Introduction

This chapter contains preliminary design of the three bridge types, a concrete girder bridge, an arch bridge and a cable-stayed bridge. The aim of the preliminary design is to determine the most suitable bridge type for the purpose of crossing the fjord Þorskafjörður. The chapter is divided in to two different sections. The first sections (sections 4.2 and 4.3) treat factors that are common for all three bridge types, i.e. loads, load combinations and materials. Sections 4.4 to 4.6 treat the three different bridge types respectively. In these sections are sizes of important bridge elements for each bridge type estimated. These sections also contain rough cost estimations and construction methods for each bridge type. Finally, in the last section of this chapter, the most suitable bridge type is determined based on the preliminary design.

4.2 Loads

For the preliminary design of this project only three loads are considered. Two permanent loads, self-weight and pavement, and one variable load, traffic load. The loads are determined according to Eurocode 1 (EC1).

4.2.1 Permanent loads

Self-weight for reinforced concrete is set to 25 kN/m^3. The self-weight of pavement and structural steel are set to 2.1 kN/m^{2}and 78.5 kN/m^3 respectively.

4.2.2 Variable loads

The variable actions, which are taken into account in this thesis, are traffic loads in vertical direction. After some discussion with the head of the bridge division of ICERA it seemed reasonable to do this simplification in the preliminary analysis.

Traffic Loads

In EC1-2, chapter 4, there are defined four different load models for traffic loads. In this case Load Model 1 (LM1) is used with two partial systems, one including axle loads (Tandem system TS) and the other including uniformly distributed loads (UDL system), see figure 4-1. LM1 is considered to cover most of the effects from traffic of lorries and cars and should be used for general and local verifications while the other load models are considered for dynamic effects, special vehicles and other situations. LM1 should be applied on each notional lane and on the remaining areas. On notional lane number i, the load magnitudes are referred to as $\alpha_{Qi}Q_{ik}$ and $\alpha_{qi}q_{ik}$, axle load and distributed load respectively. On the remaining areas, the load magnitude is referred to as $\alpha_{qr}q_{rk}$. According to chapter 4.3.2(3) in EC1-2 the recommended minimum values for the adjustment factors are:

$$\alpha_{Q1} \geq 0{,}8$$

$$\alpha_{qi} \geq 1{,}0$$

The national annex for Sweden recommends the following minimum values for the adjustment factors:

$$\alpha_{Q1} = 0{,}9$$

$$\alpha_{Q2} = 0{,}9$$

$$\alpha_{Q3} = 0$$

$$\alpha_{qi} = 1{,}0$$

$$\alpha_{qr} = 1{,}0$$

Hence, these values are used for this situation. The Swedish national annex is applied since an Icelandic national annex for this part of Eurocode 2 is not ready yet. Characteristic axle loads, Q_{ik}, and characteristic vertical distributed loads, q_{ik}, are summarized in table 4-1.

Location	Tandem system *TS*	*UDL* system
	Axle loads Q_{ik} [kN]	q_{ik} [kN/m^2]
Lane Number 1	300	9
Lane Number 2	200	2,5
Lane Number 3	100	2,5

Table 4-1: Axle loads and uniformly distributed loads.

These load arrangements are displayed on figure 4-1 and should be arranged for each case to give the most unfavorable result.

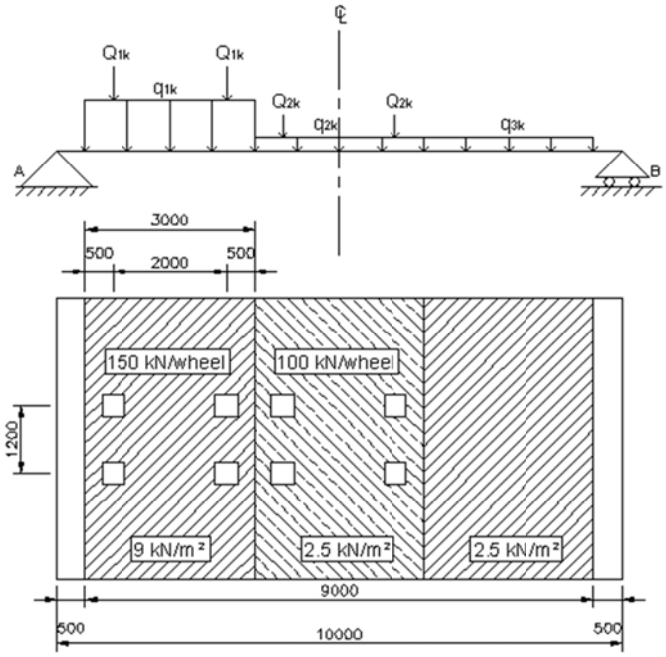

Figure 4-1: Load arrangements for load model 1 in EC1-2.

4.2.3 Load combinations

Several load combinations need to be taken into account, in the ultimate and serviceability limit states, when a bridge is analyzed and designed. But for simplification only an analysis in the ultimate limit state is made for the preliminary design of all bridge types. The design value of actions in the ultimate limit state is according to EC0, section 6.4.3.2:

$$\sum_{j\geq 1} \gamma_{G,j} G_{k,j}" + "\gamma_P P" + "\gamma_{Q,1} Q_{k,1}" + " \sum_{i>1} \gamma_{Q,i} \psi_{0,i} Q_{k,i}$$

where

$\gamma_{G,j}$ Partial factor for permanent action *j*

$G_{k,J}$ Characteristic value of permanent action *j*

γ_P Partial factor for prestressing actions

P Relevant representative value of a prestressing action

$\gamma_{Q,1}$ Partial factor for variable action *1*

$Q_{k,1}$ Characteristic value of the leading variable action *1*

$\gamma_{Q,i}$ Partial factor for variable action *i*

$\psi_{0,i}$ Factor for combination value of variable action *i*

$Q_{k,i}$ Characteristic value of the accompanying variable action *i*

Here are $\gamma_{G,j}$=1.35, γ_P=1.0 and $\gamma_{Q,1}$=1.5 the partial safety factors for permanent action, prestress and variable action respectively. The last term in this equation is not required since there is only one principal action.

4.3 Material cost

Table 4-2 summarizes unit prices for the materials used. Even though values of various expenses are not completely correct they will give a good perspective on prices for comparison of the bridge types that have been investigated. The basis of the cost estimation and prices is from courses the author has attended and other resources like discussions with contractors and engineers both in Iceland and Sweden. Workforce is included in these values and higher values are chosen where a price range is given.

Material	Cost
Concrete-superstructure	2800 SEK/m^3
Concrete-substructure	2200 SEK/m^3
Reinforcement	36 SEK/kg
Prestressing steel	46 SEK/kg
Formwork	1100 SEK/m^2
Steel	28-35 SEK/kg
Cables	100 SEK/kg cabel

Table 4-2: Unit prices for various structural materials.

To estimate the price of the steel hangers in the arch bridge, see section 4.5.4, unit price for solid steel is used (SEK/kg). To come up with a price for the stay cables of the cable-stayed bridge it is necessary to find the unit weight (kg/m) of the cables. Unit weight for cables was found in a literature from Zhuan (1998) about stay cables where the unit weight of cables that has a similar breaking load as the ones that were chosen here to use and that value is 24.1 kg/m. No lifetime cost, like maintenance or other factors, will be estimated and cost of foundations is a factor of uncertainty since the design of that is not done in the preliminary phase. Here estimation is used to calculate the cost of

the substructures with a method developed by Menn (1986) as a 23.5% of the total cost of structural elements. Included in the substructure are the piers and fundaments.

4.4 The concrete beam bridge

Bridge type no. 1 is a concrete post-tensioned girder bridge with four spans and concrete columns supporting the beams. There will be two main girders with post-tensioning cables. The total width of the bridge deck will be 10 m, see figure 4-3. Supports will be founded on concrete piles.

4.4.1 Geometry for type 1

This bridge type will have a concrete slab supported on two continuous girders. The bridge is a continuous girder bridge with 4 spans, see figure 4-2. The girders are supported on concrete columns down to the sea bed.

4.4.2 Size estimation

As was mentioned before, the total span of the bridge is 170 m. The bridge is divided into four smaller spans, two internal spans with the length 48 m and two external spans with a length of 37 m, see figure 4-2. This choice of span lengths is made to get an even moment distribution. That is achieved if the length of the external spans is about 80 % of the length of the internal ones.

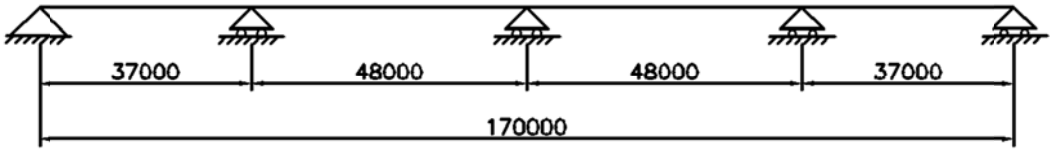

Figure 4-2: Span lengths for bridge type 1.

The first step is to decide the prestressing system to estimate the size of the girders. The chosen prestress system is VSL 6-19. The dimensions for anchorage blocks for that specific system are 290x290 mm. 3 cables are chosen in each row which results in a minimum width, b, of 1080 mm. Also an additional thickness of 300 mm is determined over the supports.

The height of the girder is determined by the slenderness, a ratio between the span length and the height, *L/h*, of the girder. A recommended slenderness ratio for a conventional cast-in-place girder bridge should be chosen in the range of 12-35 and some lower range should be considered because of economic reasons (section 7.2.1 in Menn (1986)) and a low value should also be chosen so there won't come up problems later in the design. So the estimated height becomes:

$$\frac{l}{h} = 20 \Longrightarrow h = \frac{48}{20} = 2{,}4\ m$$

The center distance between the two main girders, *a*, is chosen with the following method, Thelandersson (2009):

$$B = 1{,}8 \cdot a \Longrightarrow a = \frac{10}{1{,}8} = 5{,}6\ m$$

where *B* is the free width of the bridge.

The thickness of the slab is chosen to be 250 mm to be able to resist shear forces and moments.

The estimated cross-section of the bridge, based on the methods above, can be seen in figure 4-3.

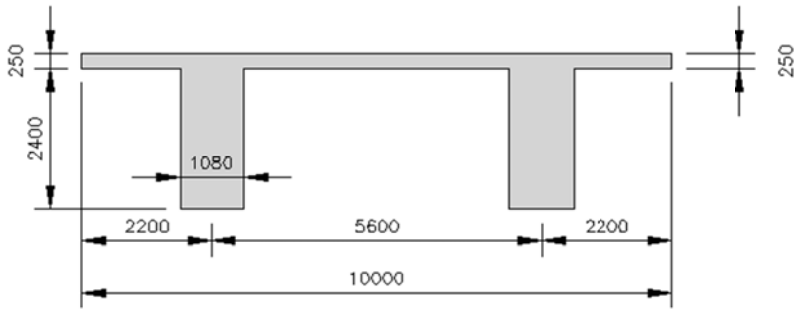

Figure 4-3: The cross-section at preliminary stage.

4.4.3 Supports

Maximum load on a column would be when the given traffic load is located as shown in figure 4-4. To estimate the most unfavorable load acting on a single beam the girder distribution factor (GDF) has to be determined. GDF tells how the traffic load is distributed between the girders. The traffic loads have to be located in the most unfavorable position on the bridge deck in the lateral direction. To find GDF, the moment is calculated around B with the lever arm for each load as displayed in figure 4-4.

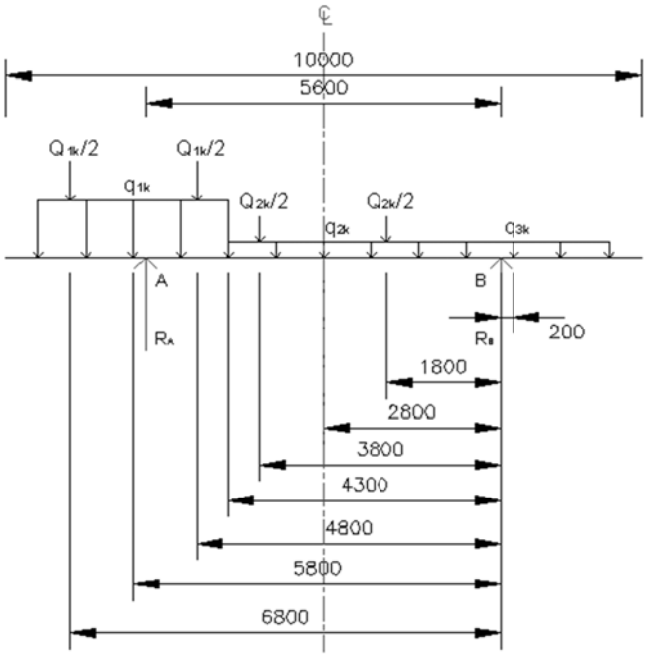

Figure 4-4: Location of traffic loads to determine GDF.

The GDFs for the two traffic loads, axle and distributed loads, are determined to be:

$$GDF_Q = 1{,}37 \quad \text{For the tandem system}$$

$$GDF_q = 1{,}16 \quad \text{For UDL system}$$

And the following traffic loads that act on one beam are:

$$Q_{traffic} = 1012\ kN$$

$$q_{traffic} = 37\ kN/m$$

where the axle loads are changed into one concentrated force (assumption). Then the bridge is analyzed in the length direction for one girder. Calculations are made for half of the bridge cross section. Figure 4-5 shows the actions and the position of actions to decide the largest shear force for the columns and the bridge section in the ultimate limit state.

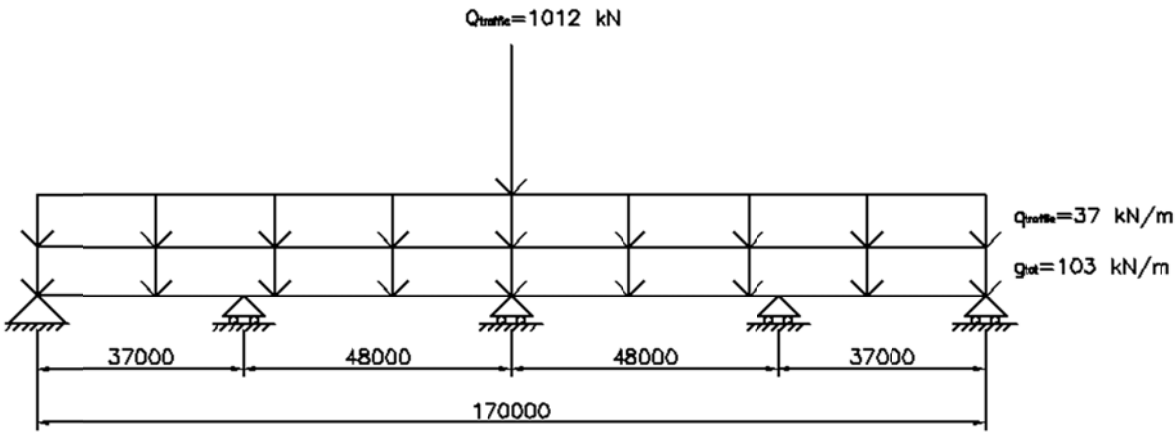

Figure 4-5: Position of traffic loads when the largest normal force at the middle support occurs.

The maximum normal force in the middle support is calculated to be 11.180 kN in the ultimate limit state. At this stage the concrete quality is assumed to be C45/55.

The width of a single girder over supports is 1.380 mm. The thickness of the support wall is calculated from a formula for preliminary design given in the ISE manual (1985):

$$N = A_c\left(0.44f_{ck} + \frac{p}{100}\left(0.67f_y - 0.44f_{ck}\right)\right)$$

with the yield strength of the reinforcement as f_y=500 MPa, characteristic cylinder strength of concrete as f_{ck}=45 MPa, the percentage of reinforcement p=2% and A_c as the gross cross-sectional area. Thus the minimum thickness of the support should be:

$$11180 \times 10^3 = 1380 \times t\left(0.44 \times 45 + \frac{2}{100}(0.67 \times 500 - 0.44 \times 45)\right) \Rightarrow t \geq 311mm$$

So for a single support the total size is determined to be *b x t* = 7500 x 450 mm.

For the piles, given that each pile resists 400 kN, gives:

$$\frac{11180}{400} \approx 28\ piles$$

Precasted 270x270 piles with 1200 mm spacing and a foundation of the size 5x10 m.

4.4.4 Construction

The construction method of a concrete girder bridge is relatively easy to perform. Concrete girder bridges are one of the most common bridges in Iceland. This bridge alternative is often chosen for similar conditions as are in this case because of economic and constructional reasons, that is, when a shallow fjord is to be crossed.

Supports and columns below the superstructure will be constructed first. They will be founded on piles. Since the level of sea depth at is shallow at the construction site the superstructure of the bridge will be casted in forms that are supported on a temporary filling under the bridge. The filling will finally be removed when the concrete has hardened and can then be used as road material.

4.4.5 Cost estimation/conclusions

To estimate the cost of this bridge type a method from Menn (1986) is used. The following is an explanation of this method.

The superstructure's costs can be reliably estimated with the help of the geometrical average span length, l_m, defined as:

$$l_m = \frac{\sum l_i^2}{\sum l_i}$$

where l_i is the length of span i.

The empirical equations given below give the quantities of concrete, reinforcing steel, and prestressing steel as functions of l_m and have been derived from samples of recently constructed bridges.

By this method the volume of concrete in the whole superstructure is obtained by multiplying the total deck surface by the effective girder depth, h_m, defined by the following expression:

$$h_m = 0.35 + 0.0045 \cdot l_m$$

where h_m and l_m are in meters. This equation is valid provided the actual girder depth, h, satisfies the following inequality:

$$\frac{1}{20} \leq \frac{h}{l_m} \leq \frac{1}{16}$$

which fulfills the criteria used earlier, l/h=20. The quantity of reinforcing steel is obtained by multiplying the total volume of concrete by the mass of steel per unit volume of concrete, m_s. The parameter m_s is estimated using the equation:

$$m_s = 90 + 0.35 \cdot l_m$$

where l_m is in meters and m_s is in kilograms per cubic meter of concrete (kg/m^3). This expression is valid provided the deck slab is not transversely prestressed. Between 65 and 70 kg/m^3 of reinforcement is required for stability during construction and crack control; this quantity is independent of span length, see Menn (1986). The transverse reinforcement required to resist loads is primarily a function of cross-section dimensions. An additional 20 to 25 kg/m^3 is required for commonly used cross-sections, regardless of span length. Most of the steel required above the

minimum 65 to 70 kg/m^3 is located in the deck slab. The deck slab should therefore be the focus of attention in the design and arrangement of the superstructure reinforcement.

The mass of prestressing steel per unit volume of concrete, m_p, is a function of span length and construction method. For girders that are casted on conventional falsework, m_p is estimated using the equation:

$$m_p = 0.4 \cdot l_m$$

where l_m is in meters and m_p is in kilograms per cubic meter of concrete. This expression is valid for girders that are not transversely prestressed. The quantity of prestressing steel is obtained by multiplying m_p by the total volume of concrete.

The estimated cost of concrete, reinforcing steel and prestressing steel in the superstructure is obtained by multiplying the estimated quantities with unit material costs. The cost of falsework (scaffolding systems that are used to temporarily support permanent structures) and formwork (temporary structure used to retain unhardened concrete until hardened) should be estimated taking into account the proposed construction sequence; if it is greater than 65 percent of the superstructure´s material costs, another construction method should be considered. Adding the bridge material, falsework and formwork costs yields the total superstructure cost. Since abutments and piers are under sea level the cost percentage of the total cost of those structural parts as well as falsework/formwork increased. These values are chosen to be 25% and 23% respectively. The remaining costs can be estimated using table 4-3, from Menn (1986).

Item	Cost (% of Total Construction Cost)		
Mobilization			8.0
Structure			
Substructure			
Foundations	18.0		
Piers and abutments	5.5		
Total substructure	23.5	23.5	
Superstructure			
Falsework, formwork	20.0		
Concrete	10.0		
Reinforcing steel	13.3		
Prestressing steel	11.2		
Total superstructure	54.5	54.5	
Total structure		78.0	78.0
Accessories			14.0
Total construction cost			100.0

Table 4-3: Table from Menn (1986) to estimate costs for various structural elements.

Here is only listed the quantity of super- and substructure materials that will be determined and below is a table that summarizes those results. These quantities are acquired based on the preliminary calculations as well as the empirical equations above. The calculated quantities are given in table 4-4.

Material	Amount	Unit
Concrete	1.306	[m^3]
Reinforcement	137.322	[kg]
Prestressing steel	22.579	[kg]

Table 4-4: Amounts of structural materials for the concrete beam bridge.

For the figures given in table 4-4, abutments and columns are included. Below is a table with prices of sub- and superstructure and the total cost based on the price values from section 4.3 and to get a total cost for this bridge type the total values for the structural elements are doubled.

Prestressed Concrete Bridge	
Material	**Cost [SEK]**
Concrete-Abutments and Piers	4,819,889
Concrete-Superstructure	3,657,584
Reinforcement	4,943,575
Prestressing Steel	1,038,619
Falsework, formwork	4,337,900
	18,797,567
Total Cost:	***37,595,133***

Table 4-5: Total cost of bridge type 1.

This result is consistent with a draft for this project made by ICERA where the estimated cost for this type of bridge was 638.500.000 ISK which is around 38.700.000 SEK with the exchange rate of 16.5 ISK/SEK. Note that this draft assumes the total length of 182 m instead of 170 m.

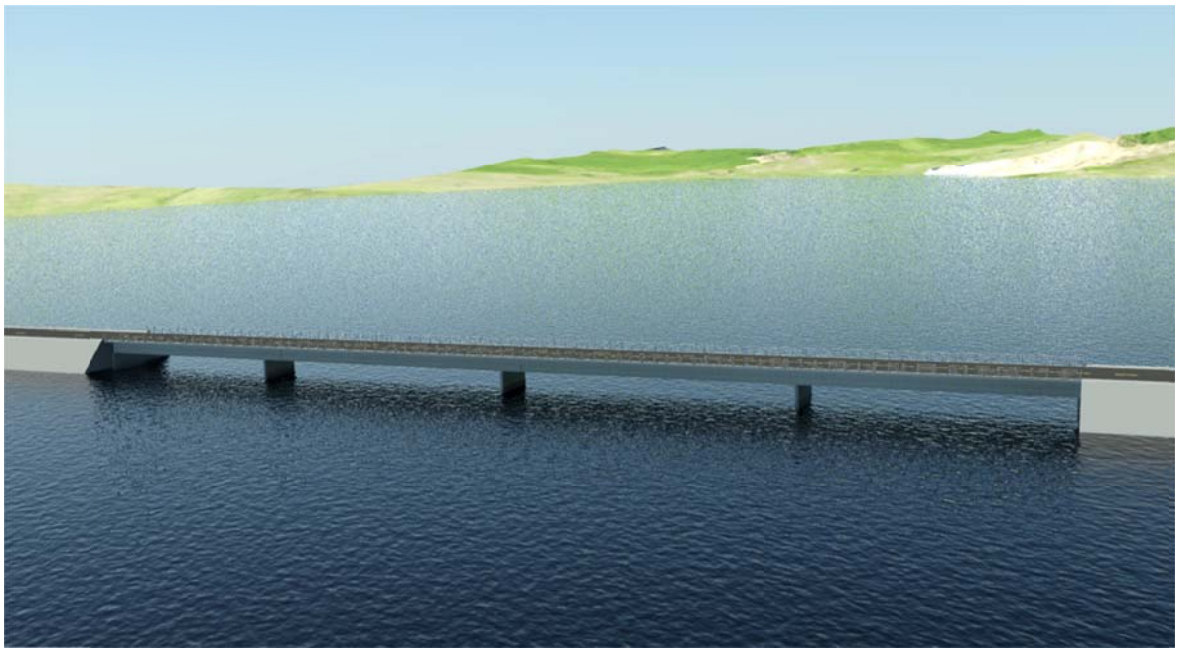

Figure 4-6: An overview of the beam bridge.

4.5 The arch bridge

Bridge type no. 2 is a conventional steel arch bridge with two separate arches above the bridge deck. Each arch will be of a steel box cross-section with steel stiffeners inside, see figure 4-11. The arches will be of zero hinged type with X-bracing between the arches to increase lateral stiffness. The bridge deck will be of composite steel/concrete. In the longitudinal direction of the bridge there will be two main girders with shear studs. To connect the two main girders there will be transversal steel beams which are connected to the arches with hangers. A reinforced concrete slab will be casted on top of the main girders, see figure 4-7.

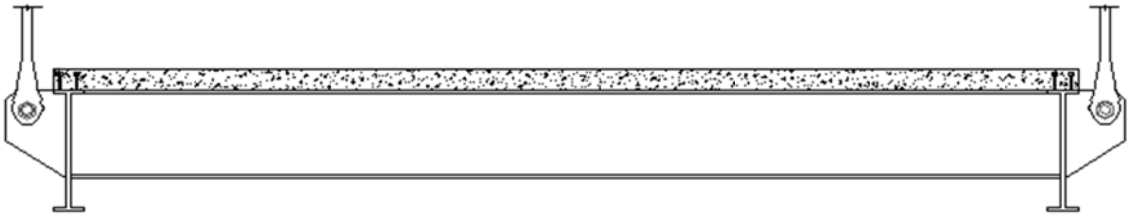

Figure 4-7: A cross-section of the bridge deck.

4.5.1 Geometry for type 2

The choice of the rise of the arch is based on the ratio between span and rise which is generally chosen between 4 and 8 see, Loretsen and Sundquist (1995). This ratio is in this case chosen to be 4 which would result in less horizontal reaction forces. This ratio is suitable because of geotechnical conditions on site (no rock – only sediment soil layers). That results in

$$\frac{span}{rise} = 4 \Rightarrow rise = \frac{170}{4} = 42{,}5\ m$$

To connect the deck to the arch vertical steel wire hangers with c/c 25 m are chosen. On figure 4-8 is a drawing of the structural model of the bridge.

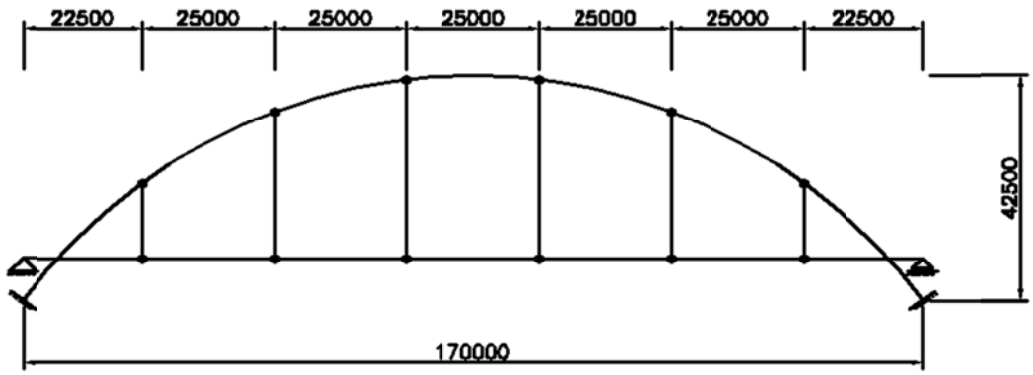

Figure 4-8: A structural model of the tied arch bridge.

To determine the section forces in the arches the GDF needs to be determined again. The GDFs are determined according to figure 4-9.

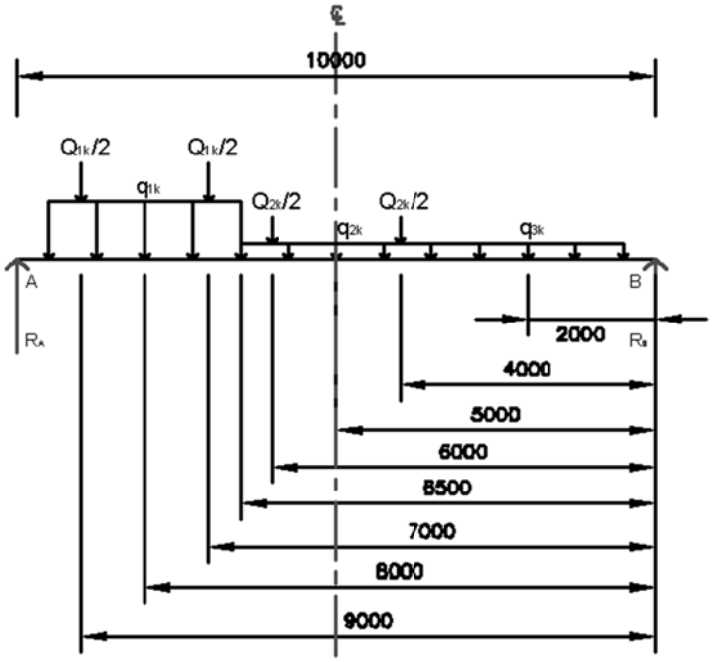

Figure 4-9: Position of traffic loads when calculating GDF.

The following GDFs are acquired:

$$GDF_Q = 1{,}13 \quad \text{For the tandem system}$$

$$GDF_q = 1{,}00 \quad \text{For UDL system}$$

And the following traffic loads that act on one girder are:

$$Q_{traffic} = 694\ kN$$

$$q_{traffic} = 27\ kN/m$$

4.5.2 Arch

To design the arch the influence lines for the arch need to be determined. 3 sections in the arch are investigated: abutment, ¼ of the arch and the middle. Influence lines for each section are made by moving a point load of 100 kN in 10 m intervals over the deck in the longitudinal direction for moment, shear force and normal force. These influence diagrams can be seen in figure 4-10.

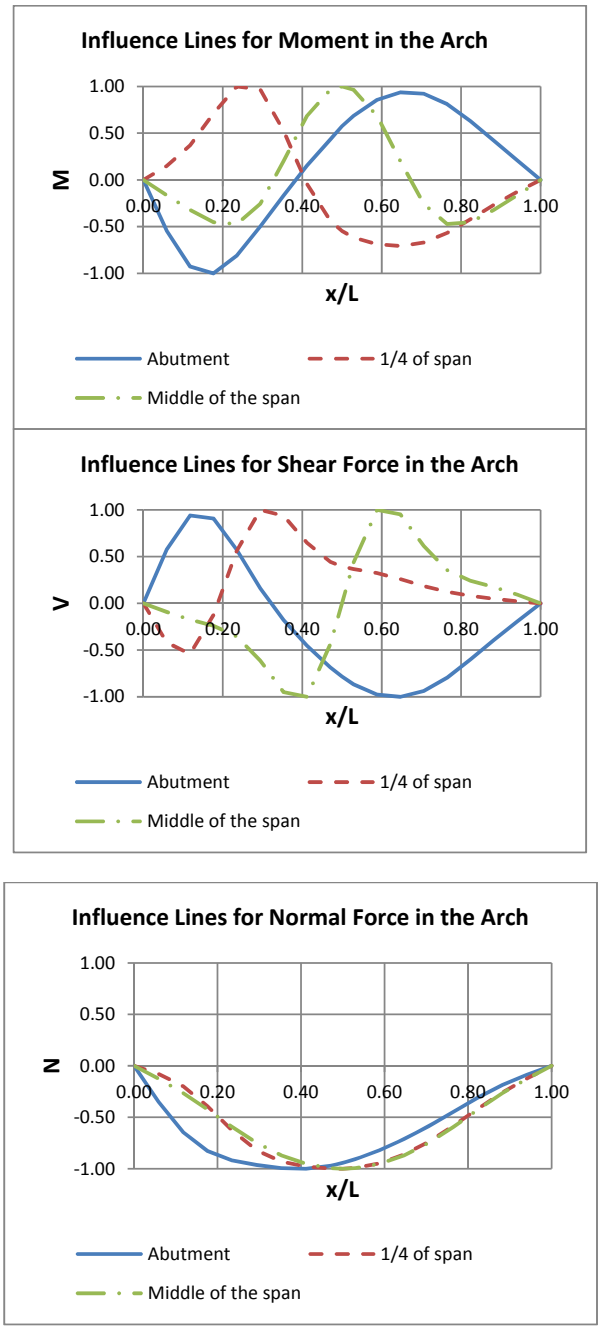

Figure 4-10: Influence lines for various section forces at most critical placements.

To calculate the important section forces for design of the cross section of the arch the traffic loads are placed on the most unfavorable position corresponding to these influence diagrams in a program called PCFrame. PCFrame is a commercial program for structural analysis of frames.

Cross Section

To design the arch in the ultimate limit state the section forces are required. The highest moment in the arch is reached when the traffic load is located in the middle of the span. The position of the point load at the first quarter of the span gave the highest normal force. So these corresponding section forces are used to design the cross section and are shown in table 4-6.

	M	N	V
	[kNm]	[kN]	[kN]
M_{max} @0,5L	15875	-9517	-454
M_{max} @0,25L	-14561	-10901	-532

Table 4-6: Design section forces in the arch.

The material qualities of the steel are given in table 4-7.

	fy	fu	E
	[N/mm^2]	[N/mm^2]	[N/mm^2]
Fe E 355	355	470	210000

Table 4-7: Material qualities of steel.

The following cross-section was determined after few trials with respect to stability in the longitudinal direction and resistance, see figure 4-11:

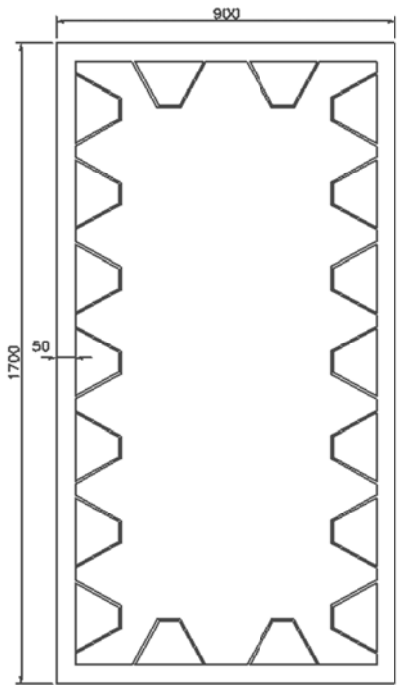

Figure 4-11: Chosen cross-section of the arch.

The cross-section is a welded box section with trapezoidal stiffeners. Further details about the dimensions of the cross section (moment of inertia, section modulus etc.) can be seen in the appendix A.

Stability

To check for stability in longitudinal direction two investigations are made; calculation by hand as well as with the help of PCFrame. To fulfill the requirements for stability the ratio between buckling load and the maximum normal force needs to be in the range from 4 to 5, see Loretsen and Sundquist

(1995). To calculate the buckling load by hand formulas presented by Austin (1971) were used. The critical buckling load is given as:

$$P_e = \pi^2 \frac{EI}{(kS)^2}$$

where S is the one-half length of the arch and k is the effective length factor, see Austin (1971). In this case S is 98525 mm and k is 0.70 for a fixed arch with a rise-span ratio as 0.25. For these values P_e is determined to be 45845 kN and the ratio between the buckling load and the maximum normal force is

$$\frac{P_e}{N} = 4.8$$

From analysis in PCFrame for this case this factor is determined to be 5.0. That matches considerably well with the calculations by hand. These calculations were the most critical ones for the determination of the cross section. The buckling mode shape for this arch is shown in figure 4-12.

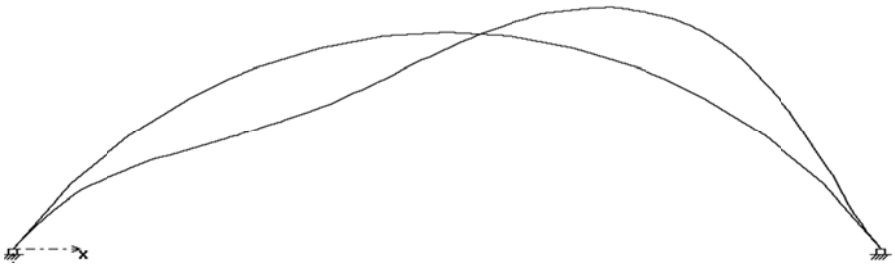

Figure 4-12: Buckling mode shape of the arch.

EC3 gives another method to determine the buckling resistance criteria for compressed members and is given in section 5.5.1 in EC3. EC3 defines the following criteria:

$$N_d \leq N_{b.Rd}$$

with N_d as the design normal force and the capacity of the cross-section, $N_{b.Rd}$, as

$$N_{b.Rd} = \chi \beta_A A f_y / \gamma_{M1}$$

Here χ is the reduction factor for the relevant buckling mode and is defined as

$$\chi = \frac{1}{\phi + \left[\phi^2 - \bar{\lambda}^2\right]^{0,5}} \quad but\ \chi < 1$$

with ϕ equal to

$$\phi = 0{,}5\left[1 + \alpha\left(\bar{\lambda} - 0{,}2\right) + \bar{\lambda}^2\right]$$

and α, an imperfection factor, obtained from an appropriate buckling curve. For buckling about the stronger axis and a welded box section with b/t_f<30, α becomes

$$\alpha = 0.49$$

$\bar{\lambda}$, the non-dimensional slenderness, is defined as

$$\bar{\lambda} = \left[\beta_A A f_y / N_{cr}\right]^{0,5}$$

where β_A is depending on the cross-section as below:

$$\beta_A = 1 \text{ for Class 1, 2 or 3 cross sections}$$

$$\beta_A = A_{eff}/A \quad \text{for Class 4 cross sections}$$

In this case β_A is equal to 1. For resistance of member to buckling the safety factor is

$$\gamma_{M1} = 1{,}1$$

Table 4-8 summarizes the results of this analysis.

γ_{M1}	f_y [MPa]	A [mm]	β_A	ϕ	α	$\bar{\lambda}$	χ	$N_{b.Rd}$ [kN]
1,1	355	285.097	1	1,918834852	0,49	1,485808	0,52115	47950

Table 4-8: Criteria for buckling resistance from EC3.

It can be seen in table 4-8 that the buckling resistance is well above the calculated normal forces in the arch.

Compression and bending capacities

To determine the compression and bending capacities the class of the cross-section has to be determined. To decide the cross section class plastic stress distribution is assumed.

In this case the cross section class is determined to be 1.

The cross-section capacities are defined in EC3 in sections 5.4.4 and 5.4.5 respectively as

$$N_{pl.Rd} = A f_y / \gamma_{M0}$$

$$M_{pl.Rd} = W_{pl} f_y / \gamma_{M0}$$

Here, $N_{pl.Rd}$ is the plastic design resistance for compression, $M_{pl.Rd}$ the plastic resistance for bending and W_{pl} the plastic section modulus. For resistance of Class 1, 2 or 3 cross-section the partial safety factor is defined as $\gamma_{M0} = 1{,}1$ in section 5.1.1 in EC3. The calculations for $N_{pl.Rd}$, $M_{pl.Rd}$ and W_{pl} can be seen in appendix A. Next a check for bending moment, compression and combined bending and axial force are made according to section 5.4 in EC3. The following design criteria are checked:

$$M_{Sd} \leq M_{c.Rd} \qquad \text{Bending}$$

$$N_{Sd} \leq N_{c.Rd} \qquad \text{Compression}$$

$$\frac{M_{Sd}}{M_{pl.Rd}} + \left[\frac{N_{Sd}}{N_{pl.Rd}}\right]^2 \leq 1 \qquad \text{Combined bending and axial force}$$

The results of this analysis are summarized in table 4-9.

	Design	Resistance	
Bending [kNm]	15875	75984	OK!
Compression [kN]	10901	92009	OK!
Combined	0,22	1,00	OK!

Table 4-9: Design values and resistance for the arch.

All the criteria are fulfilled. Also, the cross-section is assumed to resist the shear forces since they are so small and are therefore neglected. The arch is mostly in compression.

4.5.3 Bridge Deck

The bridge deck will consist of main steel girders, transversal beams and concrete slab. They will work as composite deck with steel shear studs. The composite effect is not calculated here but that will only make the structure more rigid. Estimated thickness of the concrete slab is 200 mm.

Transversal beams

The transversal beams will be made of steel and will be placed with 5 m spacing. Worst case of loading for these beams will be when the axle load from the traffic is placed exactly above one of them. These positions are show in figure 4-13. This location of the axle load will generate the highest moment and shear force in the transversal beams. These section forces are used to determine the cross-section in the ultimate limit state.

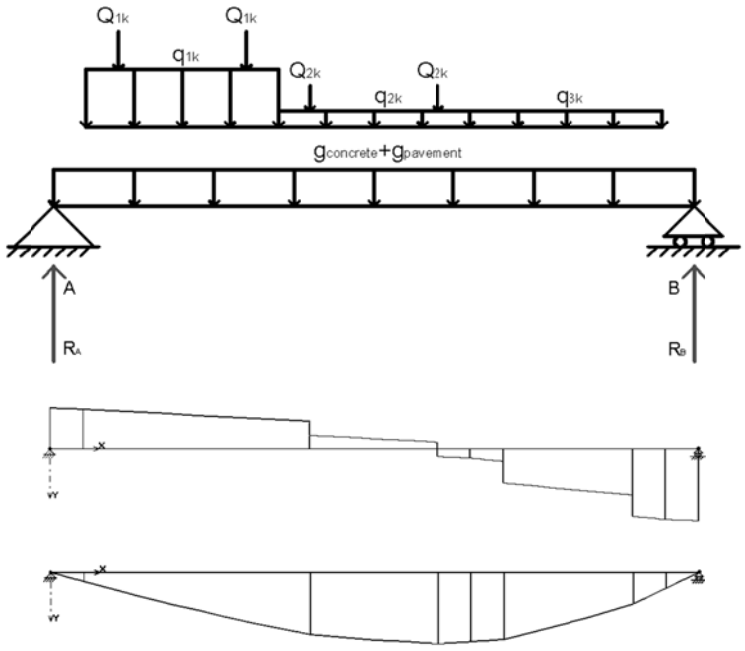

Figure 4-13: Positions of traffic loads and shear- and moment diagrams when the cross-sections of cross beams are determined.

The highest moment and shear force are determined to be 3025 kNm and 1359 kN respectively. From these section forces the cross-section can be determined. The design criteria for shear- and moment is given in sections 5.4.5 and 5.4.6 in EC3 as

$$M_{Sd} \leq M_{c.Rd} = W_{pl} f_y / \gamma_{M0} \qquad \text{For class 1 or 2 cross sections}$$

$$V_{Sd} \leq V_{pl.Rd} = A_V(\frac{f_y}{\sqrt{3}})/\gamma_{M0}$$

where the parameters are explained in the last section. The determined cross-section of the transversal beams is shown in figure 4-14. For detailed calculations, see appendix A.

Figure 4-14: Estimated size of the cross beams.

Main girders

The main girders will be connected to the transversal beams which are hanging from the arches in hangers. The largest shear force and moment in the main girders are determined to be 2087 kN and 7241 kNm respectively. Here the same criteria are checked, shear- and moment resistance, as was for the transversal beams. The determined cross-section can be seen in figure 4-15 and detailed calculations can be seen in appendix A.

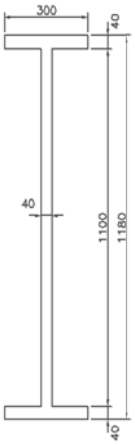

Figure 4-15: Determined size of the main girders.

4.5.4 Hangers

The hangers are the elements that connect the bridge deck to the arch. They are vertical cables. The hangers are designed to resist the largest tension force, which is determined to be 3393 kN in the ultimate limit state. This force is acquired when the axle force from the traffic load is positioned exactly at hanger number 1 closest to the support. The chosen material of these hangers is M100 carbon steel with the design yield strength as 3605 kN.

4.5.5 Transversal Bracing

The choice of X-type bracing rather than Vierendeel bracing is that the system will be more rigid with the X-type, see Bunner and Wright (2006), which results in less lateral deflections and would be analyzed as a truss system. Lateral braces will not be calculated at this time.

4.5.6 Foundations

The soil under the foundations is sediment layers. The foundation will be founded on precasted concrete piles that will be driven down to the ground. Each pile resists about 400 kN, Hafliðason (2010). The piles will have an inclination down in the direction to the arch's direction. The estimated length of the piles will be 14 m. The largest reaction force in the arch's direction is 12601 kN so the estimated amount of piles is

$$\frac{12601}{400} \approx 32\ piles$$

for each arch. The spacing between the piles will be 1.2 m. The total number of piles is determined to be 35 piles under each abutment. The piles will also be able to resist the risk of turning along with the fundament itself. The filling behind the bridge will also be able to resist some external actions and support the fundaments. A continuous foundation is chosen under the whole bridge in the lateral direction and the approximate size of it will be 7.2 x 4 x 16.8 m, see figure 4-16.

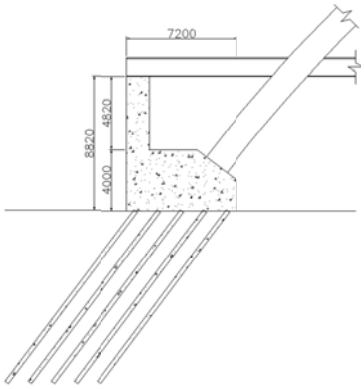

Figure 4-16: Placing of piles at the arch supports.

4.5.7 Construction

My proposal of a construction method for this bridge type is similar to the method for bridge type 1. First, foundations for the arches will be constructed and then a temporary working plane of gravel will be placed under the bridge. Then the arches will be raised. Each arch will be divided into several segments, sizes that are possible to transport. These segments will be welded together in steps, each segment at a time, supported by falsework standing on the working plane. When the arches have been placed in right positions the temporary working plane is removed and can be used as a road filling.

Next the deck is constructed. The main girders come in segments and are connected to the cross beams that are hanging in the hangers. The hangers connect the arches to the deck. Each segment is welded together and finally, when all the work with the structural steel is done, the concrete slab is casted.

4.5.8 Cost estimation/conclusions

In table 4-10 the total quantity of materials for the arches and bridge deck are summarized. These quantities are based on the preliminary calculations. The cost estimation for the foundations is based on the method in section 4.4.2 for bridge type one. These cost figures are given in table 4-11.

Material	Amount	Unit
Concrete	425	[m^3]
Reinforcement	252.872	[kg]
Steel	444.528	[kg]
Ties	17.936	[kg]

Table 4-10: Quantities of structural materials for the arch bridge.

To get a total cost the total material cost is doubled, which is a rough estimation.

Arch Bridge	
Material	**Cost [SEK]**
Concrete-Abutments and Piers	6,845,160
Concrete-Deck	1,190,000
Reinforcement-Deck	9,103,379
Steel-Deck	15,558,492
Ties	627,771
Falsework, formwork	901,000
	34,225,802
Total Cost:	***68,451,604***

Table 4-11: Total cost of bridge type 2.

This bridge type is little less than twice as expensive as the first bridge type. This mainly depends on steel cost and complexity of the structure. An overview of the arch bridge can be seen in figure 4-17.

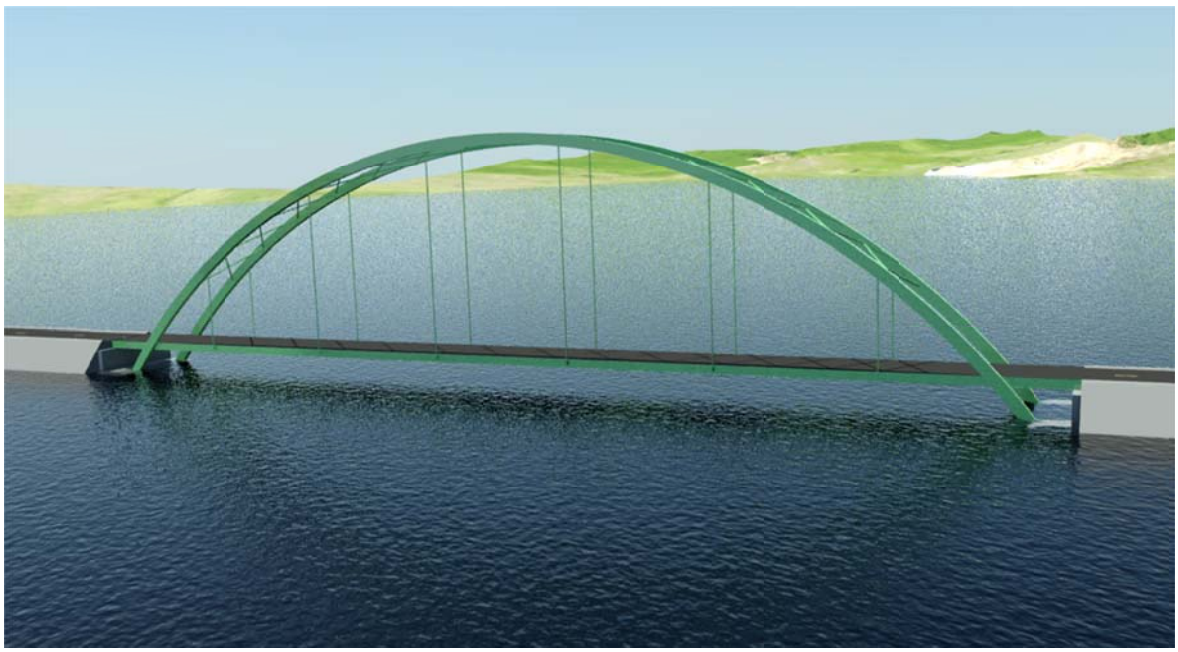

Figure 4-17: An overview of the arch bridge.

4.6 The cable-stayed bridge

Bridge type no. 3 is a back and front cable-stayed bridge, see figure 4-21. This bridge type has two pylons on each side, similar to the Öresund bridge. The bridge will consist of a composite steel/concrete deck. The cross section of the deck is similar to bridge type 2. A further discussion about the choice of the superstructure is in the next chapter where aesthetics and structural system of cable-stayed bridges are discussed.

4.6.1 Aesthetics of cable-stayed bridges

Bridge type no. 3 is a cable stayed bridge. There are several types that can come into mind when a cable stayed bridge is to be designed. The cables can be arranged in a harp-, fan- or combined configurations, see figure 4-18. The number of spans can either be two or three, see figures 4-19 and 4-20. The pylons can either be rigid, work as a cantilever, or the deck is stiff and the pylons are stabilized by the cables that are anchored into the ground.

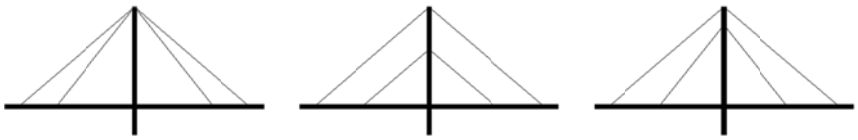

Figure 4-18: Configurations of the cables for cable-stayed bridges.

Nowadays the pylons are most often made of concrete. The deck can be made of concrete, steel orthotropic or as a composite steel/concrete deck.

Many concrete cable-stayed bridges have been built. In general, there are two construction methods for concrete cable-stayed bridges: cast-in-place construction or precast construction. A cast-in-place construction is a further development of the free cantilever construction method. For precast construction it is possible to use a more complicated cross-section because precasting is done in the yard. The segments, however, should all be similar to avoid adjustment in the precasting forms. The weight of the segment is limited by the transportation capability. Box is the preferred cross section because it is stiffer and easier to erect.

A properly designed and fabricated orthotropic deck is a good solution for a cable-stayed bridge. However, with increasing labor costs, the orthotropic deck becomes less commercially attractive except for very long spans. The use of steel in the deck is, today, two to four times as expensive as concrete. Thus the reduced self-weight of the deck slab must result in appreciable savings.

Although the steel orthotropic deck is too expensive for construction in most countries at this time, the composite deck with a concrete slab on a steel frame can be very competitive. Making the deck composite with the steel girder by shear studs reduces the steel quantity of the girder significantly. Most portions of the girder are under high compression, which is good for concrete members. However, tensile stresses may occur in the middle portion of the center span and at both ends of the end spans. Post-tensioning is usually used in these areas to keep the concrete under compression.

In this a self-anchoring system is preferable, see figure 4-19. That depends on the foundation conditions on site, the foundations will be below sea level and sediment layers are the main soil. Also there is a so called earth anchored system where the horizontal components of the cable forces are transferred to the supports at the ends of the bridge which requires favorable foundation conditions and a combination of self-anchoring and earth anchoring system. The principle of a self-anchored cable system can be seen on figure 4-19.

Figure 4-19: Self anchored system.

Let us consider an asymmetrical system with only one pylon as can be seen in figure 4-19. That could be a good choice with respect to foundation construction. An example of that structural system can be seen on figure 4-20.

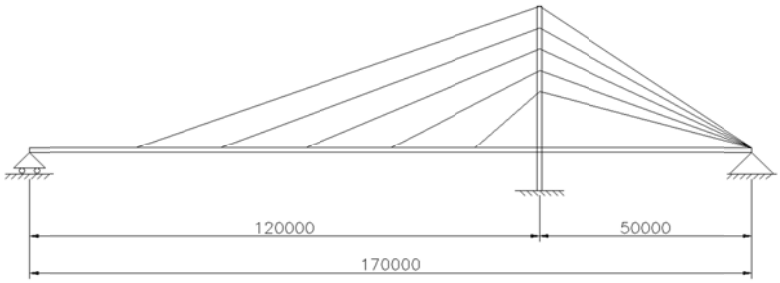

Figure 4-20: Asymmetrical system.

But, an asymmetrical system has earth-anchored cables and requires better foundation condition than a self-anchoring system.

4.6.2 Geometry for type 3

Based on the discussion above self-anchoring cable system is preferable in this specific situation. Here, a harp shape configuration of the cables is chosen. Harp shape configuration offers a very clean and delicate appearance because an array of parallel cables will always appear parallel irrespective of the viewing angle. It also allows an earlier start of the deck construction because the cable anchorages in the pylon begin at a lower elevation so that fastening of cables can start before the pylon is ready. The outer spans lengths should be around 30-40% of the main span length so the stresses in the back stays won't exceed its limits. Figure 4-21 displays the geometry of the chosen model. The bridge is modelled in SAP2000 for 3D analysis. SAP2000 is a commercial finite element program for structural analysis of structures. The deck, see figure 4-26, is 10 m wide with four pylons, two on each side. The two pylons are connected together with one cross-beam for stability. Ten cables will connect the bridge deck to each pylon. Each cable will be connected to transversal beams with 30° angle to horizontal.

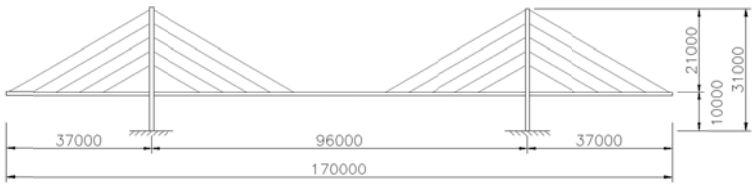

Figure 4-21: Model for bridge type 3.

4.6.3 Design

In this section the elements in the following table will be checked in the ultimate limit state.

Element	Ultimate limit state
Main girders	Bending
Cross-beams	Bending
Pylons	Bending/Compression
Cables	Tension
Foundation	Bending/Compression

Table 4-12: Elements that will be checked in ULS.

To begin with the necessary section forces and reactions are determined for the corresponding elements of the bridge that are under investigation. SAP2000 is used to create influence lines and the traffic loads are placed by using these influence lines. To create influence lines a point load of 100 kN is moved in 5 m increments along the bridge deck. On figures 4-22 to 4-24 are these influence lines displayed for those parts of the bridge that will be analyzed at this stage. The dark vertical lines indicate the position of the pylons.

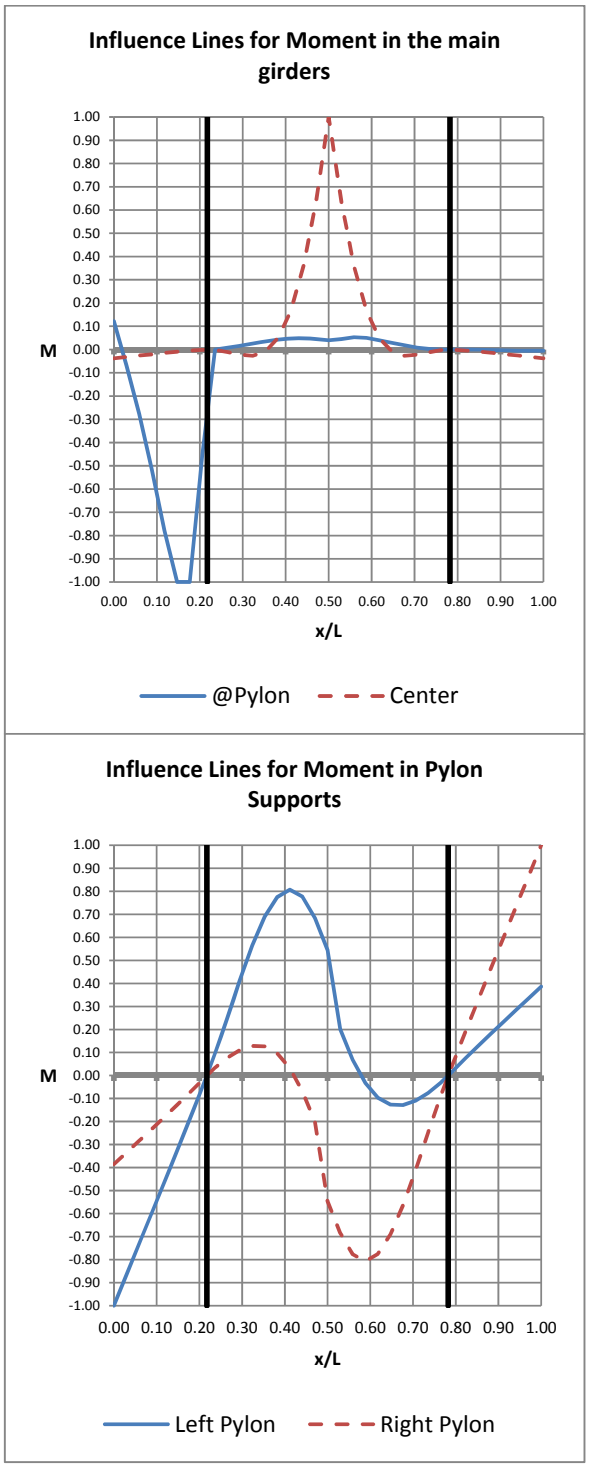

Figure 4-22: Influence lines for moments in the deck and at pylon supports.

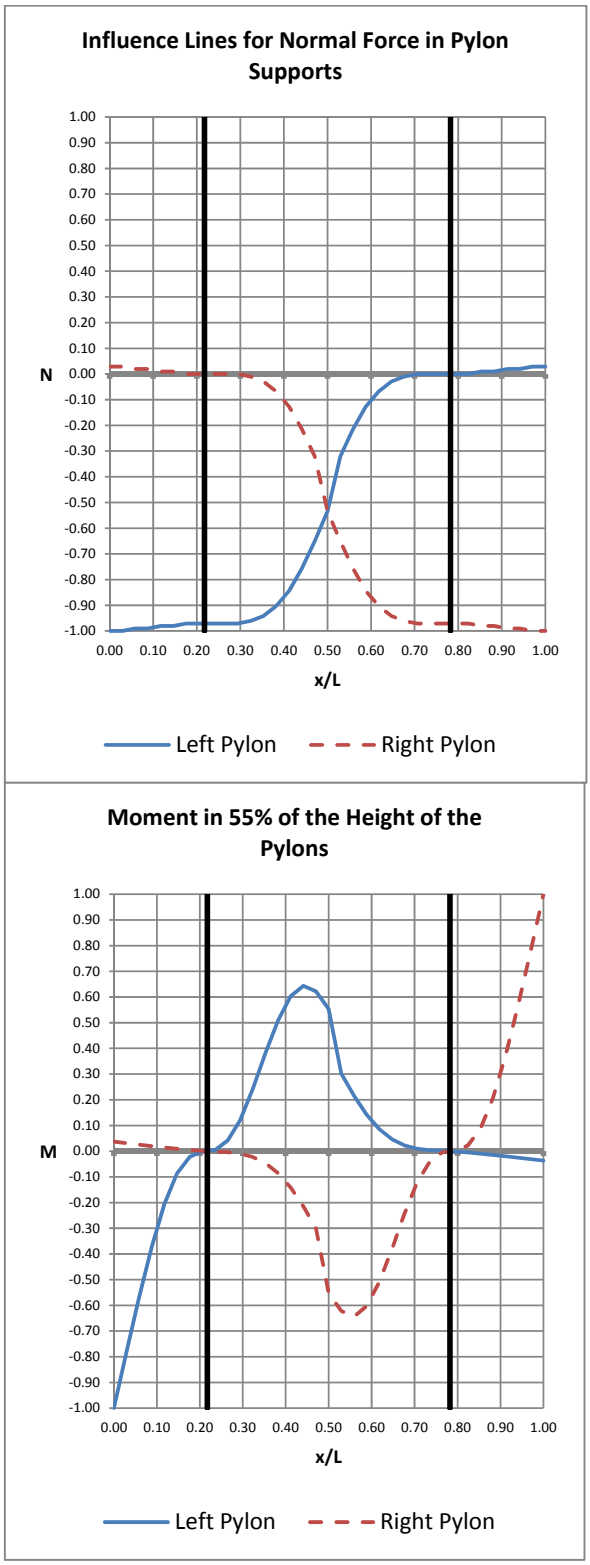

Figure 4-23: Influence lines for normal forces in pylon support and moment at 55% of the height of the pylons.

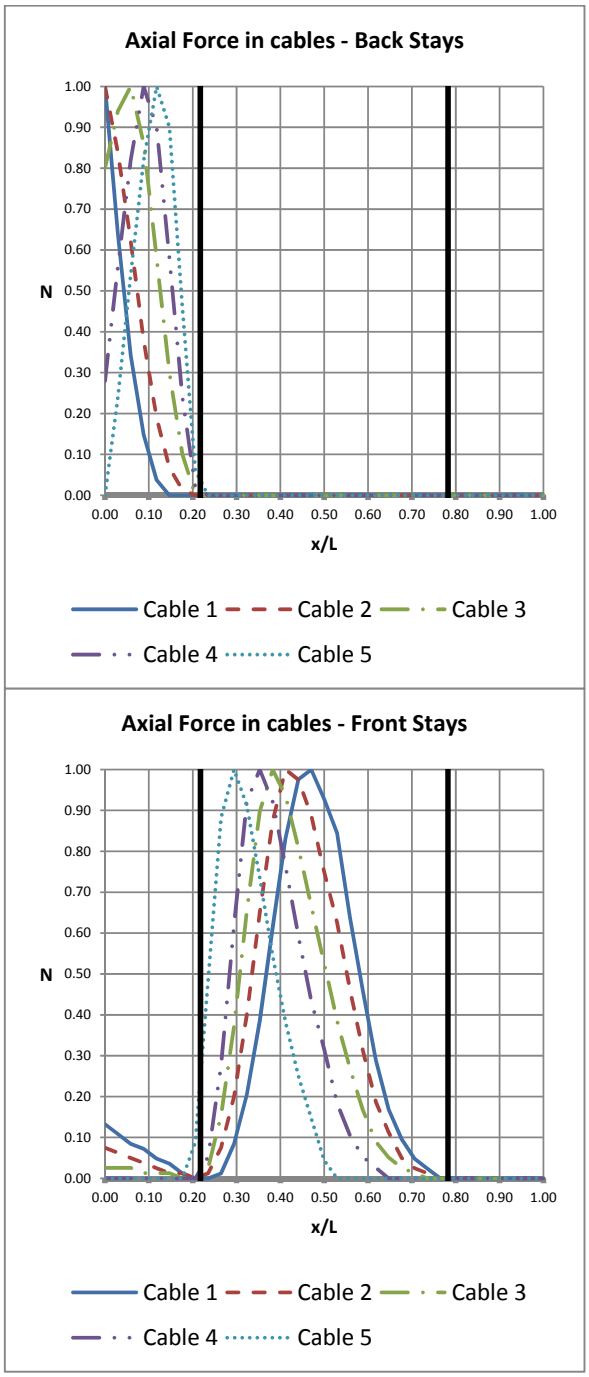

Figure 4-24: Influence lines for various parts of the structural system of the cable-stayed bridge.

After the influence lines have been created the bridge is modeled as a 3D model in SAP2000 with the forces positioned at the corresponding positions. The slab is modeled as area section elements with a meshing of 0.5 m so that the axle traffic loads can be positioned right. Main girders and cross beams in the bridge deck are modeled as frame elements as well as the pylons. The cables are modeled as cable elements with high tensional stiffness. The only supports of the model are the fixed supports under the pylons because the pylons and cables should be able to carry its self-weight under construction.

4.6.4 Deck

Concrete Slab

The concrete slab will be 250 mm thick and the concrete quality is C35/45. The slab will consist of concrete casted on site and a metal deck beneath of trapezoidal profiles. To achieve composite effects shear studs will be welded on cross beams and main girders.

Cross Beams

The cross beams will be made of steel and are placed in 5 m intervals along the deck. They are designed to resist the self-weight of the concrete slab and the traffic loads. Location of the traffic loads for the largest moment can be seen in figure 4-25.

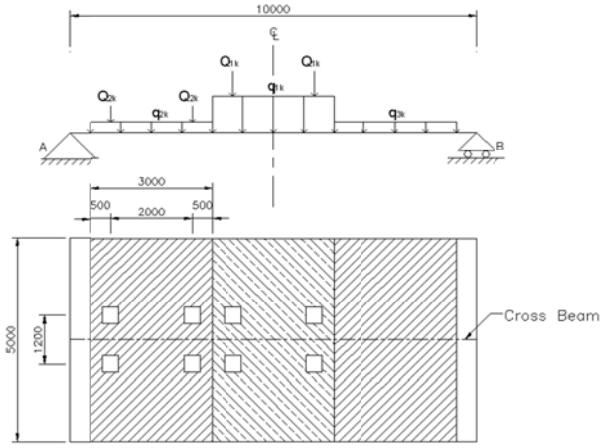

Figure 4-25: Position of the traffic loads to estimate the size of the cross beams.

When the largest moment and shear force are determined in ULS, it's possible to determine the size of the cross beams. The cross section of the beam is I shaped with the total height of 860 mm. The width of the flanges is 300 mm and the thickness of the web and flanges is 30 mm. For detailed calculation, see appendix A.

Main Girder

Largest moment in the main girders is when the traffic loads are applied at the middle of the bridge span and is determined to be 7311 kNm. The largest shear force is determined to be 1247 kN and is reached when the traffic loads are applied where the pylons are positioned. An I-shaped cross section is chosen. From these design values the size of the girder is determined. The total height is 1200 mm, the width of the flanges is 400 mm and the thickness of the web and flanges is 30 mm. For detailed calculation, see appendix A. Figure 4-26 displays the chosen bridge deck.

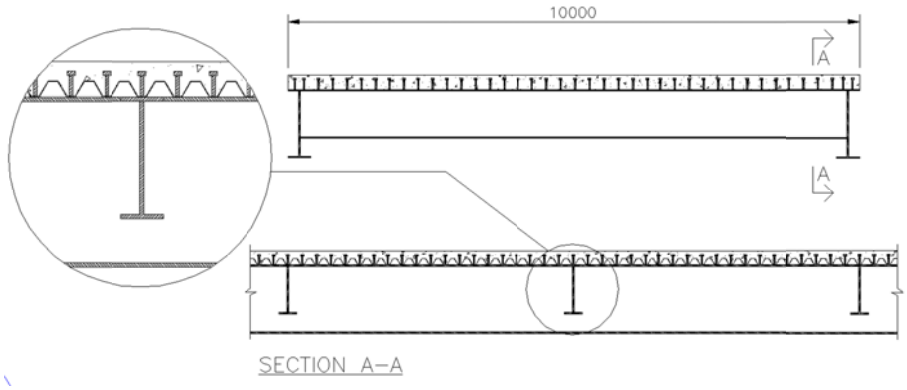

Figure 4-26: Configuration of the deck and girders with shear studs and trapezoidal profiles.

4.6.5 Pylons

The pylons will be a concrete hollow section. The concrete quality in the pylons is chosen to be C40/50. The towers have two vertical cable planes and are connected together with two transverse beams. Each pylon is designed for combined moment and normal force. The design moment and normal force were determined to be 27292 kNm and 5121 kN respectively. The size of a pylon is determined 1.5 x 2.0 m with a wall thickness as 0.3 m. The size of the cross-beams that connects the pylons is determined to be 1.2 x 2.0 m with a wall thickness of 0.25 m. Figure 4-27 displays an interaction diagram to estimate the capacity of the pylon. The star on the inside of the curve shows the design point for the above mentioned section forces. Calculations of the pylons are displayed in appendix A.

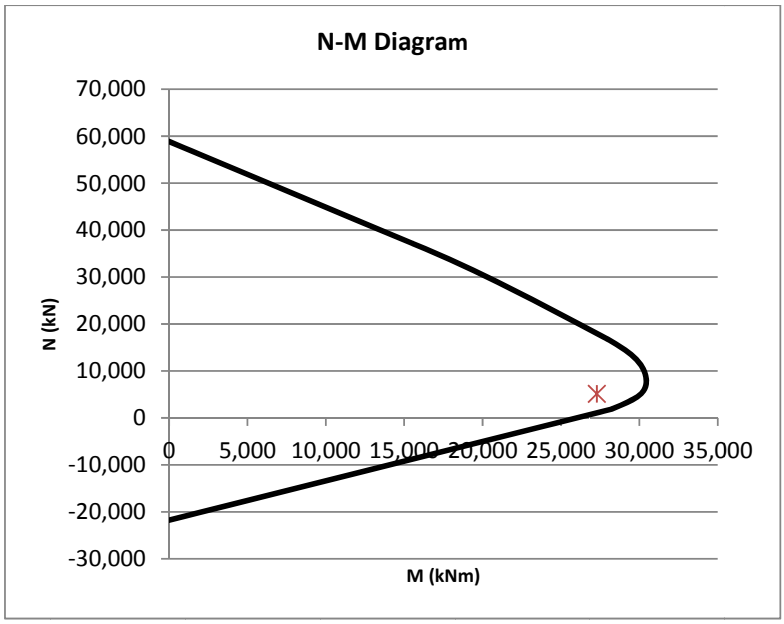

Figure 4-27: N-M interaction diagram for the pylon.

The chosen cross-section of the pylon is shown in figure 4-28.

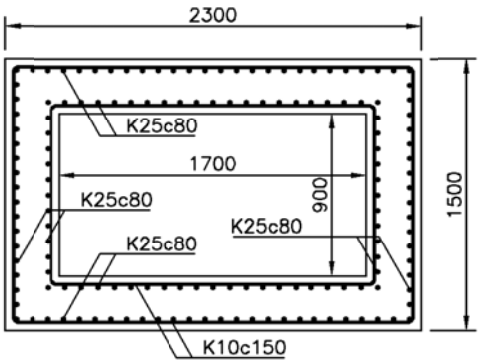

Figure 4-28: Cross section of the pylon with reinforcement.

4.6.5.1 Cables

Where the cables are connected to the bridge deck cross beams are placed to reduce torsion in the main girders. The cables are modeled as cable elements with high tensional stiffness. The largest tension force in the cables was determined to be 15888 kN. A proposal of a cable system is VSL SSI 2000 with tendon units as 6-61 with a design capacity of 17019 kN.

Finally a model of the bridge that was constructed in SAP2000 is displayed in figure 4-29.

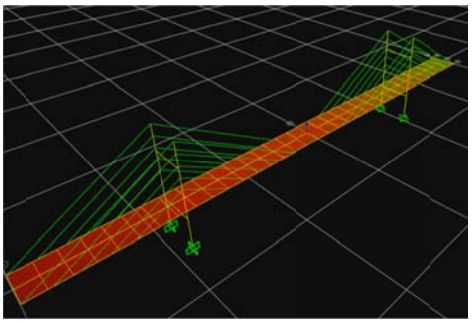

Figure 4-29: 3-D model of the cable-stayed bridge in SAP2000.

4.6.6 Foundation

The foundation under each pylon will consist of concrete footings and cohesive piles as for the other bridge types. The largest vertical reaction force and moment under one pylon is determined to be 5121 kN and 27292 kNm respectively. That implies that approximately 13 piles are needed under each pylon. The fundament along with the piles is assumed to resist the risk for overturning.

4.6.7 Construction

The foundations are to be constructed first. After that, the work with the pylons can start where each pylon will be constructed up to a height where the lowest cable is connected. Then the construction of the deck can start where the deck is connected to the cables in segments meanwhile the pylons are constructed further up. During this the cross-beams are also set in place. After the segments of the main girders and cross-beams are in place the trapezoidal profiles are fastened on the upper edges of the beams. Finally the slab is casted. This process is done for each cable row with the segments of the main girders welded togeather until the top row is reached and the deck structure meets in the middle of the span. This way, the structure works as a self-anchored system with the deck hanging from the

cables on each side of the pylons. Below, figure 4-30, is an example from one of the largest cable-stayed bridge in the world that displays how this principle works.

Figure 4-30: The Stonecutters Bridge (currently the largest cable-stayed bridge in the world) under construction.

4.6.8 Cost estimation/conclusions

The total quantities of materials are summarized in table 4-13 and cost estimation made based on the price values given in section 4.3. In table 4-14 the main materials and quantities of the super- and substructure are listed for the cost estimation. These quantities are based on the preliminary calculations but the cost estimation for the foundations is based on the method in section 4.4.2 for bridge type one.

Material	Amount	Unit
Concrete	666	[m^3]
Reinforcement	325.519	[kg]
Steel	230.719	[kg]
Cables	40	[pcs.]

Table 4-13: Amounts of structural materials for the cable-stayed bridge.

Finally the total cost of this bridge type is summarized in the table 4-14.

Cable-Stayed Bridge	
Material	**Cost [SEK]**
Concrete-Abutments and Piers	8,932,316
Concrete-Pylons	529,892
Concrete-Deck	1,190,000
Reinforcement-Slab	9,103,379
Reinforcement-Pylons	2,615,308
Steel-Deck	8,075,177
Falsework, formwork	3,636,308
Cables	10,579,200
	44,661,580
Total Cost:	***89,323,159***

Table 4-14: Total cost of bridge type 3.

This bridge type is little less than three times as expensive as the first bridge type. This mainly depends on the same factors as for bridge type 2, steel cost and complexity of the structure. But also there is quite much quantity of concrete and reinforcement that is used in the pylons and the cables are also a large factor. An overview of the arch bridge can be seen in figure 4-31.

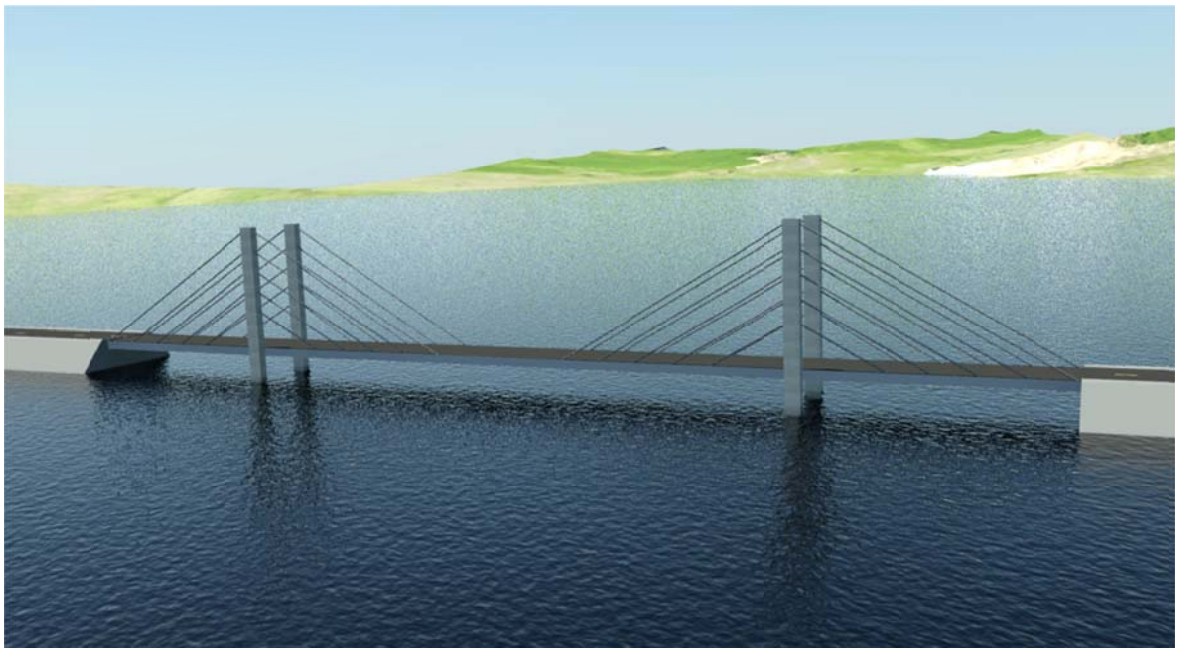

Figure 4-31: An overview of my proposal of a cable-stayed bridge.

4.7 Summary and choice of bridge type

From the total cost estimations for the bridge types it is clear that the cable-stayed bridge is the most expensive one. Also the arch bridge is quite expensive compared to the prestressed concrete bridge that is the least expensive one. From a construction point of view the prestressed bridge is also the most favorable. From these perspectives a concrete girder bridge is the obvious choice.

But, there are also other aspects that need to be taken into consideration when choosing a bridge type; aesthetics, method of construction and construction time are obvious factors that can affect which choice is made. The author will leave those decisions for others to make at later stages but chooses to design the concrete beam bridge in a more detailed manner. In the following chapter more detailed calculations will be performed for the superstructure of bridge type 1. Calculations of the post-tensioned cables are performed where the prestress force and eccentricity of the cable profile are determined. Following that all cable losses are determined and then the secondary effects of prestress. Finally the ultimate moment capacity is determined for relevant members of the superstructure.

5 Final design

5.1 Introduction

Prestressed concrete structures, using high-strength materials to improve serviceability and durability, are an attractive alternative for long-span bridges, and have been used worldwide since the 1950s. The presence of cracks that can develop in tensile members can lead to corrosion of the reinforcement due to its exposure to water and chemical contaminants. Corrosion is generally only a problem for structures in aggressive exterior environments (bridges, marine structures, etc.) and is not critical in the majority of buildings. The effect of cracking of members can lead to substantial loss in stiffness which occurs after cracking and the second moment of area of the cracked section is far less than the second moment of area before cracking. Thus, allowing cracks to develop can cause a large increase in the deformation of the member. For prestressed concrete, compressive stresses are introduced into a member to reduce or nullify the tensile stresses which result from bending due to the applied loads. The compressive stresses are generated in a member by tensioned steel anchored at the ends of the members and/or bonded to the concrete.

There are two types of prestressing systems: pre-tensioning and post-tensioning systems. Pre-tensioning systems are methods in which the strands are tensioned before the concrete is placed. This method is generally used for mass production of prefabricated members. Post-tensioning systems are methods in which the tendons are tensioned after concrete has reached a specified strength. This technique is often used in projects with very large elements. The main advantage of post-tensioning is its ability to post-tension cast-in-place members. Mechanical prestressing jacking is the most common method used in bridge structures.

The post-tensioning process involves three fundamental stages. In the first stage of the process, the concrete is cast around a hollow duct. After the concrete has set or hardened, a tendon, consisting of a number of strands, is pushed through the duct (alternatively, the tendon can be placed in the duct before casting). Thus, the tendon can be fixed in any desired linear or curved profile along the member. By varying the eccentricity of the tendon from the centroid, the maximum effectiveness of a constant prestressing force can be utilized by applying the prestress only where it is required. Once the concrete has achieved sufficient strength in compression, the tendon is jacked from one or both ends using hydraulic jacks, thus putting the concrete into compression. When the required level of prestress is achieved, the tendon is anchored at the ends of the member. After anchorage, the ducts are usually filled with grout under pressure. The grout is provided mainly to prevent corrosion of the tendon but it also forms a bond between the tendon and the concrete which reduces the dependence of the beam on the integrity of the anchor and hence improves its robustness.

When prestressed concrete elements are designed the following factors need to be considered:

- The prestressing reinforcement is determined by concrete stress limits under service load.
- Bending and shear capacities are determined for the ultimate limit state
- Deformations are determined in the serviceability limit state.

5.2 Design

Throughout the design process, one girder is designed with properties of half the cross-section. The loads are calculated with respect to that. After iteration of the calculations in this chapter the size of the girders is changed from what was chosen in chapter 4.4 with a height of 1800 mm instead of 2400 mm.

5.2.1 Building codes

The bridge shall be designed according to the following standards:

- FS ENV 1991 Eurocode 1 (Loading)
- FS ENV 1992 Eurocode 2 (Concrete Design)

5.2.2 Loading

Self-weight and traffic loads are the same as in the pre-design phase. But in this detailed design also the load generated by prestressing is taken into account.

5.2.3 Materials

In this section the most common physical properties of all materials used are summarized.

5.2.3.1 Concrete

High strength concrete is always used in post-tensioned structural members. In this case the chosen concrete quality is C45/55. For this quality the modulus of elasticity is E_{cm}=36000 MPa and the concrete compression strength is f_{ck}=45 MPa. The self-weight of reinforced concrete is 25 kN/m^3.

The effects of creep need to be taken into account for calculation of long-term deflection. The definition of creep is that under compression the concrete member will contract with time due to constant stress. To take account for creep in the design of concrete members the modulus of elasticity, E_{cm}, is reduced to an effective elastic modulus, $E_{c,eff}$. $E_{c,eff}$ is determined with the following formula:

$$E_{c,eff} = \frac{E_c}{1+\varphi}$$

where φ is the creep coefficient. φ is taken from EC2 and shown in table 5-1.

Age of concrete at loading (days)	Notional size, $2A_c/u$ (mm)					
	50	150	600	50	150	600
	Dry atmospheric conditions, i.e. inside (RH = 50%)			Humid atmospheric conditions, i.e. outside (RH = 80%)		
1	5.5	4.6	3.7	3.6	3.2	2.9
7	3.9	3.1	2.6	2.6	2.3	2.0
28	3.0	2.5	2.0	1.9	1.7	1.5
90	2.4	2.0	1.6	1.5	1.4	1.2
365	1.8	1.5	1.2	1.1	1.0	1.0

Table 5-1: Creep coefficient, φ, for normal weight concrete.

In this case, there is a humid atmospheric condition at the bridge site of 80% and the age when the concrete is loaded is 28 days. The circumference of the section, u, is:

$$u = 27700\ mm$$

The cross sectional area of the concrete is:

$$A_c = 6460000\ mm^2$$

The notional size is calculated to be:

$$\frac{2A}{u} = 466$$

which gives after interpolation the creep coefficient as φ =1.56, see table 5-1, and the effective modulus of elasticity is determined to $E_{c,eff}$=14066 MPa.

5.2.3.2 Reinforcement

The quality of the reinforcement is chosen to be B500B with characteristic yield strength f_{yk}=500 MPa.

5.2.3.3 Prestress system

As mentioned in chapter 4 for bridge type 1, the prestressing system is VSL 6-31. All technical information concerning VSL systems are acquired from technical brochures published by VSL International Ltd. (2010). Each tendon consists of 28 strands each consisting of 7 wires with a diameter of 15.7 mm with a total nominal cross-section A_p=4200 mm^2, where each strand has a nominal cross section of 150 mm^2. The steel quality of the wires is $f_{p0,1k}/f_{pk}$=1640/1860 MPa. The breaking load of each tendon is 7812 kN. The cables will be placed before casting in a group around a centerline that counteracts the moment from the self-weight of the bridge. The cables will be anchored individually with conical devices at each end of the bridge. When the concrete has achieved sufficient strength large multi-cable hydraulic jacks are used at both ends of the bridge to prestress the structure. When the required level of prestress is achieved the tendons are anchored at each end of the member. After anchorage, the ducts around the tendons are filled with cement grout under pressure, called bonded tendons. The cement grout is provided mainly to prevent corrosion of the tendons, but also it forms bond in the integrity of the anchor and hence improves its robustness. The prestressing process will be done in that manner that first the two internal spans will be constructed and prestressed and then finally the two external spans will be constructed and prestressed. To simplify the calculations it is assumed that the cables are calculated as one element, stressed from both ends of the bridge.

5.2.4 Exposure classes and service life

According to Eurocode 2 (EN 1992-1-1) a structure should be classified after environmental conditions, chemical and physical. This structure will be classified in the following classes:

- Corrosion induced by carbonation: XC4
- Corrosion induced by chlorides: XD3
- Corrosion induced by chlorides from sea water: XS3
- Freeze/Thaw Attack: XF4

These classifications give a structural class of S4 according to table 4.3N in EC2. For that class the minimum concrete cover for reinforcement steel is $c_{min,dur}$=45 mm and for prestressing steel $c_{min,dur}$=55 mm. Also, for post-tensioned members, the concrete cover should not be less than the diameter of the duct. In this case the external diameter of the duct is 117 mm. According to EC0, table 2.1, the service life (indicative design working life) for bridges is 100 years.

5.2.5 Tendon alignment and prestress force

The position of the centroid of the tendons should be chosen to give the highest effective depth. The alignment is based on concrete cover, the number and size of the tendons, the size of the cable ducts

and stresses. Roughly, a good moment distribution is obtained if the positions of cables in the cross-section are chosen as $0.17h$ from the bottom extreme fiber at bay and as $0.12h$ from the top extreme fiber at supports. The total height of the cross-section, h, is 2050 mm. Hence,

$$0.17h = 348.5\ mm$$

$$0.12h = 246\ mm$$

These values will be used in the beginning of the calculations. Minimum spacing of the cables, is given in section 8.10.1.3 in EC2, and should not be less than the diameter of the duct, in this case 117 mm. Maximum moments from self-weight in external bays occur at 0.375L or 13.875 m and in the center of the internal bays. These values will be checked later when the amount of cables has been decided with respect to minimum concrete cover and minimum distances between ducts. Figure 5-1 displays the moment curve from self-weight. In the prestressing stage only the self-weight from the superstructure will be taken into account.

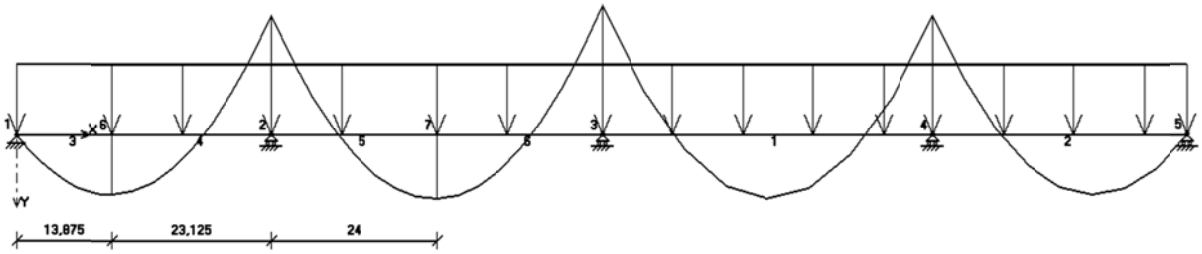

Figure 5-1: Moment distribution in the girder from self-weight.

At each end of the bridge the tendons are placed at the centroids of the T-section (half the cross-section). Eurocode 2, part 1.1, section 5.10.2, is used to determine the maximum allowed stresses at different times. The maximum allowed pre-tensioning stress during tensioning is the smaller of:

$$\sigma_s \leq \begin{cases} 0.8\, f_{pk} = 0.8 \cdot 1860 = 1488\ MPa \\ 0.9\, f_{p0.1k} = 0.9 \cdot 1640 = 1476\ MPa \end{cases}$$

Immediately after the cables are released from the jacks the maximum stresses in the cables are given as the smaller of:

$$\sigma_s \leq \begin{cases} 0.75\, f_{pk} = 0.75 \cdot 1860 = 1395\ MPa \\ 0.85\, f_{p0.1k} = 0.85 \cdot 1640 = 1394\ MPa \end{cases}$$

At the same time, excessive compressive and tensile stresses must not arise in the concrete. The acceptable value depends on the length of time during which the concrete has hardened. Eurocode 2 suggests that an acceptable compressive stress is:

$$\sigma_c \leq 0.60\, f_{ck}(t)$$

with $f_{ck}(t)$ as the characteristic compression strength as a function of time of the prestressing operation. $f_{ck}(t)$ is defined in section 3.1.2 in Eurocde 2 and is found with the following method:

$$f_{ck}(t) = f_{cm}(t) - 8\ (MPa) \qquad \text{for } 3 < t < 28 \text{ days}$$

$$f_{ck}(t) = f_{ck} \qquad \text{for } t \geq 28 \text{ days}$$

$f_{cm}(t)$ is estimated from the following expressions:

$$f_{cm}(t) = \beta_{cc}(t) f_{cm}$$

With $\beta_{cc}(t)$ as:

$$\beta_{cc}(t) = \exp\left\{ s\left[1 - \left(\frac{28}{t}\right)^{\frac{1}{2}}\right]\right\} = \exp\left\{0.25\left[1 - \left(\frac{28}{10}\right)^{\frac{1}{2}}\right]\right\} = 0.85$$

where s is chosen to 0.25 which is valid for cement of strength classes CEM Class N at 10 days and f_{cm} is 53 MPa. From this $f_{cm}(t)$ is determined to 44.79 MPa and $f_{ck}(t)$ to 36.79 MPa. Hence, the compressive strength at transfer becomes:

$$\sigma_c \leq 0.6\, f_{ck}(t) = 0.6 \cdot 36.79 = 22.07\ MPa$$

And the concrete strength at service time is:

$$\sigma_c \leq 0.6\, f_{ck} = 0.6 \cdot 45 = 27\ MPa$$

EC2 does not lay down any compulsory permissible tension stresses so the choice of concrete tension stress limits is left to the discretion of the designer. Hence the design is restricted by not allowing high tensile stresses to develop at service and only the concrete tensile strength at transfer:

$$\sigma_{ctk.0,05} \leq 2.7\ MPa$$

And at service the maximum tensile stress is chosen to:

$$\sigma_t \leq 2.0\ MPa$$

The stresses in the cross-section are calculated according to Navier's formula:

$$\sigma = -\frac{P}{A} + \frac{M_g - P e_s}{I} y$$

where P is the normal force, A is the area of the cross-section and I is the moment of inertia. M_g is the moment generated by self-weight, e_s is the eccentricity of the normal force and y is the location in the section where the stresses are calculated. In this equation P and e_s are unknown and have to be determined. The prestress force and eccentricity will be determined by developing a Magnel diagram, a method to determine a Magnel diagram is descriped in O'Brien (1999). Magnel diagrams are determined for the critical sections where the maximum transfer- and service moments occur. An estimation of the ratio between the prestress force at service and the prestress force at transfer, ρ, is made (generally from 0.75-0.90) and is chosen here to be 0.75. The critical sections that will be checked are external and internal spans and supports B and C. Figure 5-2 displays the load arrangements to establish the largest moments at each section at service stage. These load arrangements are determined based on influence lines that are created by the same method as in section 4 and can be seen in appendix B.

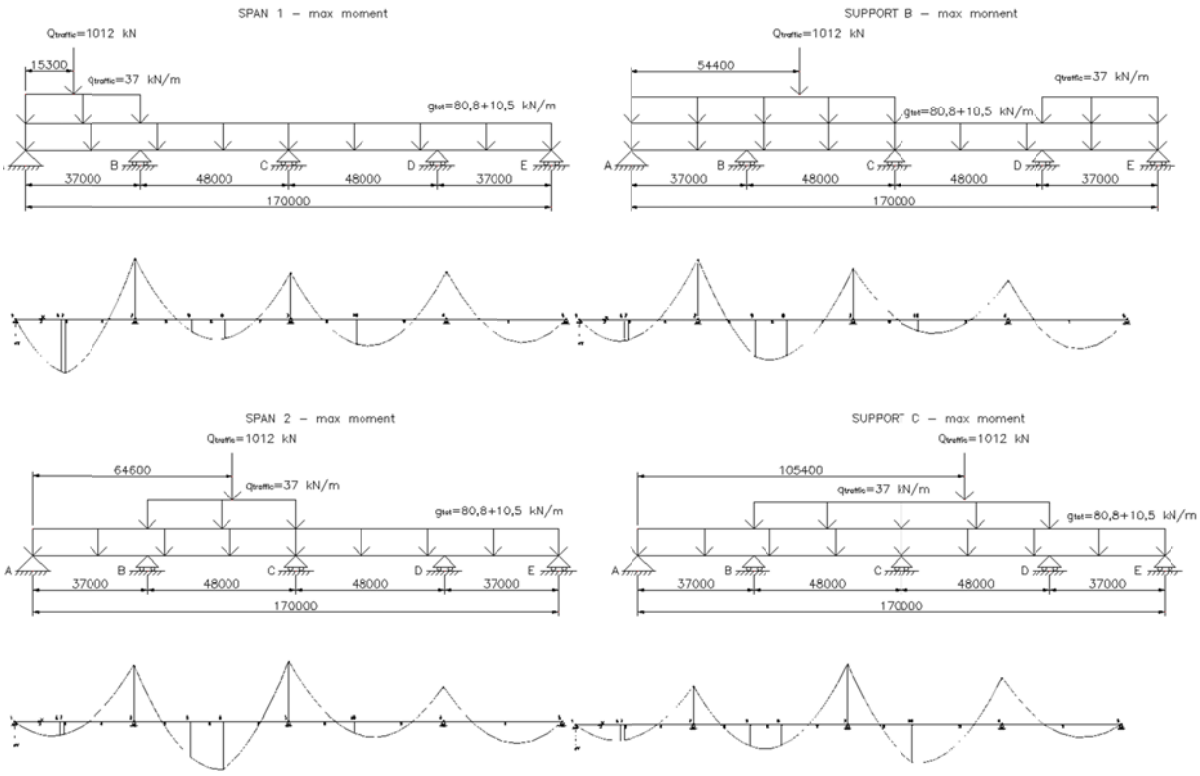

Figure 5-2: Moment distributions and load arrangement for moments at service for the calculated sections.

These moments are calculated in the computer program PCFRAME after influence lines have been developed for each section and the moments can be seen in table 5-2.

[kNm]	@SPAN 1	@SUPPORT B	@SPAN 2	@SUPPORT C
M_0	7463	-14648	7970	-15931
M_S	21040	-28880	22148	-30959

Table 5-2: Maximum moments at each section where M_0 is the moment at transfer and M_s the moment at service.

Below is a list that defines necessary notation, sign conventions and formulas for the calculations that follow.

σ_{tmin}: minimum stress at extreme top fibre.

σ_{tmax}: maximum stress at extreme top fibre.

σ_{bmin}: minimum stress at extreme bottom fibre.

σ_{bmax}: maximum stress at extreme bottom fibre.

These stresses are determined according to:

$$\sigma_{tmin} = greater\ of\ \left(p_{0min} - \frac{M_0}{W_t}\right)\ and\ \frac{1}{\rho}\left(p_{Smin} - \frac{M_S}{W_t}\right)$$

$$\sigma_{tmax} = lesser\ of\ \left(p_{0max} - \frac{M_0}{W}\right)\ and\ \frac{1}{\rho}\left(p_{Smax} - \frac{M_S}{W_t}\right)$$

$$\sigma_{bmin} = greater\ of\ \left(p_{0min} - \frac{M_0}{W_b}\right)\ and\ \frac{1}{\rho}\left(p_{Smin} - \frac{M_S}{W_b}\right)$$

$$\sigma_{tmax} = lesser\ of\ \left(p_{0max} - \frac{M_0}{W_b}\right)\ and\ \frac{1}{\rho}\left(p_{Smax} - \frac{M_S}{W_b}\right)$$

where W is the section modulus (I/y). W_b is at bottom and is a negative value and W_t is at top and is a positive value, A is area of the cross-section, e is the eccentricity of prestress tendons (above the centroid is positive and below negative) and M are applied moments (M_0 is the moment at transfer and M_S at service), see table 5-2. Sag moments are positive and hog moments are negative. These values are shown in appendix B. The notation for permissible stresses in these equations is the following:

ρ_{omin}: minimum permissible stress at transfer.

ρ_{omax}: maximum permissible stress at transfer.

ρ_{Smin}: minimum permissible stress at service.

ρ_{Smax}: maximum permissible stress at service.

In table 5-3 the numerical values for these permissible stresses are given.

p_{0min}	p_{Smin}	p_{0max}	p_{Smax}
[N/mm^2]	[N/mm^2]	[N/mm^2]	[N/mm^2]
-2,7	-2	22	27

Table 5-3: Permissible stresses.

And finally the results for these top and bottom stresses are listed in table 5-4.

	σ_{tmin}	σ_{tmax}	σ_{bmin}	σ_{bmax}
	[N/mm^2]	[N/mm^2]	[N/mm^2]	[N/mm^2]
SPAN 1	-6.88	17.90	24.36	29.26
SUPPORT B	17.27	29.66	-14.31	5.49
SPAN 2	-7.16	17.61	25.78	29.75
SUPPORT C	18.71	30.32	-15.32	3.29

Table 5-4: Maximum stresses at top and bottom fibers.

Note that for these calculations compressive stresses are considered positive and tensile stresses negative.

The following four inequalities are used to determine the feasible zone for the prestressing force on the Magnel diagrams:

$$\frac{1}{P}\sigma_{tmin} \leq \frac{1}{A} + \frac{e}{W_t} \qquad Inequality\ 1$$

$$\frac{1}{A} + \frac{e}{W_t} \leq \frac{1}{P}\sigma_{tmax} \qquad Inequality\ 2$$

$$\frac{1}{P}\sigma_{bmin} \leq \frac{1}{A} + \frac{e}{W_b} \qquad Inequality\ 3$$

$$\frac{1}{A} + \frac{e}{W_b} \leq \frac{1}{P}\sigma_{bmax} \qquad Inequality\ 4$$

These inequalities represent half-planes bounded by the line on which the stress limits are just satisfied. To determine which half-plane represents the inequality, the origin of the Magnel diagram is substituted into inequality 1, *1/P=0* and *e=0*, and gives the following:

$$0 \leq \frac{1}{A} \qquad Inequality\ 1$$

If this is true (A is positive), the correct half-plane is the one containing the origin and the same procedure is done for the three remaining inequalities.

$$\frac{1}{A} \leq 0 \qquad Inequality\ 2$$

$$0 \leq \frac{1}{A} \qquad Inequality\ 3$$

$$\frac{1}{A} \leq 0 \qquad Inequality\ 4$$

Thus, for inequality 1 the half-plane contains the origin, for inequality 2 it doesn't, for inequality 3 the half-plane contains the origin and for inequality 4 it doesn't. For further information see appendix B and O'Brien (1999).

After some calculation the Magnel diagrams are established (Appendix B) and the appropriate prestress force and eccentricity are chosen. The chosen prestress force is 46.512 kN ($1/P=2.15 \times 10^{-8}$ N^{-1}) which is based on the maximum allowable eccentricity that is at supports B and C. That requires approximately 8 tendons each with a breaking load of 7812 kN. The eccentricity limits at each section are given below, based on these Magnel diagrams.

Section at support A: -180 mm ≤ *e* ≤ 283.6 mm

Section at span 1: -210 mm ≤ *e* ≤ -410 mm

Section at support B: 200 mm ≤ *e* ≤ 283.6 mm

Section at span 2: -300 mm ≤ *e* ≤ -420 mm

Section at support C: 250 mm ≤ *e* ≤ 283.6 mm

On figure 5-3 is the longitudinal feasible zone and the cable layout displayed. That zone is based on the calculations above.

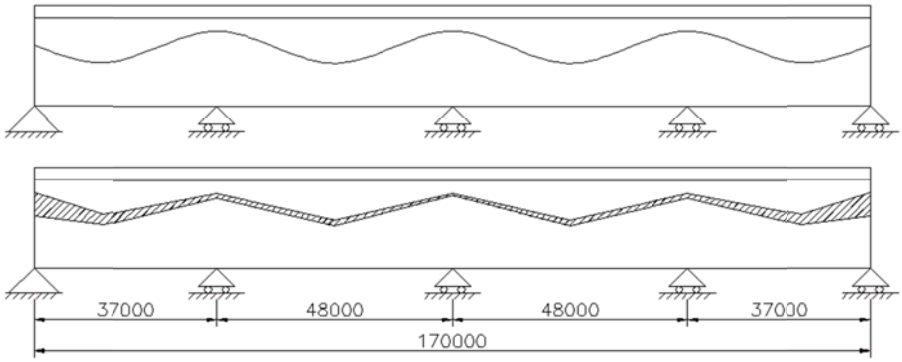

Figure 5-3: Longitudinal feasible zone of the cable (the beam size has the scale of 10 in vertical direction).

On figure 5-4 the chosen eccentricities are displayed.

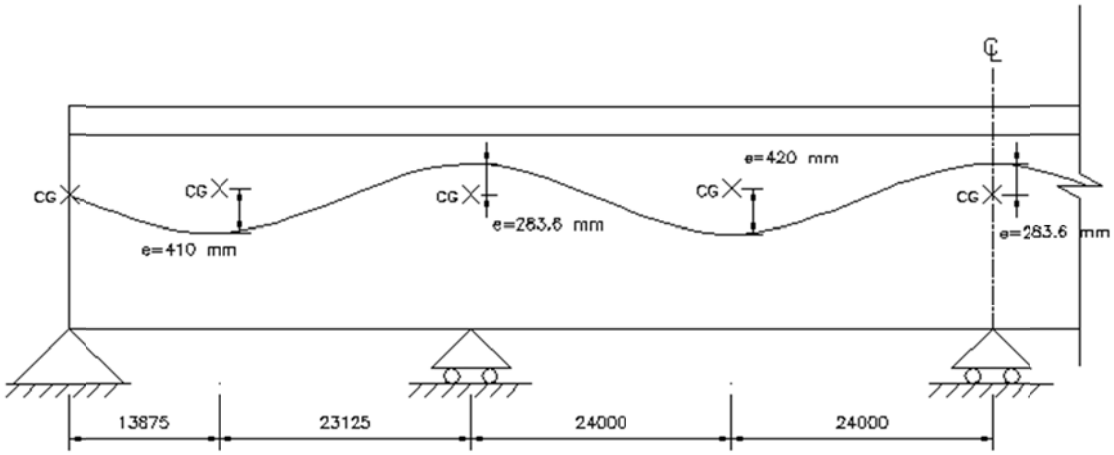

Figure 5-4: Chosen eccentricities for the cable line.

5.2.6 Prestress losses

The effective prestress force is not generally equal to the applied jacking force nor is it constant along the length of the member. Therefore, in order to determine the effective stress due to prestress at transfer and service, the losses in prestress must first be calculated at each design section. These losses can be divided into two groups in accordance with the time when they occur. Losses which occur prior to the point in time when stress is first felt by the concrete are called pre-transfer losses and losses which occur after the prestress is transferred to the concrete are called post-transfer losses. The pre-transfer losses consist of:

- Elastic shortening of the cross-section.
- Friction between the tendons and the surrounding ducts (in case of post-tension).

The post-transfer losses consist of:

- Time dependent losses, which are from relaxation of the steel and by creep and shrinkage of the concrete.
- Loss due to slippage of the tendons at the anchorage known as draw-in loss (in case of post-tension).

5.2.6.1 Friction losses

The loss of prestress force from friction is caused by two sources:

- Friction due to curvature of the tendon
- Friction due to unintentional variation of the duct from its prescribed profile or 'wobble'.

The friction loss at section *i* due to curvature is:

$$curvature\ loss_i = P_{jack}(1 - e^{-\mu \sum_{i=1}^{n} \theta_i})$$

where μ is a friction coefficient and θ_i is the aggregate change in slope in radians between the jack and section *i* and n is the total number of sections. The system producer recommends a value of the friction coefficient as μ=0.2. To calculate the angle changes at each section the following equation is used:

$$\theta_i = 2(\frac{y_i}{x_i})$$

where y_i is the vertical change in height between the sections that are calculated and x_i is the horizontal distance between the corresponding sections. These sections are displayed on figure 5-5.

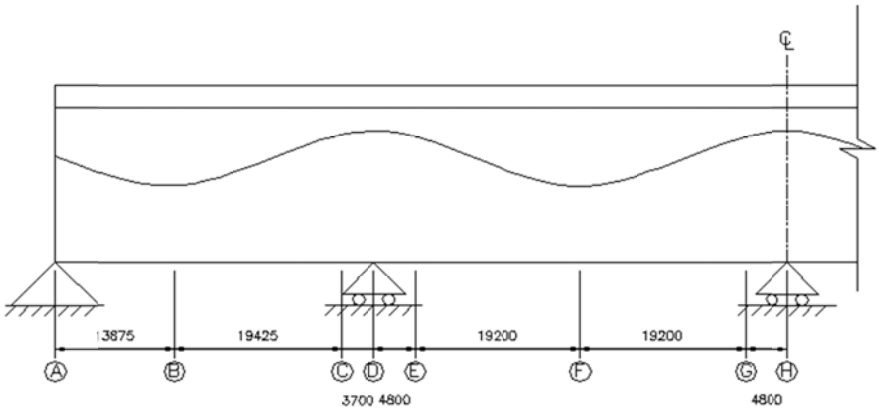

Figure 5-5: Sections of the beam for calculations of friction losses and elastic shortening losses.

The friction loss at section *i* due to wobble is:

$$wobble\ loss_i = P_{jack}(1 - e^{-\mu k \sum_{i=1}^{n} x_i})$$

k is a wobble coefficient which depends on the quality of workmanship, the distance between tendon supports, the degree of vibration used in placing the concrete and the type of the duct. For the chosen system the producer recommends k=0.0008 m^{-1}. The term x_i is the distance (in meters) from the jack to section number *i*. Hence, the total friction loss becomes:

$$total\ friction\ loss_i = P_{jack}(1 - e^{-\mu \sum_{i=1}^{n} (\theta + kx)})$$

The results of the calculated friction losses are displayed in table 5-5.

Segment	y [m]	x [m]	$\theta = 2(y/L)$ [rad]	$\Sigma\theta$ [rad]	Wobble, k [m^{-1}]	Σx [m]	$(\mu\Sigma\theta+k\Sigma x)$	$e^{-(\mu\Sigma\theta+k\Sigma x)}$	Friction loss $P_{jack}(1-e^{-(\mu\Sigma\theta+k\Sigma x)})$ [kN]
AB	0.353	13.875	0.0509	0.0509	0.0008	13.875	0.0213	0.9789	979
BC	0.595	19.425	0.0613	0.1121	0.0008	33.3	0.0491	0.9521	2227
CD	0.042	3.7	0.0227	0.1348	0.0008	37	0.0566	0.9450	2558
DE	0.067	4.8	0.0279	0.1628	0.0008	41.8	0.0660	0.9361	2970
EF	0.58	19.2	0.0604	0.2232	0.0008	61	0.0934	0.9108	4149
FG	0.579	19.2	0.0603	0.2835	0.0008	80.2	0.1209	0.8862	5295
GH	0.067	4.8	0.0279	0.3114	0.0008	85	0.1303	0.8778	5681

Table 5-5: Friction losses.

5.2.6.2 Elastic shortening losses

As the prestress is transferred to the concrete, the concrete undergoes elastic shortening. This can cause a slackening of the strand which results in a loss of prestress force. The losses due to elastic shortening in each tendon of post-tensioned members are different. The maximum loss is in the tendon that is released first and then less in the next one and etc. The elastic shortening loss in the tendon that is released first is:

$$elsastic\ shortening\ loss\ in\ tendon\ 1 = P_2 A_{p1} \frac{E_p}{E_c}\left(\frac{1}{A_g} + \frac{e_1 e_2}{I_g}\right)$$

where index 1 and 2 indicate tendon 1 and 2 respectively. P and e are the prestressing force and eccentricity respectively. A_g is the area of the cross-section. The results of the calculated elastic shortening loss for the whole cable group in one girder are displayed in table 5-6.

Segment	e [mm]	I_g [mm^4]	A_g [mm^2]	Total elastic shortening loss [kN]
AB	410	1.35E+12	3230000	3793
BC	185	1.35E+12	3230000	2924
CD	284	1.56E+12	3770000	2764
DE	160	1.35E+12	3230000	2869
EF	420	1.35E+12	3230000	3846
FG	159	1.35E+12	3230000	2866
GH	284	1.56E+12	3770000	2764

Table 5-6: Elastic shortening losses.

5.2.6.3 Draw-in losses

After jacking the tendons are released from the jacks and the force is applied directly through the anchorages to the concrete. This process results in a loss due to slippage or 'draw-in' of the strands at the anchors. The ´draw-in´ of the tendons results in a loss of strain of ε_{jack} at the anchorage. However,

because of friction, this loss decreases along the length of the member to zero at a distance L_d from the jack. The extent of draw-in losses is determined with the following equation:

$$L_d = \sqrt{\frac{\Delta_s E_p A_p}{(P_{jack} - P_L)/L}}$$

where $(P_{jack}-P_L)/L$ is the slope of the distribution of prestress force if the friction loss is assumed to vary linearly. Δ_s is the total shortening of the tendon. The magnitude of the draw-in loss at the anchorage is then given by the following equation:

$$\Delta P = 2\frac{(P_{jack} - P_L)}{L} L_D$$

where ΔP is the draw-in loss. The distribution of the prestress force after the draw-in loss is displayed in figure 5-6 where the decrease of this loss along the length of the member becomes zero at distance L_d approximately 15 m from the jack.

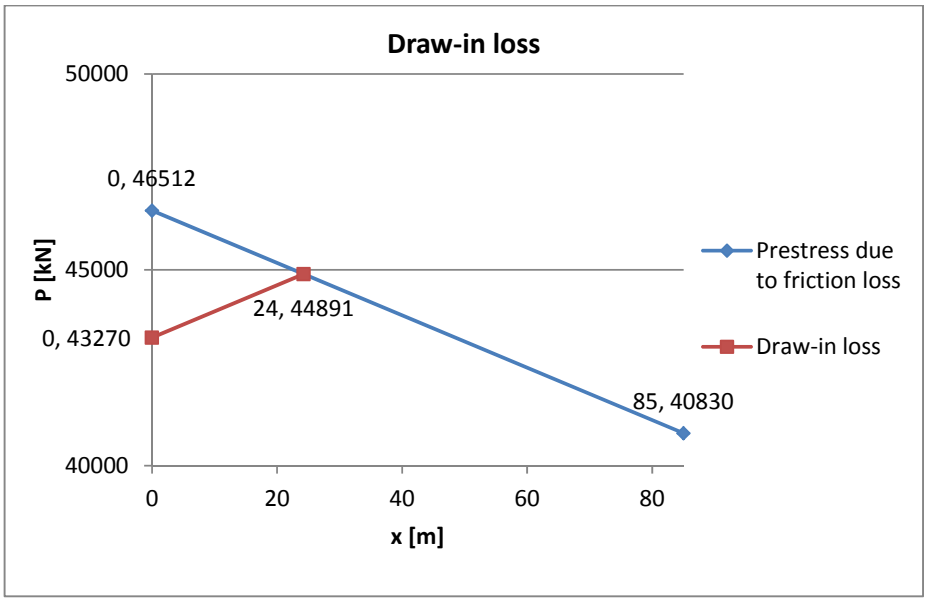

Figure 5-6: Distribution of the prestress force after the draw-in loss for half of the total span.

5.2.6.4 Time-dependent losses

Losses in prestress which occur gradually over time are caused by shortening of the concrete due to creep and shrinkage and due to relaxation of the prestressing steel. Shrinkage is a time-dependent strain which occurs as the concrete sets and for a period after setting. The shrinkage strain approaches final value at infinite time. When maintained at a constant tensile strain, steel gradually loses its stress with time due to relaxation. The extent of the loss of stress in prestressing strands due to relaxation is determined by the stress to which the steel is tensioned, the ambient temperature and the class of steel. Maximum allowable value for relaxation losses of the prestressing steel are specified by the manufacturer as 2.5% for 15 mm strands. To determine the loss EC2 suggests that it should be based on the 1000 hour values given in figure 5-7. These values should be trebled to determine the final relaxation losses.

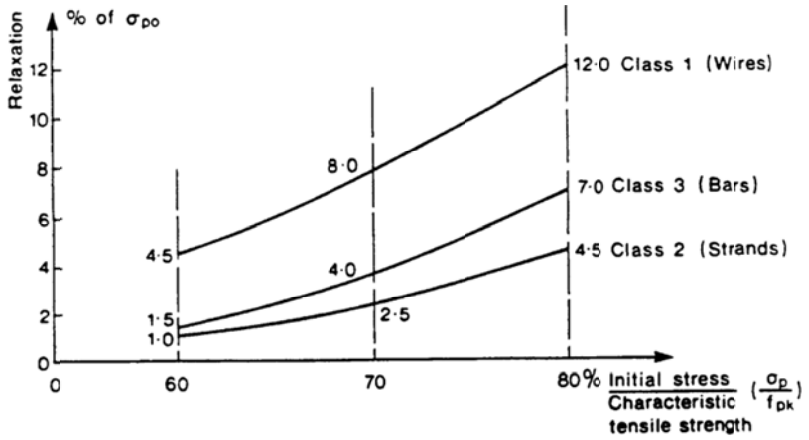

Figure 5-7: Relaxation of prestressing steel.

The phenomenon of creep is essentially the same as that of relaxation. The distinction is that relaxation refers to the loss of stress under constant strain while creep is the increase of strain which occurs at constant stress. For prestressed concrete, relaxation occurs in the steel while creep occurs in the concrete.

EC2 recommends that these two prestress losses, creep and shrinkage, should be calculated with the following formula:

$$\Delta\sigma_{p,tot} = \frac{\varepsilon_{cs}E_p + \Delta\sigma_{p,r}m\varphi\sigma_c}{1 + \frac{mA_p}{A_g}\left(1 + \frac{A_g e^2}{I_g}\right)(1 + 0.8\varphi)}$$

where

$\Delta\sigma_{p,tot}$ = loss of stress in steel due to creep, shrinkage and relaxation.

ε_{cs} = final shrinkage strain calculated according to section 3.1.4 (6) in EC2. Calculated value of this strain is ε_{cs}=0.000256.

E_p = modulus of elasticity of the prestressing steel.

$\Delta\sigma_{p,r}$ = loss of stress in the tendons at the design section due to relaxation.

m = modular ratio, E_p/E_c.

φ = final creep coefficient taken from table 5-1.

σ_c = stress in the concrete at the level of the tendons due to permanent loads plus prestress.

A_p = area of prestressing steel.

A_g, I_g = gross area and second moment of area of section.

e = eccentricity of tendons from centroid section.

The final shrinkage strain is composed of two components, the drying shrinkage strain, ε_{cd}, and the autogenous shrinkage strain, ε_{ca}. For detailed explanations of calculations of the final shrinkage strain author refers to section 3.1.4 (6) in EC2. The loss of stress in the tendons due to relaxation, $\Delta\sigma_{p.r}$, is

derived from figure 5-7 with the ratio of steel stress/characteristic tensile strength as (σ_p/f_{pk}) with σ_p at the section that is calculated as:

$$\sigma_p = \frac{P}{A_p} + \frac{E_p}{E_c}\frac{M_s e}{I_g}$$

and the loss of stress in the tendons due to relaxation as:

$$\Delta\sigma_{p,r} = 3 \times relaxation\ loss \times \frac{P}{A_p}$$

The stress, σ_c, in the concrete at the level of tendons due to permanent loads plus prestress is calculated using the following equation:

$$\sigma_c = \frac{P}{A_g} + \frac{(Pe + M_s)e}{I_g}$$

Following these calculations the total time-dependent loss of stress in the tendons can be calculated. From these results and from the calculations of the draw-in losses the applied prestress at service can then be calculated. The results of the calculated time-dependent losses are displayed in table 5-7.

	L [m]	P [kN] (after draw-in)	M_s [kNm]	e_p [mm]	I_g [mm^4]	σ_p [N/mm^2]	A_g [mm^2]	σ_p/f_{pk}	Relaxation (max 2,5%)	$\Delta\sigma_{p,r}=3*\%*P/A_p$ [N/mm^2]	σ_c [N/mm^2]	$\Delta\sigma_{p,tot}$ [N/mm^2]	Total time loss [kN]	Prestress at service [kN]	Ratio of prestress at service to transfer, ρ
Supp. A	0	43270	0	0.0	1.56E+12	1288	3.77E+06	0.69	0.025	96.6	11.48	219.6	7379	35890	0.77
Span 1	13.875	44197	21040	-410.0	1.35E+12	1281	3.23E+06	0.69	0.025	98.7	12.79	217.9	7322	36875	0.79
Supp. B	37	44039	-28880	283.6	1.56E+12	1282	3.77E+06	0.69	0.025	98.3	8.71	196.4	6598	37441	0.81
Span 2	61	42434	22148	-420.0	1.35E+12	1225	3.23E+06	0.66	0.025	94.7	11.79	206.9	6952	35482	0.76
Supp. C	85	40830	-30959	283.6	1.56E+12	1185	3.77E+06	0.64	0.025	91.1	7.32	179.6	6035	34795	0.75

Table 5-7: Time-dependent losses.

5.2.7 Secondary effects of prestress

For statically indeterminate structures the prestress moment consists of two components, primary moment and secondary moment. The primary moment is the product of prestressing force and eccentricity, the secondary moment is moment caused by reactions developed at intermediate supports during prestressing. To determine the secondary moment there are two common methods; support displacement method and equivalent load method. In this thesis the equivalent load method is applied. The equivalent load is a uniformly distributed load established by considering a simple beam with a parabolic tendon profile. The bending moment at any point due to this prestressing force is given by $M_1=Pe$. If an equivalent uniform upward load, w, is assumed to act on the beam, see figure 5-8, the maximum moment at mid-span is equal to:

$$M_2 = \frac{wL^2}{8}$$

Since the equation of the bending moment for uniformly loaded simply supported beam is also parabolic, the moments must be equal in the two beams at any point. Thus

$$M_1 = M_2$$

Application of this equation at the mid-span gives

$$Pe = \frac{wL^2}{8}$$

and

$$w = \frac{8Pe}{L^2}$$

where *e* is the distance from the cable to the eccentricity of the beam at mid-span.

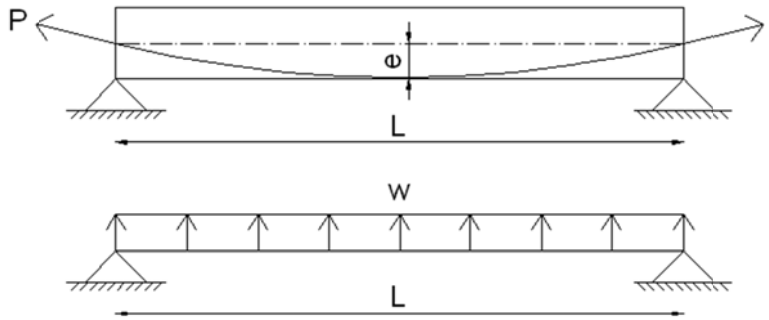

Figure 5-8: Calculation of the equivalent load for curved tendons.

In the case when the vertical position of the cables at supports is not the same at two adjacent supports *e* is the eccentricity at mid span from the cable to the line that connects these two positions of the cable, see figure 5-9.

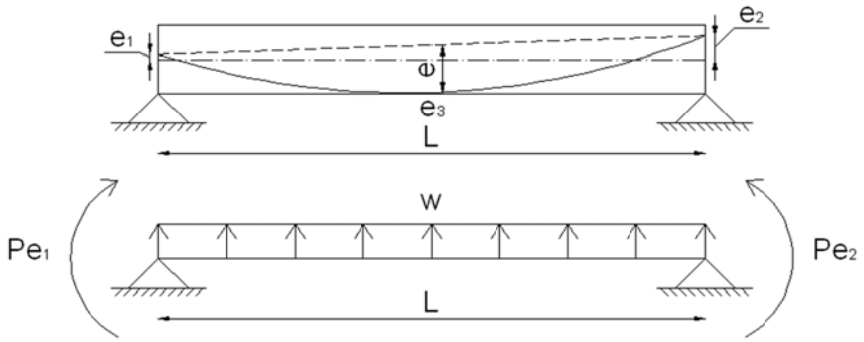

Figure 5-9: Determination of e for cable with eccentricity e_1 and e_2.

Thus, the eccentricity becomes:

$$e = e_3 + \frac{e_1 + e_2}{2}$$

To determine the moment at the intermediate supports the three-moment equation (Clapeyron´s theory) is used. The calculation procedure of the three-moment equation is in the following order:

- Draw a free body diagram of the first two spans.
- Label the spans L_1 and L_2 and the supports A, B and C.
- Use the three-moment equation to solve the unknown moments.
- Move one span further and repeat the procedure above.

- Repeat as needed, always moving one span to the right and writing a new set of moment equations.
- Solve 3 simultaneous equations for 4 spans to get the internal moments.

In this case these moment equations are three since there are four spans and three unknown moments, M_A, M_B and M_C. They are the following:

$$M_A L_1 + 2M_B(L_1 + L_2) + M_C L_2 = -6(EI\theta_1 + EI\theta_2)$$

$$M_B L_2 + 2M_C(L_2 + L_3) + M_D L_3 = -6(EI\theta_2 + EI\theta_3)$$

$$M_C L_3 + 2M_D(L_3 + L_4) + M_E L_4 = -6(EI\theta_3 + EI\theta_4)$$

The notation for the formulas above is displayed on figure 5-10.

Figure 5-10: Notation for calculations with the three-moment equation.

The terms on the right hand side of these equations are acquired with the following formula for beams with uniformly distributed load on span no. n:

$$EI\theta_n = \frac{w_n L_n^3}{24}$$

In table 5-8 the calculated values for *w* and the prestress moments are listed and on figure 5-11 the moment diagrams for the corresponding moments. The secondary moment is linear between supports. More detailed calculations to obtain the secondary moment are in appendix B.

	L [m]	e_m [mm]	w [kN/m]	$M_{primary}$ [kNm]	$M_{secondary}$ [kNm]	$M_{primary+secondary}$ [kNm]
Support A				0	0	0
Span 1 (0,375*37)	37	460	99.023	-15119	2068	-13050
Support B				10618	5516	16134
Span 2 (37+0,5*48)	48	647	79.685	-14902	5265	-9638
Support C				9868	5014	14882

Table 5-8: Prestress moment.

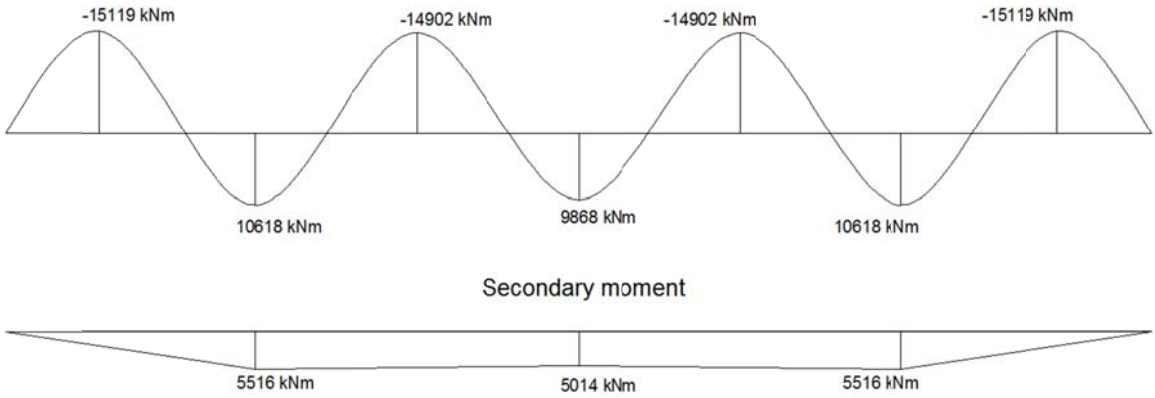

Figure 5-11: Diagrams of primary and secondary moments.

When the total moment has been obtained in the beam, the ultimate moment capacity can be calculated. That is done in the next chapter.

5.3 Ultimate moment capacity

When the member has been designed to satisfy the transfer and service stress limits it is necessary to check for moment capacity in the ultimate limit state. As for ordinary reinforced concrete, the ultimate moment capacity of a prestressed section is calculated by equilibrium of forces at the corresponding section. The compressive strain in the concrete due to prestress, ε_{ce}, at the level of the prestressing tendon is given with the following formula:

$$\varepsilon_{ce} = \frac{1}{E_c}\left(\frac{P}{A_g} + \frac{M_p e}{I_g}\right)$$

where M_p is the moment due to prestress and P is the prestress force, both after all losses, at the section that is calculated. The tendon strain is defined as (contraction positive):

$$\varepsilon_{pu} = -\frac{P}{A_p E_p} + \varepsilon_{ct} - \varepsilon_{ce}$$

where A_p is the area of the prestress reinforcement and E_p is its modulus of elasticity. ε_{ct} is the total ultimate strain in the concrete and is found with the following equation:

$$\varepsilon_{ct} = -\frac{\varepsilon_{ult}(d - x)}{x}$$

EC2 recommends that ε_{ult} should be taken as 0.0035. Here d is the effective depth, distance from extreme fibre in compression to the center of tension reinforcement, and x is the distance from extreme fibre in compression to neutral axis. To calculate the equilibrium of forces the force in the steel, F_p, and the compressive force acting on the concrete in compression, F_c, are required:

$$F_p = A_p(E_p \varepsilon_{pu})$$

$$F_c = 0.8xb\frac{\alpha f_{ck}}{\gamma_c}$$

Here b is the width of the section which F_c is acting on. α is a coefficient which takes into account the long-term effects on the compressive strength and is 1.0. γ_c is the partial safety factor for concrete strength and is equal to 1.5 according to EC2. Now the following equation for equilibrium of forces is established and solved to find x:

$$F_p + F_c = 0$$

When x is found a check is made to see if the steel has yielded by substituting x into the equation for the tendon strain defined above. The initial yield strain for prestressing steel is $f_{pk}/\gamma_p E_p$ where γ_p is the partial safety factor for reinforcement strength and is equal to 1.15 according to EC2. ε_{pu} cannot exceed the initial strain, otherwise the steel has yielded. Finally the ultimate moment capacity can be determined with the following formula:

$$M_{ult} = F_p z = F_c z$$

with z as:

$$z = (d - 0.4x)$$

In appendix B are detailed calculations of the moment capacity of each section displayed. In table 5-9 are the bending moments in ULS with prestress and the moment capacity summarized for each section.

	M_{total} [kNm]	M_{ult} [kNm]
Span 1	17264	22256
Support B	24704	43846
Span 2	22317	22532
Support C	28855	42982

Table 5-9: Total design moment in the ULS with prestress (M_{total}) and the ultimate moment capacity (M_{ult}).

Finally, the cross-section with the cable elevation is displayed for each section in figure 5-12.

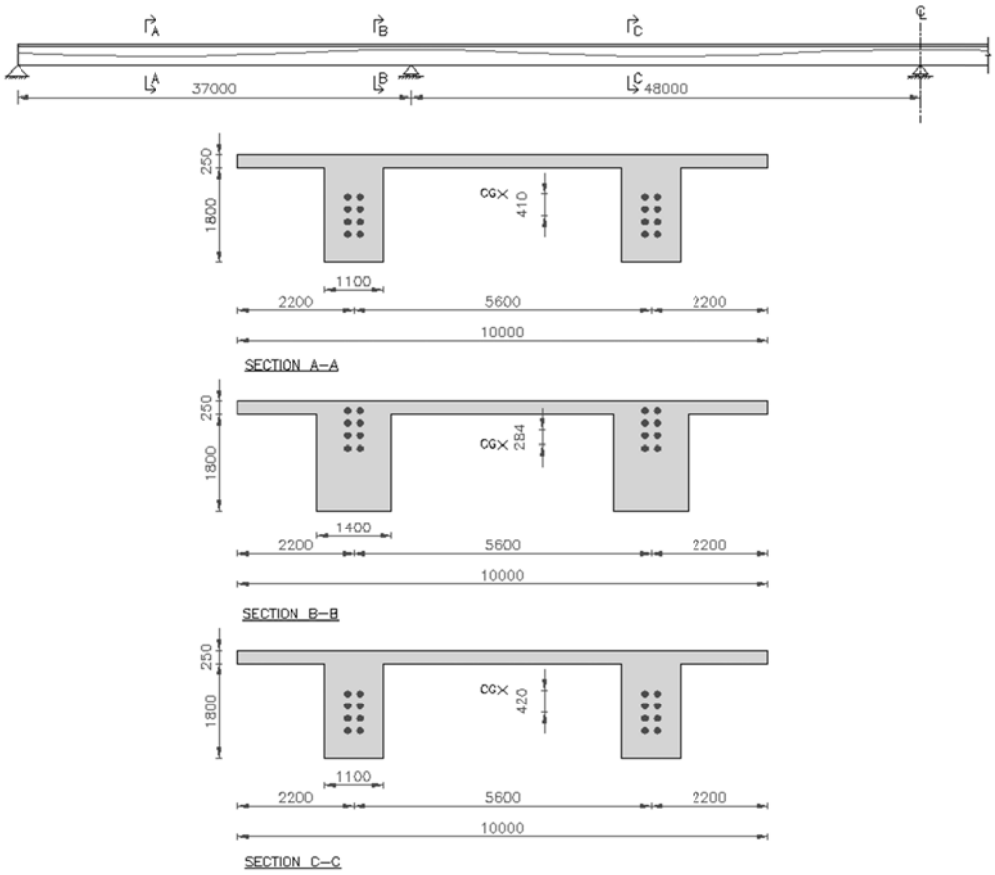

Figure 5-12: Cross-section and cable elevation.

6 References

6.1 Literature

Austin, W.J., (1971), "*IN-PLANE BENDING AND BUCKLING OF ARCHES*", Journal of the Structural Division, May 1971, pp. 1575-1591.

Bunner, M. and Wright, K., (2006), "*Selecting the Shape of a Steel Arch*", *Bridgeline, Volume 15, NO. 1, April 2006.*

Chen, W. and Duan, L., (2000), "*Bridge Engineering Handbook*", CRC Press LLC, Florida.

EN 1990:2002. Eurocode - Basis of Structural Design. CEN, 2002.

EN 1991:2002. Eurocode - Actions on Structures. CEN, 2002.

EN 1992:2004. Eurocode – Design of Concrete Structures. CEN, 2004.

EN 1993:1992. Eurocode – Design of Steel Structures. CEN, 1992.

Ghoneim, M. and El-Mihilmy, M., (2008), "*Design of Reinforced Concrete Structures*", Vol. 3, Cairo University, Cairo.

Gilbert, R. I., and Mickleborough, N. C., (2004), "*Design of Prestressed Concrete*", Spon Press, London.

ISE manual, (1985), I. Struct. E./ICE Joint committee, *"Manual for the Design of Reinforced Concrete Building Structures",* Institution of Structural Engineers, London.

Loretsen, M. and Sundquist, H., (1995), "*Bågkonstruktioner"*, KTH.

Loretsen, M. and Sundquist, H., (1995), "*Hängkonstruktioner*", KTH.

Menn, C., (1986), "*Prestressed Concrete Bridges",* Springer-Verlag, Wien.

Nawy, E. G., (2008), "*Concrete Construction Engineering Handbook*", 2nd edition, CRC Press LLC, Florida.

O'Brien, E. J. and Dixon, A. S., (1999). "*Reinforced and Prestressed Concrete Design"*, Pearson Education Limited, Edinburgh.

"*Prestress Manual*", (2005), State of California, Department of Transportation, Engineering Services.

Thelandersson, S., (2009), "*Design of bridges – Structural design project"*, Lund University, Structural engineering.

Zhuan M. Q. and Guo. X. J., (1998), "*PE Shelled Large Pitch Twisted Stay Cable, For Construction Use",* Shanghai PuJiang Cable Co. Ltd. Shanghai.

6.2 Computer programs

AutoCAD 2009, Autodesk.

CSI SAP2000, version 14, Computers & Structures.

Microsoft Office Excel 2007, Microsoft.

Microsoft Office Word 2007, Microsoft.

PCFrame, version 2.15, AEC AB.

6.3 Other references

Hafliðason, E. (2010), personal communication with Hafliðason at ICERA.

Earthquake Engineering Research Centre, University of Iceland.

VSL Post-Tensioning Systems, Technical Data, (2010), VSL International Ltd.

http://www.ingvason.com/

Appendix A

CALCULATIONS OF GDF FOR BRIDGE TYPE 1

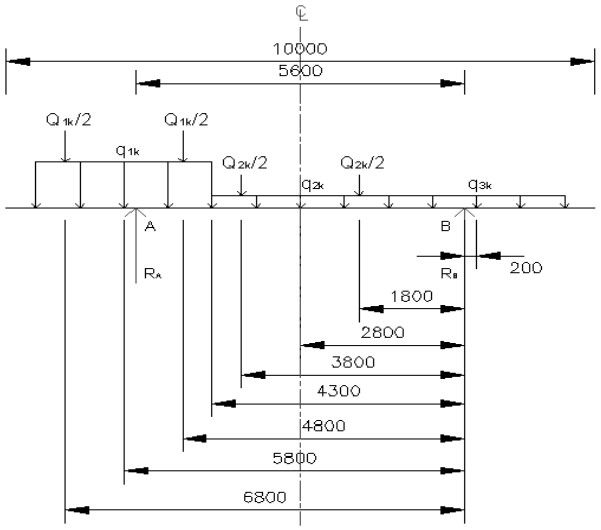

Q_{1k}=	300	α_{Q1}=	0,9	$\alpha_{Q1}\cdot Q_{1k}$=	270	kN
Q_{2k}=	200	α_{Q2}=	0,9	$\alpha_{Q2}\cdot Q_{2k}$=	180	kN
q_{1k}=	9	α_{q1}=	1	$\alpha_{q1}\cdot q_{1k}$=	9	kN/m^2
q_{2k}=	2,5	α_{q2}=	1	$\alpha_{q2}\cdot q_{2k}$=	2,5	kN/m^2
q_{3k}=	2,5	α_{q3}=	1	$\alpha_{q3}\cdot q_{3k}$=	2,5	kN/m^2

For Q		
F	**z**	**M**
R_A	5,6	$R_A\cdot x$
135	6,8	918
135	4,8	648
90	3,8	342
90	1,8	162
	∑M=	2070
	R_A=	369,64
	GDF_Q=	**1,37**
	R_B=	80,36

For q			
q	**l**	**z**	**M**
R_A		5,6	$R_A\cdot x$
9	3	5,8	156,6
2,5	3	2,8	21
2,5	3	-0,2	-1,5
		∑M=	176,1
		R_A=	31,45
		GDF_q=	**1,16**
		R_B=	10,55

Total actions on half of the cross section for traffic loads in the length direction

$Q=2*GDF_Q*R_A$=	**1012**	kN
$q=GDF_q*R_A$=	**37**	kN/m

Calculations for Area, Moment of Inertia and Section Modulus for Bridge Type 1

Note: All cross-section calculations are done from the bottom fibre

In the middle of the span									
Part	**b**	**h**	**A**	**y_0**	**$S=Ay_0$**	**$y-y_0$**	**I_0**	**$A(y-y_0)^2$**	**I_x**
nr.	mm	mm	mm^2	mm	mm^3	mm	mm^4	mm^4	mm^4
1	1080	2400	2592000	1200	3,11E+09	431,1	1,24E+12	4,82E+11	1,73E+12
2	1080	2400	2592000	1200	3,11E+09	431,1	1,24E+12	4,82E+11	1,73E+12
3	10000	250	2500000	2525	6,31E+09	-893,9	1,30E+10	2,00E+12	2,01E+12
$\sum$			7684000		1,25E+10				5,46E+12

y= 1631,1 mm **W_{Top}=** 5,36E+09 mm^3

h= 2650 mm **W_{Bottom}=** 3,35E+09 mm^3

Creep - Effective elastic modulus

Perimeter:	u=	30100	mm
Notional size:	2A/u=	511	mm
Creep coefficient:	φ=	1,54	
Effective elastic modulus:	$E_{c,eff}$=	14175	N/mm^2

In the middle of the span - Half cross section									
Part	**b**	**h**	**A**	**y_0**	**$S=Ay_0$**	**$y-y_0$**	**I_0**	**$A(y-y_0)^2$**	**I_x**
nr.	mm	mm	mm^2	mm	mm^3	mm	mm^4	mm^4	mm^4
1	5000	250	1250000	2525	3,16E+09	-893,9	6,51E+09	9,99E+11	1,01E+12
2	1080	2400	2592000	1200	3,11E+09	431,1	1,24E+12	4,82E+11	1,73E+12
$\sum$			3842000		6,27E+09				2,73E+12

y= 1631,1 mm **W_{Top}=** 2,68E+09 mm^3

h= 2650 mm **W_{Bottom}=** 1,67E+09 mm^3

Over a support									
Part	**b**	**h**	**A**	**y_0**	**$S=Ay_0$**	**$y-y_0$**	**I_0**	**$A(y-y_0)^2$**	**I_x**
nr.	mm	mm	mm^2	mm	mm^3	mm	mm^4	mm^4	mm^4
1	1380	2400	3312000	1200	3,97E+09	363,1	1,59E+12	4,36548E+11	2,03E+12
2	1380	2400	3312000	1200	3,97E+09	363,1	1,59E+12	4,36548E+11	2,03E+12
3	10000	250	2500000	2525	6,31E+09	-961,9	1,30E+10	2,31335E+12	2,33E+12
$\sum$			9124000		1,43E+10				6,38E+12

y= 1563,1 mm W_{Top}= 5,87E+09 mm^3

h= 2650 mm W_{Bottom}= 4,08E+09 mm^3

Over a support - Half cross section									
Part	**b**	**h**	**A**	**y_0**	**$S=Ay_0$**	**$y-y_0$**	**I_0**	**$A(y-y_0)^2$**	**I_x**
nr.	mm	mm	mm^2	mm	mm^3	mm	mm^4	mm^4	mm^4
1	5000	250	1250000	2525	3,16E+09	-961,9	6,51E+09	1,16E+12	1,16E+12
2	1380	2400	3312000	1200	3,97E+09	363,1	1,59E+12	4,37E+11	2,03E+12
$\sum$			4562000		7,13E+09				3,19E+12

y= 1563,1 mm W_{Top}= 2,51E+09 mm^3

h= 2650 mm W_{Bottom}= 2,04E+09 mm^3

Creep - Effective elastic modulus

Perimeter:	u=	30100	mm
Notional size:	2A/u=	606	mm
Creep coefficient:	φ=	1,50	
Effective elastic modulus:	$E_{c,eff}$=	14416	N/mm^2

Summary	**A**	**$W_{,Top}$**	**$W_{,Bottom}$**	**I**	**Weight**
	mm^2	mm^3	mm^3	mm^4	kN/m
In the Middle of the Span	7684000	5,36E+09	3,35E+09	5,46E+12	192,1
In the middle of the Span - half	3842000	2,68E+09	1,67E+09	2,73E+12	96,05
Over a support	9124000	5,87E+09	4,08E+09	6,38E+12	228,1
Over a support - half	4562000	2,51E+09	2,04E+09	3,19E+12	114,05

$\gamma_{concrete}$= 25 kN/m^3

$\gamma_{pavement}$= 2,1 kN/m^2

Self weight of concrete for half of the bridge section

$g_{concrete}$= 96,1 kN/m

$g_{pavement}$= 10,5 kN/m

g_{tot}= 106,6 kN/m

E_c= 36000 N/mm^2

CALCULATIONS OF GDF FOR BRIDGE TYPE 2

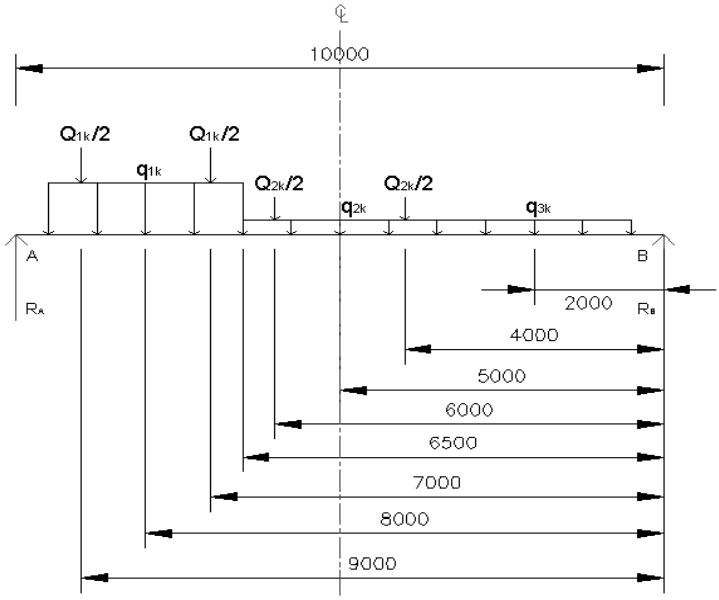

Q_{1k}=	300	α_{Q1}=	0,9	$\alpha_{Q1}\cdot Q_{1k}$=	270	kN
Q_{2k}=	200	α_{Q2}=	0,9	$\alpha_{Q2}\cdot Q_{2k}$=	180	kN
q_{1k}=	9	α_{q1}=	1	$\alpha_{q1}\cdot q_{1k}$=	9	kN/m^2
q_{2k}=	2,5	α_{q2}=	1	$\alpha_{q2}\cdot q_{2k}$=	2,5	kN/m^2
q_{3k}=	2,5	α_{q3}=	1	$\alpha_{q3}\cdot q_{3k}$=	2,5	kN/m^2

For Q		
F	**z**	**M**
R_A	10	$R_A\cdot x$
135	9	1215
135	7	945
90	6	540
90	4	360
	∑M=	3060
	R_A=	306,00
	GDF_Q=	**1,13**
	R_B=	144,00

For q			
q	**l**	**z**	**M**
R_A		10	$R_A\cdot x$
9	3	8	216
2,5	3	5	37,5
2,5	3	2	15
		∑M	268,5
		R_A	26,85
		GDF_q=	**0,99**
		R_B=	15,15

Total actions on half of the cross section for traffic loads in the length direction

$Q=2*GDF_Q*R_A$=	**694**	kN
$q=GDF_q*R_A$=	**27**	kN/m

Relevant distances for cross-section calculations of the arch

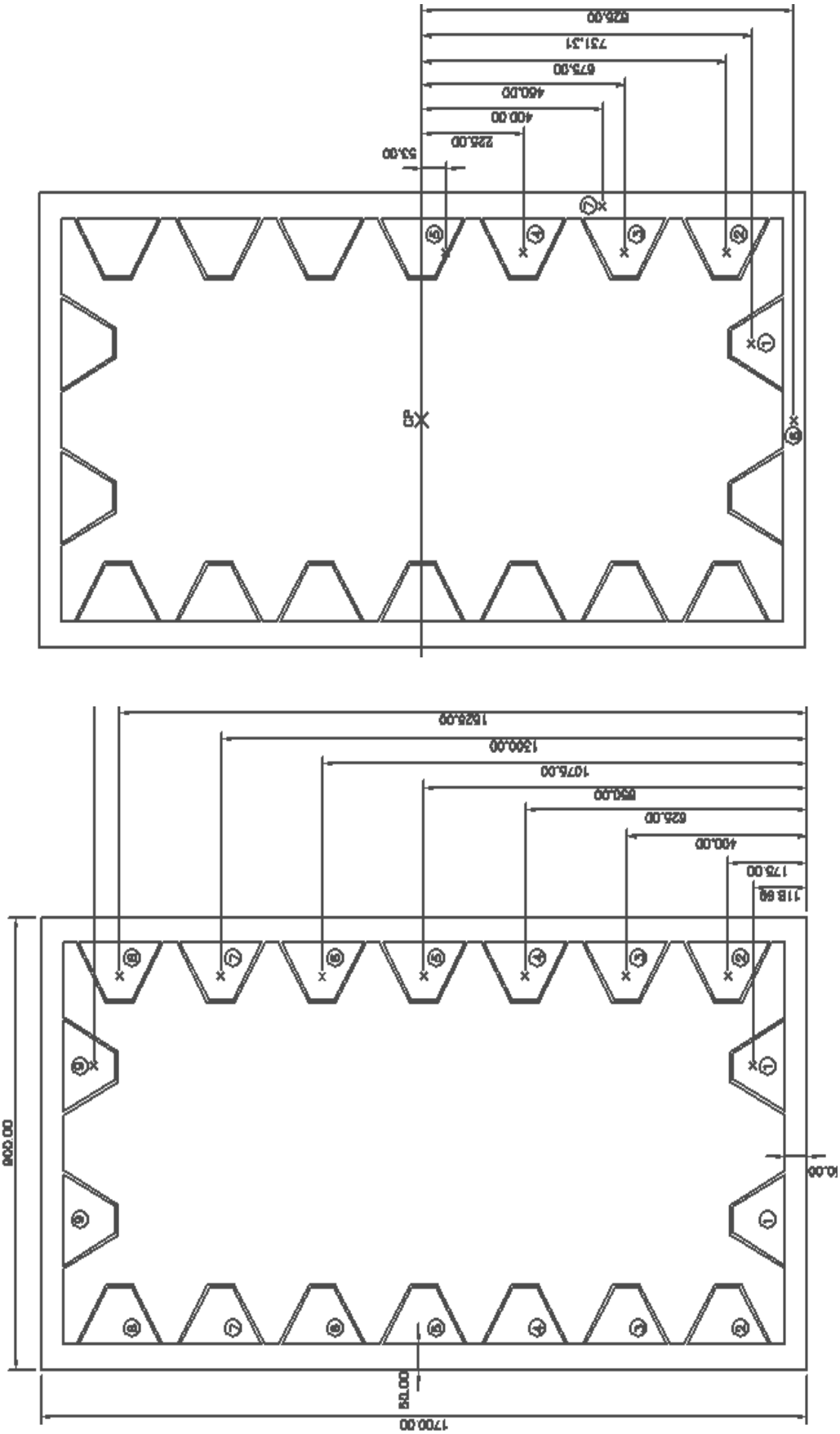

Stiffeners

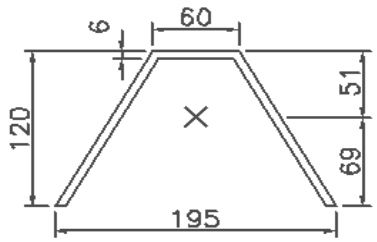

A	1949,8	mm^2
I_x	2,80E+06	mm^4
I_y	6,70E+06	mm^4

Calculations for Area, Moment of Inertia and Section Modulus For the Stronger Axis

Part	**b**	**h**	**t**	**A**	**y_0**	**$S=Ay_0$**	**$y-y_0$**	**I_0**	**$A(y-y_0)^2$**	**I_x**
nr.	mm	mm	mm	mm^2	mm	mm^3	mm	mm^4	mm^4	mm^4
Box Section	900	1700	50	250.000	850,00	2,13E+08	0,0	9,54E+10	0,00E+00	9,54E+10
Stiffeners Nr. 1	-	-	-	3.900	118,69	4,63E+05	731,3	5,60E+06	2,09E+09	2,09E+09
Stiffeners Nr. 2	-	-	-	3.900	175,00	6,82E+05	675,0	1,34E+07	1,78E+09	1,79E+09
Stiffeners Nr. 3	-	-	-	3.900	400,00	1,56E+06	450,0	1,34E+07	7,90E+08	8,03E+08
Stiffeners Nr. 4	-	-	-	3.900	625,00	2,44E+06	225,0	1,34E+07	1,97E+08	2,11E+08
Stiffeners Nr. 5	-	-	-	3.900	850,00	3,31E+06	0,0	1,34E+07	0,00E+00	1,34E+07
Stiffeners Nr. 6	-	-	-	3.900	1075,00	4,19E+06	-225,0	1,34E+07	1,97E+08	2,11E+08
Stiffeners Nr. 7	-	-	-	3.900	1300,00	5,07E+06	-450,0	1,34E+07	7,90E+08	8,03E+08
Stiffeners Nr. 8	-	-	-	3.900	1525,00	5,95E+06	-675,0	1,34E+07	1,78E+09	1,79E+09
Stiffeners Nr. 9	-	-	-	3.900	1581,31	6,17E+06	-731,3	5,60E+06	2,09E+09	2,09E+09
$\sum$				**285.097**		**2,42E+08**				**1,05E+11**

y=	**850,0**	mm
h=	**1700**	mm
W_{el}=	**1,24E+08**	mm^3

Calculations of plastic section modulus of the section

Part	A	y	n	W_{xi}	Type
nr.	mm^2	mm		mm^3	
1	1949,8	731,31	4	5703690	Stiffener
2	1949,8	675,00	4	5264518	Stiffener
3	1949,8	450,00	4	3509679	Stiffener
4	1949,8	225	4	1754839	Stiffener
5	80000	53,00	4	1,7E+07	Stiffener
6	45000	825,00	2	7,4E+07	Flange
7	80000	400	4	1,3E+08	Web
		W_{xpl}=		**2,35E+08**	

ENV 1993-1-1

5.4.5 and 5.4.5.2 Bending Moment (page 65)

$$M_{Sd} \le M_{c.Rd}$$

M_{sd}= 15875 kNm

a) Design plastic resistance moment

$$M_{pl,Rd} = W_{pl} \cdot f_y / \gamma_{M0}$$

f_y= 355 MPa

γ_{M0}= 1,1

$M_{pl.Rd}$= 75984 kNm

5.4.4 Compression ((1) and (2)) (page 65)

$$N_{Sd} \le N_{c.Rd}$$

N_{Sd}= -10901 kN

a) Design plastic resistance compression

$$N_{pl.Rd} = A f_y / \gamma_{M0}$$

$N_{pl.Rd}$= 92009 kN

5.4.8.1 Bending and axial force

$$\frac{M_{Sd}}{M_{pl,Rd}} + \left[\frac{N_{Sd}}{N_{pl.Rd}}\right]^2 \le 1$$

@ center of arch: 0,22

@ 1/4 of arch: 0,21

	Design	Resistance	
Bending [kNm]	15875	75984	OK!
Compression [kN]	10901	92009	OK!
Combined	0,22	1,00	OK!

Main girders - Bridge type 2

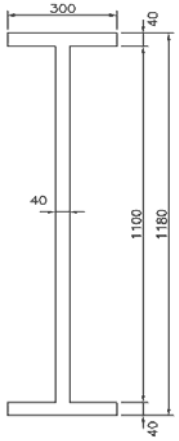

Part	b	h	A	y_0	$S=Ay_0$	$y-y_0$	I_0	$A(y-y_0)^2$	I_y
	[mm^2]	[mm^2]	[mm^2]	[mm]	[mm^2]	[mm]	[mm^4]	[mm^4]	[mm^4]
Top Flange	300	40	12000	1160	1,39E+07	-570	1,60E+06	3,90E+09	3,90E+09
Web	40	1100	44000	590	2,60E+07	0	4,44E+09	0,00E+00	4,44E+09
Bottom Flange	300	40	12000	20	2,40E+05	570	1,60E+06	3,90E+09	3,90E+09
∑			**68000**		4,01E+07				**1,22E+10**

y= **590** [mm]
h= **1180** [mm]
W_{el}= **2,07E+07** [mm^3]

Part	y	A	W_{pl}
	[mm]	[mm^2]	[mm^3]
Top Flange	570	12000	6,84E+06
Web 1	275	22000	6,05E+06
Web 2	275	22000	6,05E+06
Bottom Flange	570	12000	6,84E+06
∑	**W_{pl}=**		**2,58E+07**

Shear area: $A_v=\Sigma(dt_w)$= 44000 mm^2

Cross Section Class, table 5.3.1 in EC3

	ε	0,81	
Flange	d	1100	
	t_w	40	
	α	0,5	
	d/t_w	27,5	
	Class	**Class 1**	→d/tw ≤ 33ε
Web	c	150	
	t_f	40	
	c/tf	3,75	
	Class	**Class 1**	→c/tf ≤ 9ε

5.4 Restistance of cross-sections in EC3

γ_{M0}= 1,1 f_y= 355 MPa

$$M_{Sd} \le M_{c.Rd}$$

$$V_{Sd} \le V_{pl.Rd}$$

Where

$$V_{Sd} \le V_{pl.Rd} = A_v(f_y/\sqrt{3})/\gamma_{M0}$$

Design values:

$M_{Sd,max}$= -7241 kNm
$V_{Sd,max}$= 2087 kN

Resistance:

Moment	8320	kNm	OK!
Shear	8198	kN	OK!
Combined	No reduction needed!		

Provided that the design value of the shear force V_{sd} does not exceed 50% of the design plastic shear resistance $V_{pl.Rd}$ no reduction need be made

Cross-beams - Bridge type 2

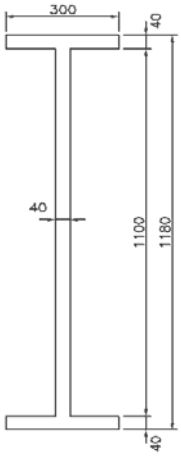

Part	b	h	A	y_0	$S=Ay_0$	$y-y_0$	I_0	$A(y-y_0)^2$	I_y
	[mm^2]	[mm^2]	[mm^2]	[mm]	[mm^2]	[mm]	[mm^4]	[mm^4]	[mm^4]
Top Flange	200	30	6000	845	5,07E+06	-415	4,50E+05	1,03E+09	1,03E+09
Web	30	800	24000	430	1,03E+07	0	1,28E+09	0,00E+00	1,28E+09
Bottom Flange	200	30	6000	15	9,00E+04	415	4,50E+05	1,03E+09	1,03E+09
∑			**36000**		1,55E+07				**3,35E+09**

y= **430** [mm]
h= **860** [mm]
W_{el}= **7,79E+06** [mm^3]

Part	y	A	W_{pl}
	[mm]	[mm^2]	[mm^3]
Top Flange	415	6000	2,49E+06
Web 1	200	12000	2,40E+06
Web 2	200	12000	2,40E+06
Bottom Flange	415	6000	2,49E+06
∑	**W_{pl}=**		**9,78E+06**

Shear area: $A_v=\Sigma(dt_w)$= 24000 mm^2

Cross Section Class, table 5.3.1 in EC3

	ε	0,81
Flange	d	800
	t_w	30
	α	0,5
	d/t_w	26,67
	Class	**Class 1**
Web	c	100
	t_f	30
	c/tf	3,333
	Class	**Class 1**

5.4 Restistance of cross-sections in EC3

γ_{M0}= 1,1 f_y= 355 MPa

$$M_{Sd} \le M_{c.Rd}$$

$$V_{Sd} \le V_{pl.Rd}$$

Where

$$V_{Sd} \le V_{pl.Rd} = A_v(f_y/\sqrt{3})/\gamma_{M0}$$

Design values:

$M_{Sd,max}$= 3025 kNm

$V_{Sd,max}$= 1359 kN

Resistance:

Moment	3156	kNm	OK!
Shear	4472	kN	OK!
Combined	No reduction needed!		

Provided that the design value of the shear force V_{sd} does not exceed 50% of the design plastic shear resistance $V_{pl.Rd}$ no reduction need be made

CALCULATIONS OF GDF FOR BRIDGE TYPE 3

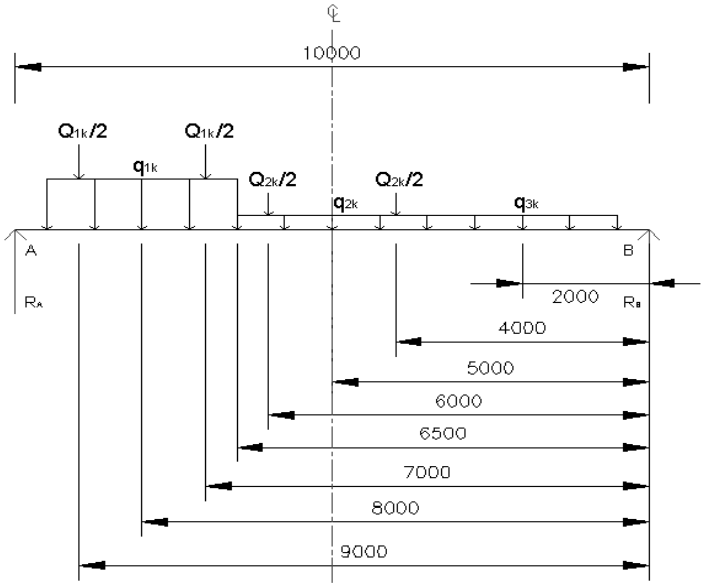

Q_{1k}=	300	α_{Q1}=	0,9	$\alpha_{Q1}\cdot Q_{1k}$=	270	kN
Q_{2k}=	200	α_{Q2}=	0,9	$\alpha_{Q2}\cdot Q_{2k}$=	180	kN
q_{1k}=	9	α_{q1}=	1	$\alpha_{q1}\cdot q_{1k}$=	9	kN/m^2
q_{2k}=	2,5	α_{q2}=	1	$\alpha_{q2}\cdot q_{2k}$=	2,5	kN/m^2
q_{3k}=	2,5	α_{q3}=	1	$\alpha_{q3}\cdot q_{3k}$=	2,5	kN/m^2

For Q		
F	**z**	**M**
R_A	10	$R_A\cdot x$
135	9	1215
135	7	945
90	6	540
90	4	360
	∑M=	3060
	R_A=	306,00
	GDF_Q=	**1,13**
	R_B=	144,00

For q			
q	**l**	**z**	**M**
R_A		10	$R_A\cdot x$
9	3	8	216
2,5	3	5	37,5
2,5	3	2	15
		∑M	268,5
		R_A	26,85
		GDF_q=	**0,99**
		R_B=	15,15

Total actions on half of the cross section for traffic loads in the length direction

$Q=2*GDF_Q*R_A$=	**694**	kN
$q=GDF_q*R_A$=	**27**	kN/m

Cross-beams - Bridge type 3

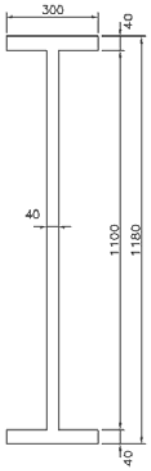

M_{max}

V_{max}

Part	b	h	A	y_0	$S=Ay_0$	$y-y_0$	I_0	$A(y-y_0)^2$	I_y
	[mm^2]	[mm^2]	[mm^2]	[mm]	[mm^2]	[mm]	[mm^4]	[mm^4]	[mm^4]
Top Flange	300	30	9000	845	7,61E+06	-415	6,75E+05	1,55E+09	1,55E+09
Web	30	800	24000	430	1,03E+07	0	1,28E+09	0,00E+00	1,28E+09
Bottom Flange	300	30	9000	15	1,35E+05	415	6,75E+05	1,55E+09	1,55E+09
∑			**42000**		1,81E+07				**4,38E+09**

y= **430** [mm]
h= **860** [mm]
W_{el}= **1,02E+07** [mm^3]

Part	y	A	W_{pl}
	[mm]	[mm^2]	[mm^3]
Top Flange	415	9000	3,74E+06
Web 1	200	12000	2,40E+06
Web 2	200	12000	2,40E+06
Bottom Flange	415	9000	3,74E+06
∑	**W_{pl}=**		**1,23E+07**

Shear area: $A_v=\Sigma(dt_w)$= 24000 mm^2

Cross Section Class

	ε	0,81	
Flange	d	800	
	t_w	30	
	α	0,5	
	d/t_w	26,67	
	Class	**Class 1**	→d/tw ≤ 33ε
Web	c	150	
	t_f	30	
	c/tf	5	
	Class	**Class 1**	→c/tf ≤ 9ε

5.4 Restistance of cross-sections in EC3

γ_{M0}= 1,1 f_y= 355 MPa

$$M_{Sd} \le M_{c.Rd}$$

$$V_{Sd} \le V_{pl.Rd}$$

Where

$$V_{Sd} \le V_{pl.Rd} = A_v(f_y/\sqrt{3})/\gamma_{M0}$$

Design values:

$M_{Sd,max}$= 3237 kNm
$V_{Sd,max}$= 672 kN

Resistance:

Moment	3960	kNm	OK!
Shear	4472	kN	OK!
Combined	No reduction needed!		

Provided that the design value of the shear force V_{sd} does not exceed 50% of the design plastic shear resistance $V_{pl.Rd}$ no reduction need be made

Main girder - Bridge type 3

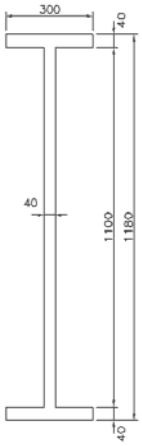

Part	b	h	A	y_0	$S=Ay_0$	$y-y_0$	I_0	$A(y-y_0)^2$	I_y
	[mm^2]	[mm^2]	[mm^2]	[mm]	[mm^2]	[mm]	[mm^4]	[mm^4]	[mm^4]
Top Flange	400	30	12000	1185	1,42E+07	-585	9,00E+05	4,11E+09	4,11E+09
Web	30	1140	34200	600	2,05E+07	0	3,70E+09	0,00E+00	3,70E+09
Bottom Flange	400	30	12000	15	1,80E+05	585	9,00E+05	4,11E+09	4,11E+09
∑			**58200**		3,49E+07				**1,19E+10**

y= **600** [mm]
h= **1200** [mm]
W_{el}= **1,99E+07** [mm^3]

Part	y	A	W_{pl}
	[mm]	[mm^2]	[mm^3]
Top Flange	585	12000	7,02E+06
Web 1	285	17100	4,87E+06
Web 2	285	17100	4,87E+06
Bottom Flange	585	12000	7,02E+06
∑	**W_{pl}=**		**2,38E+07**

Shear area: $A_v=\Sigma(dt_w)$= 34200 mm^2

Cross Section Class

	ε	0,81	
Flange	d	1140	
	t_w	30	
	α	0,5	
	d/t_w	38	
	Class	**Class 1**	→d/tw ≤ 33ε
Web	c	200	
	t_f	30	
	c/tf	6,67	
	Class	**Class 1**	→c/tf ≤ 9ε

5.4 Restistance of cross-sections in EC3

γ_{M0}= 1,1 f_y= 355 MPa

$$M_{Sd} \le M_{c.Rd}$$

$$V_{Sd} \le V_{pl.Rd}$$

Where

$$V_{Sd} \le V_{pl.Rd} = A_v(f_y/\sqrt{3})/\gamma_{M0}$$

Design values:

$M_{Sd,max}$= 7311 kNm

$V_{Sd,max}$= 1247 kN

Resistance

Moment	7677	kNm	OK!
Shear	6372	kN	OK!
Combined	No reduction needed!		

Provided that the design value of the shear force V_{sd} does not exceed 50% of the design plastic shear resistance $V_{pl.Rd}$ no reduction need be made

Column

	t_x	L	l	t_y	B	b
mm	300	1500	900	300	2300	1700

A 1920000 mm^2

Reinforcement

		Outside Bars				Inside Bars			
	Cover	x (Pcs.)	Sox	y (Pcs.)	Soy	x (Pcs.)	Sox	y (Pcs.)	Soy
mm	50	18	80,9	26	80,6	13	85,4	21	83,0

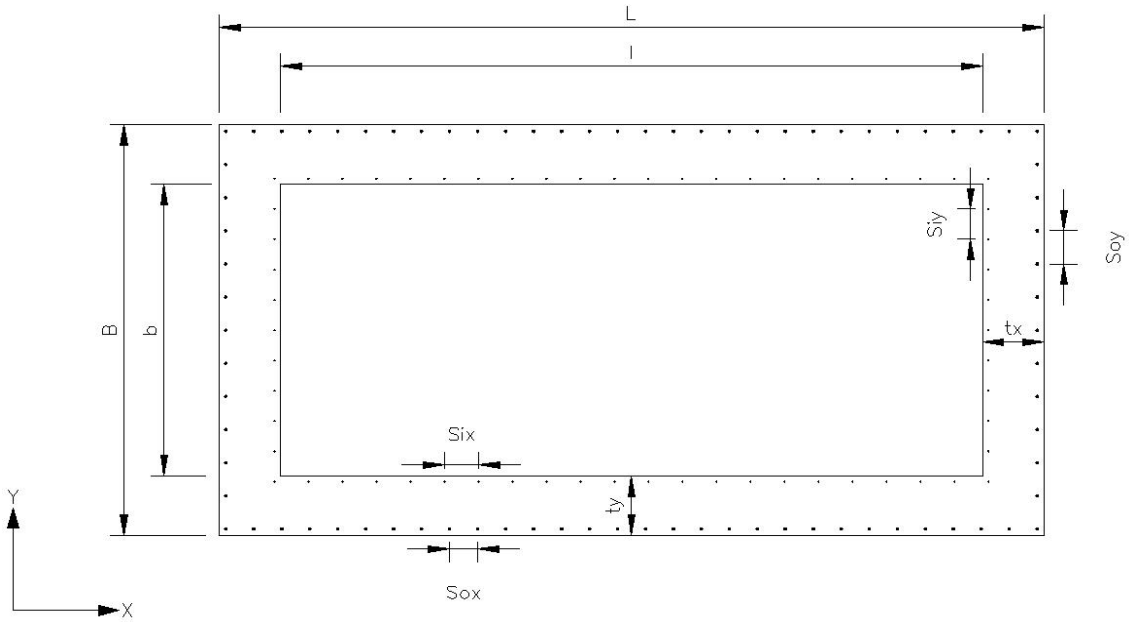

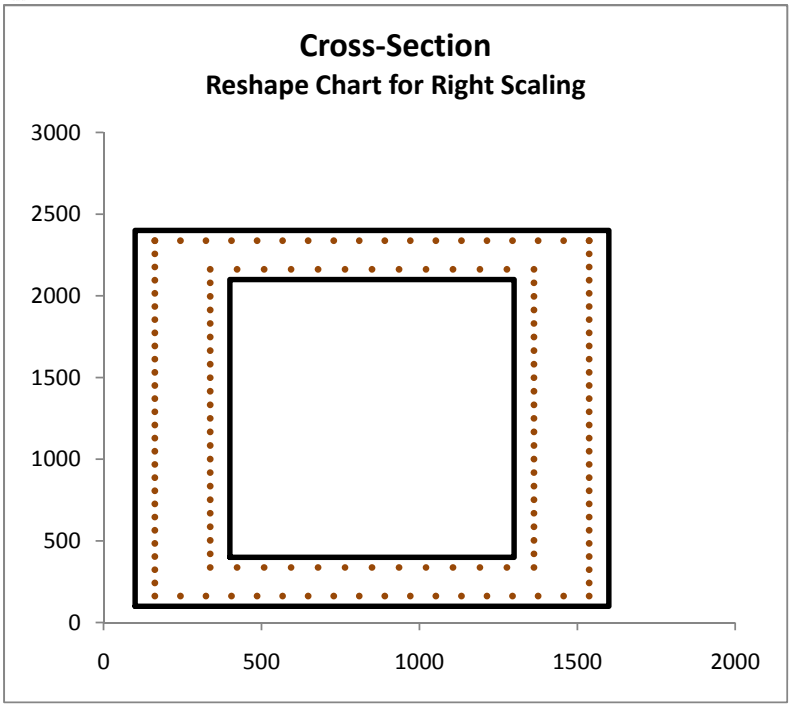

Materials

Safety Class	3	⇒	γ_n	1,2			
Concrete	C40/50						

Outside Bars	1	⌀	25	⇒	A_{slo}	490,9	mm^2/Bar
Inside Bars	1	⌀	25	⇒	A_{slo}	490,9	mm^2/Bar
Stirrups	2	⌀	10	⇒	A_{sv}	78,5	mm^2/Bar
Creep, RH %	95	φ	1				

Reinforcement	**#**
Ks40	**1**
Ks60	**2**
Ss260S	**3**
B500B	**4**
Ks600S	**5**
Ns500	**6**
Nps500	**7**

Creep, RH %	
Innomhus i uppvärmde lokaler	**55**
Normalt utomhus samt inomhus i icke uppvärmde lokaler	**75**
Mycket fuktig miljö	**⩾ 95**

Concrete	f_{cck}	f_{cc}	f_{ctk}	f_{ct}	E_{ck}	E_c	$E_{c,eff}$	ε_{cu}
	MPa	MPa	MPa	MPa	MPa	MPa	MPa	-
	38	19,8	2,4	1,33	35.000	24.306	12.153	0,0035

Rebars	f_{yk}	f_{st}	E_{sk}	E_s	ε_{sy}
	MPa	MPa	MPa	MPa	-
Outside Bars	500	435	200.000	200.000	0,00217
Inside Bars	500	435	200.000	200.000	0,00217
Stirrups	500	435	200.000	200.000	0,00217

Load

N_{Sd}= 5121 kN

M_{Sd}= 27292 kNm

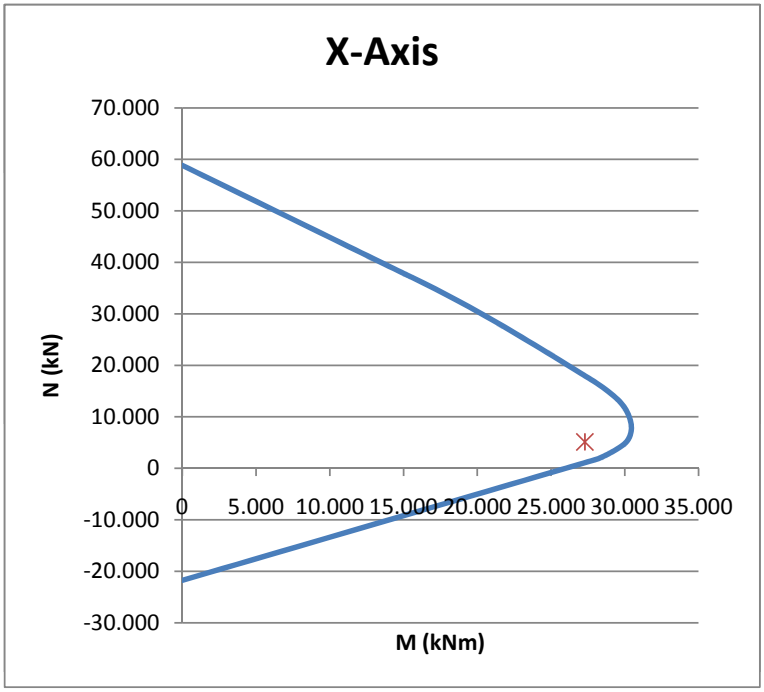

Appendix B

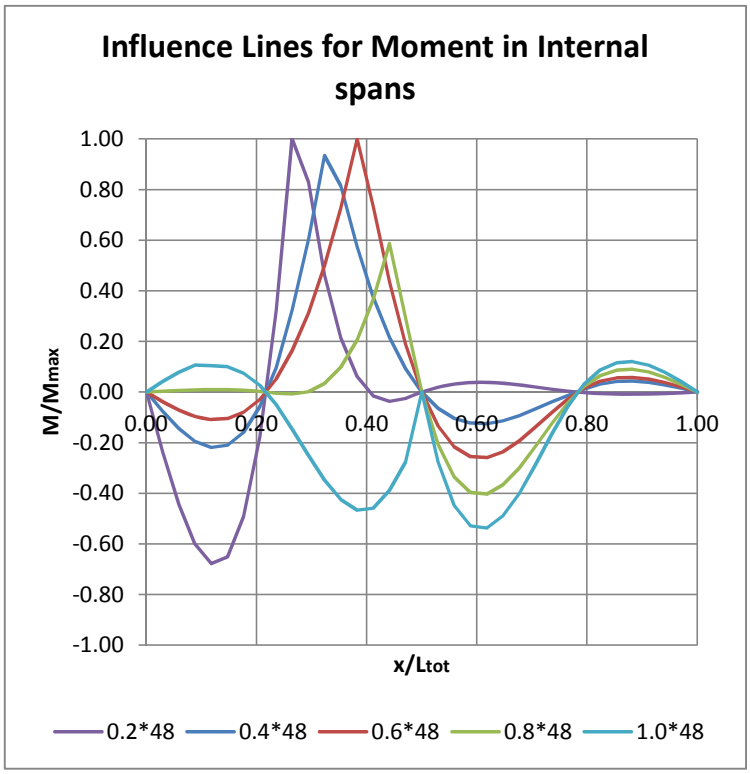
Influence Lines for Moment in Internal spans
1.00
0.80
0.60
0.40
0.20
0.00
-0.20
-0.40
-0.60
-0.80
-1.00
0.00
0.20
0.40
0.60
0.80
1.00
M/Mmax
x/Ltot
0.2*48
0.4*48
0.6*48
0.8*48
1.0*48

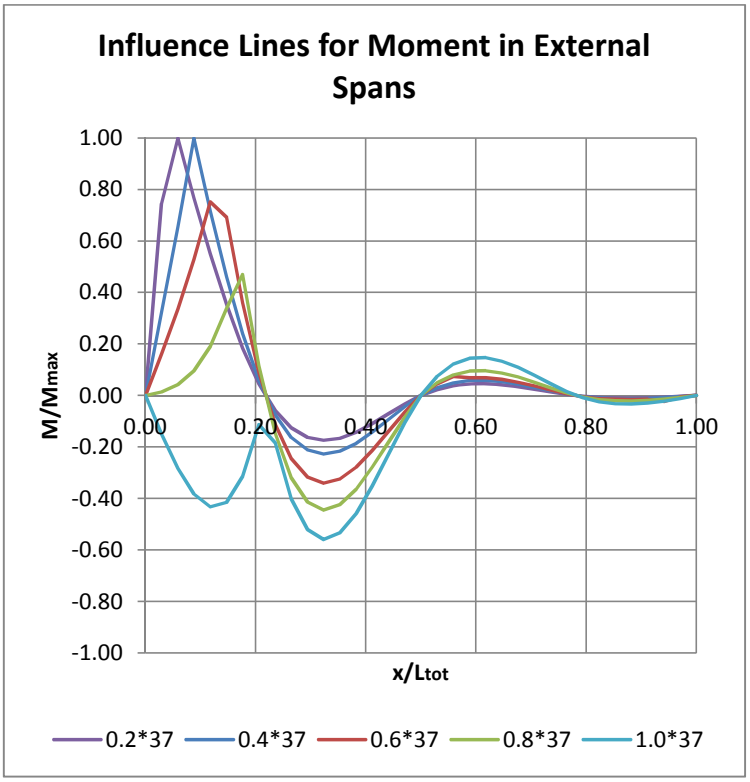
Influence Lines for Moment in External Spans
1.00
0.80
0.60
0.40
0.20
0.00
-0.20
-0.40
-0.60
-0.80
-1.00
0.00
0.20
0.40
0.60
0.80
1.00
M/Mmax
x/Ltot
0.2*37
0.4*37
0.6*37
0.8*37
1.0*37

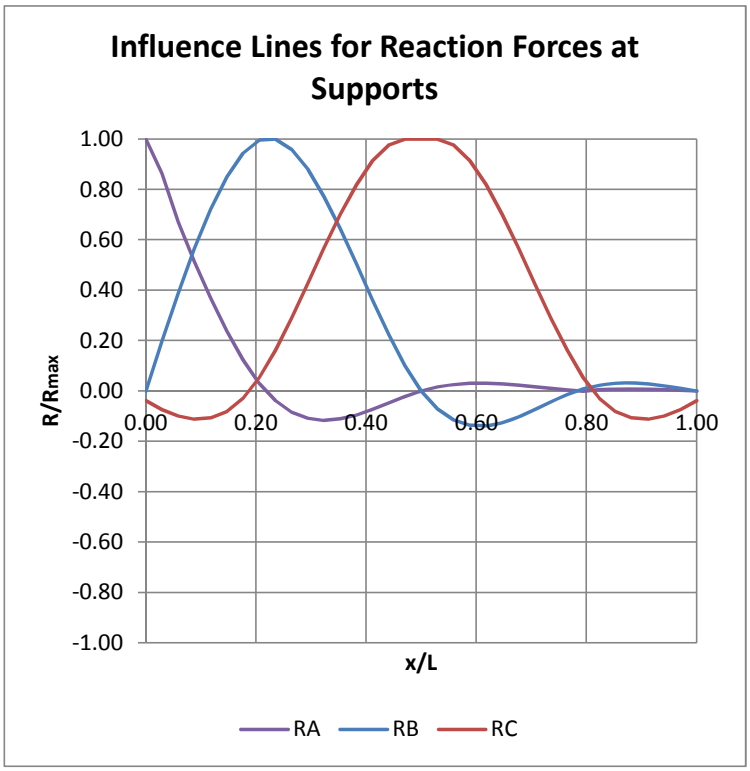
Influence Lines for Reaction Forces at Supports
1.00
0.80
0.60
0.40
0.20
0.00
-0.20
-0.40
-0.60
-0.80
-1.00
R/Rmax
0.00
0.20
0.40
0.60
0.80
1.00
x/L
RA
RB
RC

Half cross section, in the middle of the span									
Part	b	h	A	y_0	$S=Ay_0$	$y-y_0$	I_0	$A(y-y_0)^2$	I_x
nr.	mm	mm	mm^2	mm	mm^3	mm	mm^4	mm^4	mm^4
1	5000	250	1250000	1925	2406250000	-628.3	6.51E+09	4.935E+11	5.00E+11
2	1100	1800	1980000	900	1782000000	396.7	5.346E+11	3.1155E+11	8.46E+11
∑			3230000		4.19E+09				1.35E+12

y= 1296.672 mm W_{top}= 1.79E+09 mm^3

h= 2050 mm W_{bottom}= 1.04E+09 mm^3

Half cross section, over a support									
Part	b	h	A	y_0	$S=Ay_0$	$y-y_0$	I_0	$A(y-y_0)^2$	I_x
nr.	mm	mm	mm^2	mm	mm^3	mm	mm^4	mm^4	mm^4
1	5000	250	1250000	1925	2406250000	-685.1	6.51E+09	5.8678E+11	5.93E+11
2	1400	1800	2520000	900	2268000000	339.9	6.804E+11	2.9106E+11	9.71E+11
∑			3770000		4.67E+09				1.56E+12

y= 1239.854 mm W_{top}= 1.93E+09 mm^3

h= 2050 mm W_{bottom}= 1.26E+09 mm^3

CALCULATIONS FOR FEASIBLE ZONE OF THE PRESTRESS FORCE

AT TRANSFER - for one girder (half cross section)												
SPAN 1			**SUPPORT B**			**SPAN 2**			**SUPPORT C**			
Compression in top fibre			Compression in bottom fibre			Compression in top fibre			Compression in bottom fibre			
M_0=	7.46E+09	Nmm	M_0=	-1.46E+10	Nmm	M_0=	7.97E+09	Nmm	M_0=	-1.59E+10	Nmm	
W_t=	1.79E+09	mm^3	W_b=	-1.26E+09	mm^3	W_t=	1.79E+09	mm^3	W_b=	-1.26E+09	mm^3	
Tension in the bottom fibre			Tension in the top fibre			Tension in the bottom fibre			Tension in the top fibre			
W_b=	-1.04E+09	mm^3	W_t=	1.93E+09	mm^3	W_b=	-1.04E+09	mm^3	W_t=	1.93E+09	mm^3	

AT SERVICE - for one girder (half cross section)												
SPAN 1			**SUPPORT B**			**SPAN 2**			**SUPPORT C**			
Compression in top fibre			Compression in bottom fibre			Compression in top fibre			Compression in bottom fibre			
M_s=	2.10E+10	Nmm	M_s=	-2.89E+10	Nmm	M_s=	2.21E+10	Nmm	M_s=	-3.10E+10	Nmm	
W_t=	1.79E+09	mm^3	W_b=	-1.26E+09	mm^3	W_t=	1.79E+09	mm^3	W_b=	-1.26E+09	mm^3	
Tension in the bottom fibre			Tension in the top fibre			Tension in the bottom fibre			Tension in the top fibre			
W_b=	-1.04E+09	mm^3	W_t=	1.93E+09	mm^3	W_b=	-1.04E+09	mm^3	W_t=	1.93E+09	mm^3	

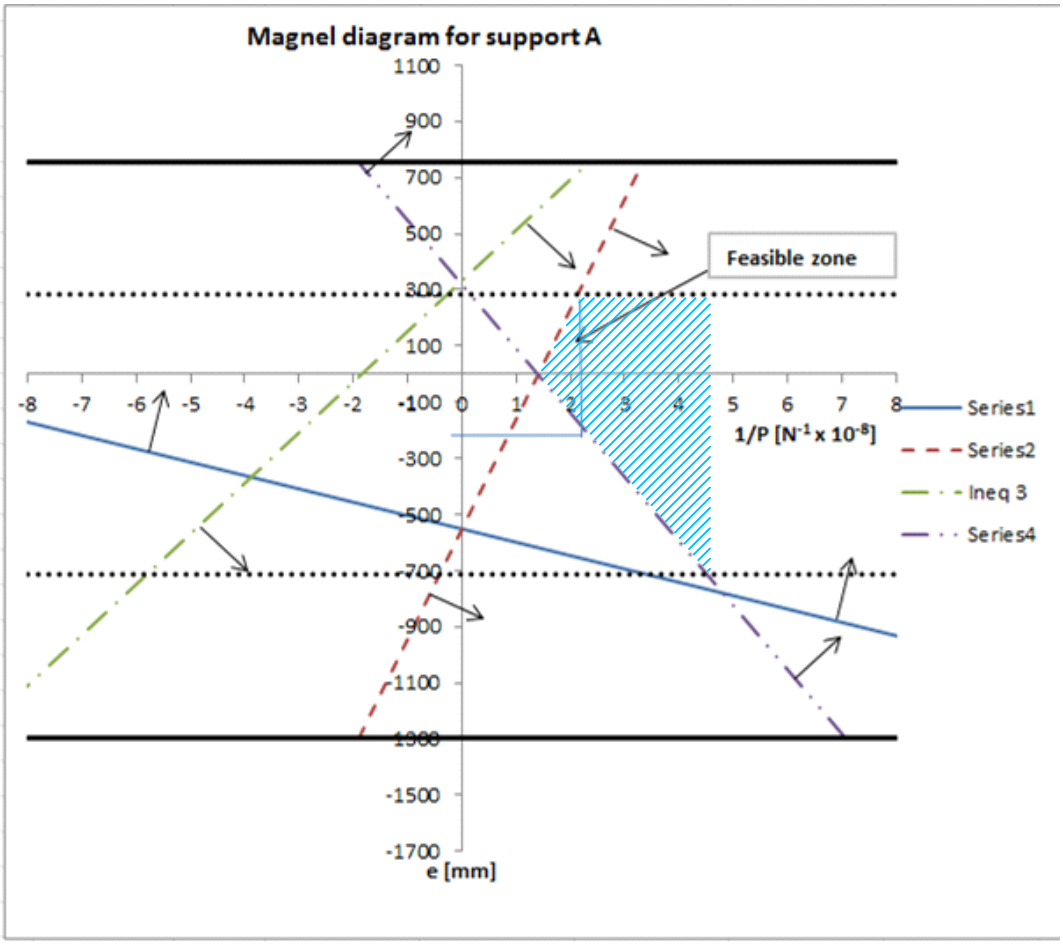
Magnel diagram for support A
Feasible zone
1/P [N-1 x 10-8]
e [mm]
Series1
Series2
Ineq 3
Series4

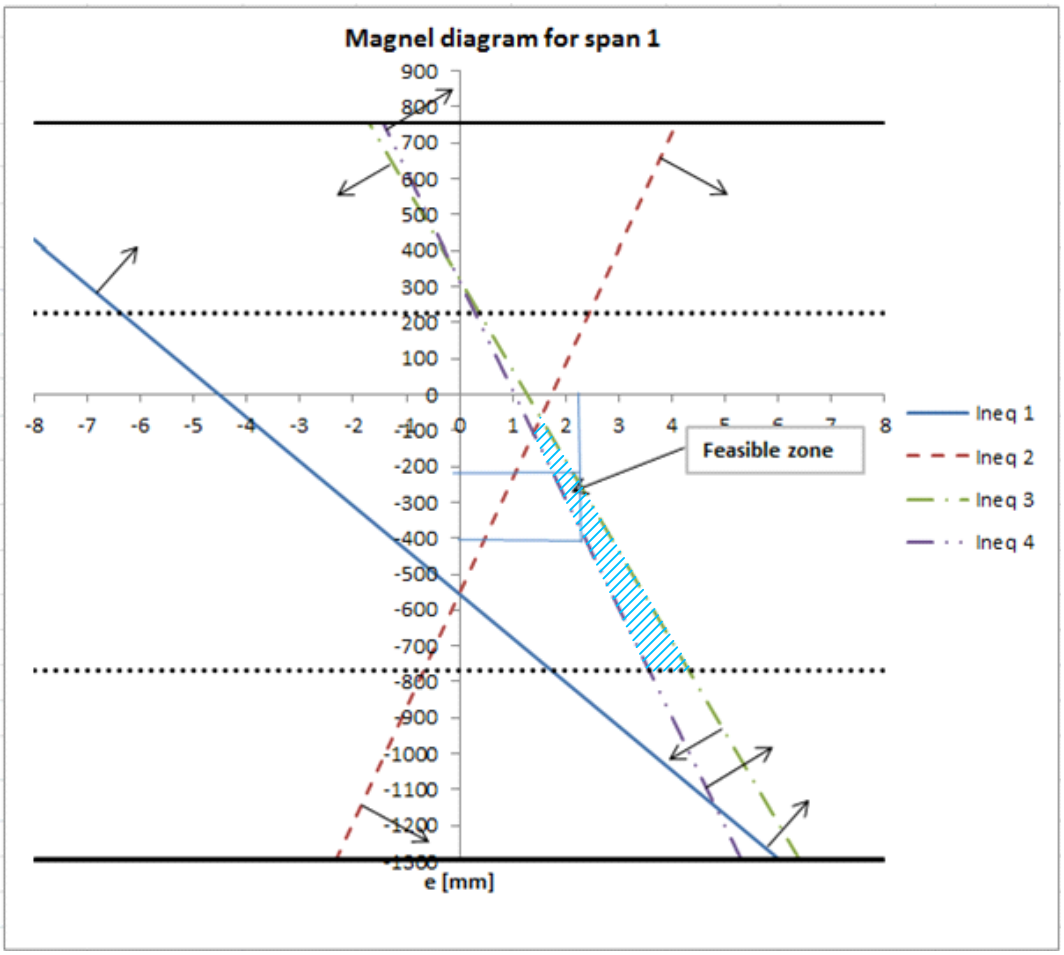
Magnel diagram for span 1
Feasible zone
e [mm]
Ineq 1
Ineq 2
Ineq 3
Ineq 4

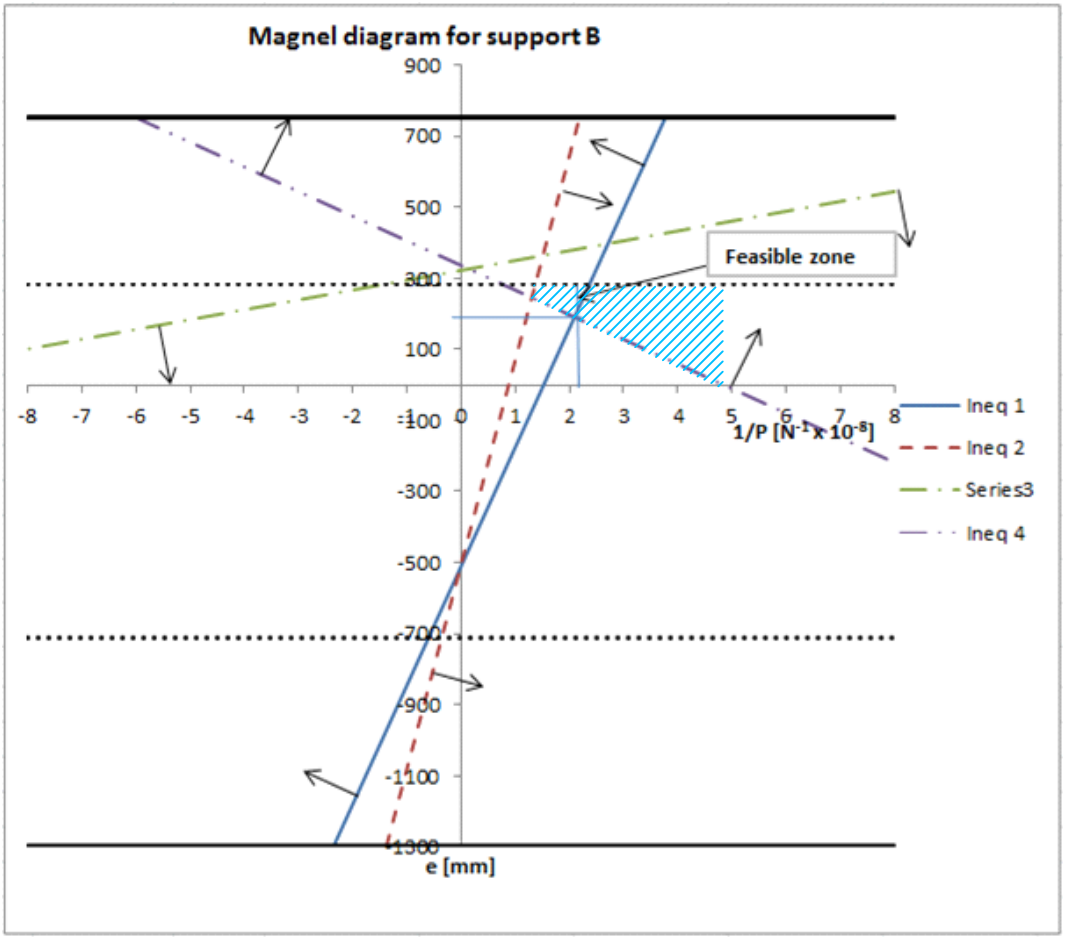
Magnel diagram for support B
900
700
500
300
100
-100
-300
-500
-700
-900
-1100
-1300
-8 -7 -6 -5 -4 -3 -2 -1 0 1 2 3 4 5 6 7 8
1/P [N-1 x 10-8]
e [mm]
Feasible zone
Ineq 1
Ineq 2
Series3
Ineq 4

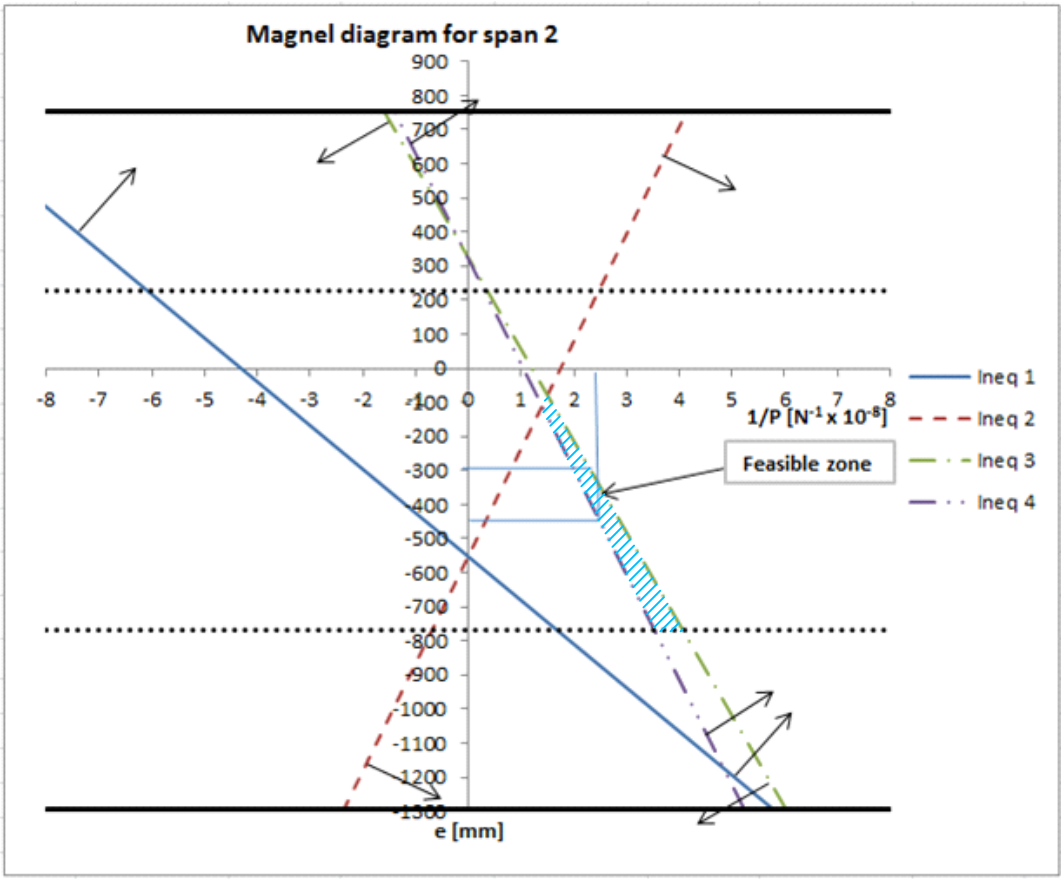
Magnel diagram for span 2
900
800
700
600
500
400
300
200
100
0
-100
-200
-300
-400
-500
-600
-700
-800
-900
-1000
-1100
-1200
-1300
-8 -7 -6 -5 -4 -3 -2 -1 0 1 2 3 4 5 6 7 8
1/P [N-1 x 10-8]
e [mm]
Feasible zone
Ineq 1
Ineq 2
Ineq 3
Ineq 4

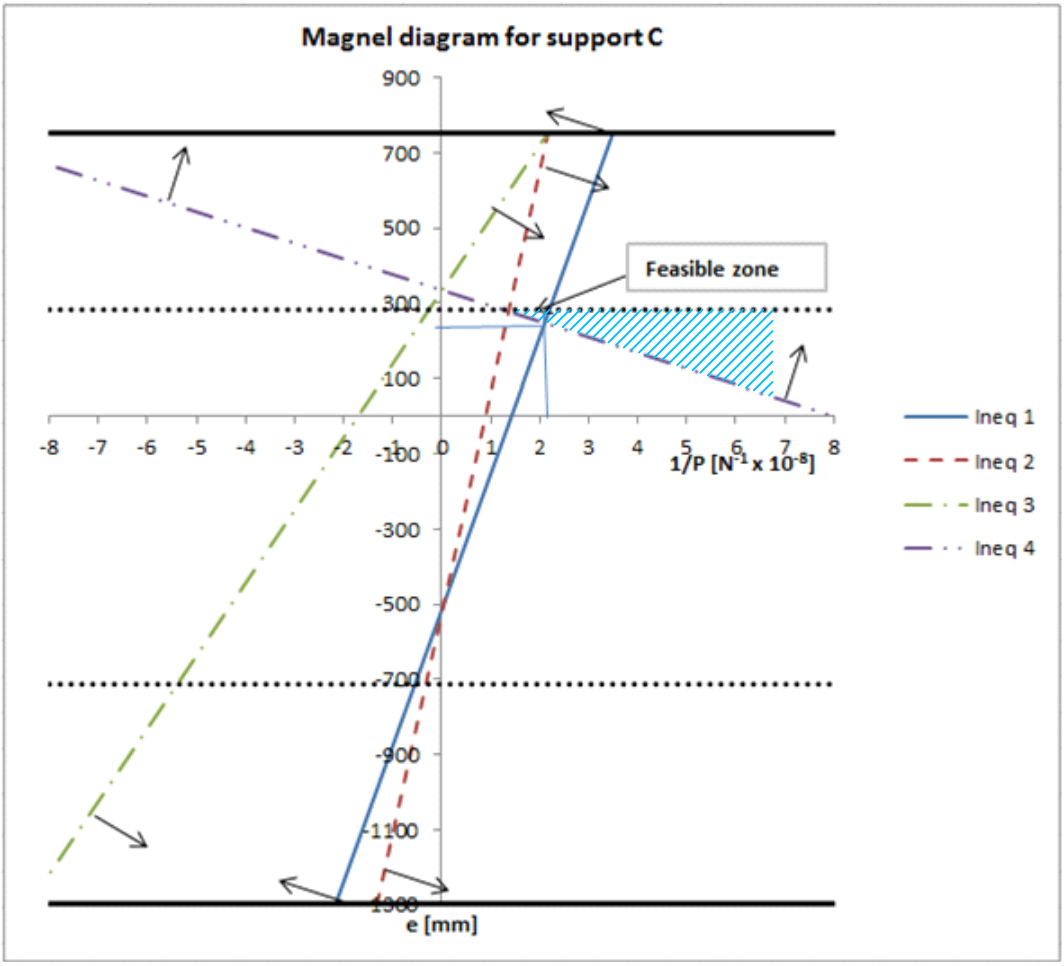
Magnel diagram for support C
900
700
500
300
100
-100
-300
-500
-700
-900
-1100
-1300
-8 -7 -6 -5 -4 -3 -2 -1 0 1 2 3 4 5 6 7 8
1/P [N-1 x 10-8]
e [mm]
Feasible zone
Ineq 1
Ineq 2
Ineq 3
Ineq 4

Calculations of secondary moment with the three-moment equation

$w_1 := -99.023 \frac{kN}{m}$ $w_2 := -79.685 \frac{kN}{m}$

Span lengths:

$L_1 := 37m$ $L_2 := 48m$

$L_4 := L_1$ $L_3 := L_2$

$M_A := 0kN \cdot m$ $M_E := 0kN \cdot m$

$M_B := 1kN \cdot m$

$M_C := 1kN \cdot m$

$M_D := 1kN \cdot m$

$EI\theta_1 := \frac{w_1 \cdot L_1^{3}}{24}$ $EI\theta_2 := \frac{w_2 \cdot L_2^{3}}{24}$

$EI\theta_4 := EI\theta_1$ $EI\theta_3 := EI\theta_2$

Given

$M_A \cdot L_1 + 2 \cdot M_B \cdot (L_1 + L_2) + M_C \cdot L_2 = -6 \cdot (EI\theta_1 + EI\theta_2)$

$M_B \cdot L_2 + 2 \cdot M_C \cdot (L_2 + L_3) + M_D \cdot L_3 = -6 \cdot (EI\theta_2 + EI\theta_3)$

$M_C \cdot L_3 + 2 \cdot M_D \cdot (L_3 + L_4) + M_E \cdot L_4 = -6 \cdot (EI\theta_3 + EI\theta_4)$

Thus, solving these equations, the total moment, with primary and secondary effects, are:

$$\begin{pmatrix} M_B \\ M_C \\ M_D \end{pmatrix} := \text{Find}(M_B, M_C, M_D) = \begin{pmatrix} 16134 \\ 14882 \\ 16134 \end{pmatrix} \cdot kN \cdot m$$

Secondary moment from prestress

Prestress forces at service and eccentrities at corresponding positions after losses:

$P_{supportA} := 35890kN$ $e_A := 0mm$ $M_{primaryA} := P_{supportA} \cdot e_A = 0 \cdot kN \cdot m$

$P_{span1} := 36875kN$ $e_1 := -410mm$ $M_{primaryspan1} := P_{span1} \cdot e_1 = -15119 \cdot kN \cdot m$

$P_{supportB} := 37441kN$ $e_B := 283.6mm$ $M_{primaryB} := P_{supportB} \cdot e_B = 10618 \cdot kN \cdot m$

$P_{span2} := 35482kN$ $e_2 := -420mm$ $M_{primaryspan2} := P_{span2} \cdot e_2 = -14902 \cdot kN \cdot m$

$P_{supportC} := 34795kN$ $e_C := 283.6mm$ $M_{primaryC} := P_{supportC} \cdot e_C = 9868 \cdot kN \cdot m$

Hence the secondary moments become:

$M_{secondaryA} := 0kN \cdot m$

$M_{secondaryB} := M_B - M_{primaryB} = 5515 \cdot kN \cdot m$

$M_{secondaryspan1} := \frac{13875}{37000} \cdot M_{secondaryB} = 2068 \cdot kN \cdot m$

$M_{secondaryC} := M_C - M_{primaryC} = 5015 \cdot kN \cdot m$

$M_{secondaryspan2} := M_{secondaryB} + \frac{M_{secondaryC} - M_{secondaryB}}{2} = 5265 \cdot kN \cdot m$

Total bending from prestress:

$M_{pA} := M_{secondaryA} + M_{primaryA} = 0 \cdot kN \cdot m$

$M_{p1} := M_{secondaryspan1} + M_{primaryspan1} = -13050 \cdot kN \cdot m$

$M_{pB} := M_{secondaryB} + M_{primaryB} = 16134 \cdot kN \cdot m$

$M_{p2} := M_{secondaryspan2} + M_{primaryspan2} = -9637 \cdot kN \cdot m$

$M_{pC} := M_{secondaryC} + M_{primaryC} = 14882 \cdot kN \cdot m$

Calculations of ultimate moment capacity

$A_{p1} := 4200mm^2$ $E_p := 195000MPa$

$A_p := 8 \cdot A_{p1}$ $E_c := 36000MPa$

$I_{gsupport} := 1.5648 \cdot 10^{12} mm^4$ $A_{gsupport} := 3770000mm^2$

$I_{gspan} := 1.3462 \cdot 10^{12} mm^4$ $A_{gspan} := 3230000mm^2$

Bending from self-weight and traffic loads in ULS:

$M_{supportA1} := 0kN \cdot m$

$M_{span11} := 30314kN \cdot m$

$M_{supportB1} := -40838kN \cdot m$

$M_{span21} := 31954kN \cdot m$

$M_{supportC1} := -43737kN \cdot m$

Bending in ULS with prestress:

$M_{A.ULS} := M_{supportA1} + M_A = 0 \cdot kN \cdot m$

$M_{1.ULS} := M_{span11} + M_{secondaryspan1} + M_{primaryspan1} = 17264 \cdot kN \cdot m$

$M_{B.ULS} := M_{supportB1} + M_{secondaryB} + M_{primaryB} = -24704 \cdot kN \cdot m$

$M_{2.ULS} := M_{span21} + M_{secondaryspan2} + M_{primaryspan2} = 22317 \cdot kN \cdot m$

$M_{C.ULS} := M_{supportC1} + M_{secondaryC} + M_{primaryC} = -28855 \cdot kN \cdot m$

Effective depth, d:

$d_1 := 1163.3mm$

$d_B := 1523.5mm$

$d_2 := 1173.3mm$

$d_C := 1523.5mm$

$f_{ck} := 45MPa$

$\gamma_c := 1.5$

$\alpha := 1$

Width of the girder:

$b_{span} := 1100mm$

$b_{support} := 1400mm$

Allowable yield strength of the steel (figure 3.10 in EC2):

$f_{pk} := 1860MPa$ $f_{p0.1k} := 1640MPa$

$\gamma_p := 1.15$

$f_{pd} := \frac{f_{p0.1k}}{\gamma_p} = 1426 \cdot MPa$ $\frac{f_{pd}}{E_p} = 0.007313$

$\varepsilon_{ud} := 0.02$ Strain limit recommended by EC2.

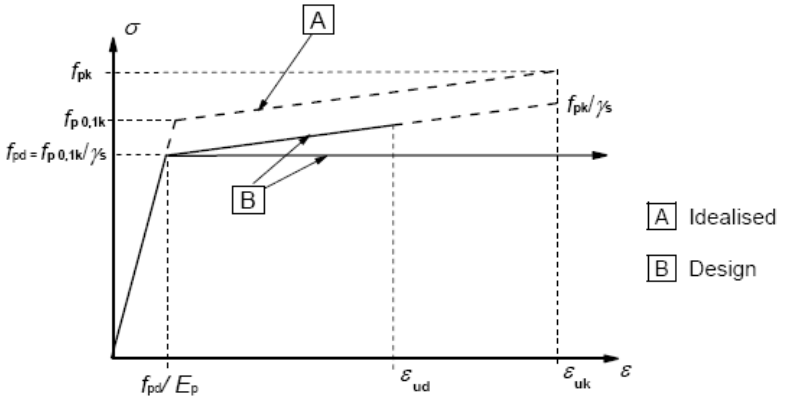

Figure 3.10: Idealised and design stress-strain diagrams for prestressing steel (absolute values are shown for tensile stress and strain)

Ultimate moment capacity at span 1:

Ultimate compressive strain in concrete:

$$\varepsilon_{ult} := 0.0035$$

Concrete strain due to prestress at the level of the tendon:

$$\varepsilon_{ce.1} := \frac{1}{E_c}\cdot\left(\frac{P_{span1}}{A_{gspan}} + \frac{M_{p1}\cdot e_1}{I_{gspan}}\right) = 0.000428$$

Total ultimate strain in concrete at the level of the tendons:

$$\varepsilon_{ct.1} = \frac{-\varepsilon_{ult}\cdot\left(d_1 - x_1\right)}{x_1}$$

Tendon strain:

$$\varepsilon_{pu.1} = \frac{-P_{span1}}{A_p\cdot E_p} + \varepsilon_{ct.1} - \varepsilon_{ce.1}$$

Concrete compressive force:

$$F_{c.1} = 0.8\cdot x_1\cdot b_{span}\cdot\frac{\alpha\cdot f_{ck}}{\gamma_c}$$

Total force in tendon:

$$F_{p.1} = A_p\cdot\left(E_p\cdot\varepsilon_{pu.1}\right)$$

Equilibrium of forces:

$$F_{p.1} + F_{c.1} = 0$$

Which leads to:

$$x_1 := 1\text{mm}$$

Given

$$A_p\cdot\left[E_p\cdot\left[\frac{-P_{span1}}{A_p\cdot E_p} + \frac{-\varepsilon_{ult}\cdot\left(d_1 - x_1\right)}{x_1} - \varepsilon_{ce.1}\right]\right] + 0.8\cdot b_{span}\cdot x_1\cdot\frac{\alpha\cdot f_{ck}}{\gamma_c} = 0$$

$$x_1 := \text{Find}\left(x_1\right) = 1.371\,\text{m}$$

Check if steel stress is ok:

$$\varepsilon_{ct.1} := \frac{-\varepsilon_{ult}\cdot\left(d_1 - x_1\right)}{x_1} = 0.000531$$

$$\varepsilon_{pu.1} := \frac{-P_{span1}}{A_p\cdot E_p} + \varepsilon_{ct.1} - \varepsilon_{ce.1} = -0.005525$$ Less than f_{pd}/E_p=0.007313

Ultimate moment capacity:

$z_1 := \left(d_1 - 0.4 \cdot x_1\right) = 0.615 \cdot m$

$F_{c1} := 0.8 \cdot b_{span} \cdot x_1 \cdot \frac{\alpha \cdot f_{ck}}{\gamma_c} = 36199 \cdot kN$

$M_{ult1} := F_{c1} \cdot z_1 = 22256 \cdot kN \cdot m$

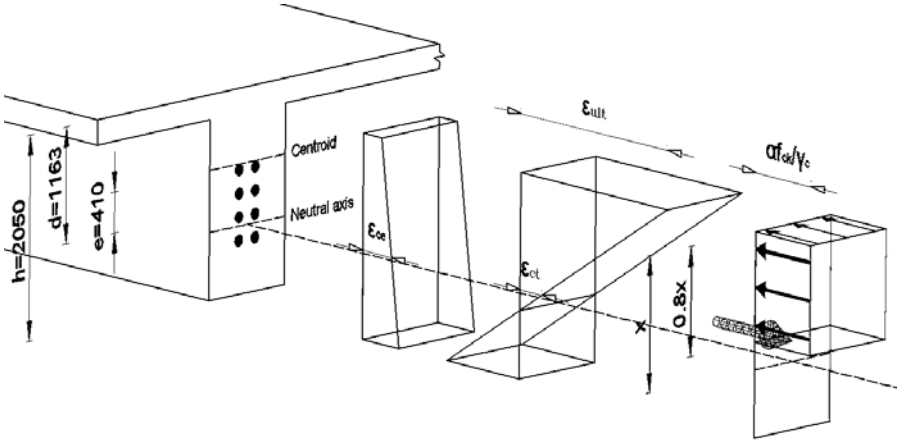

Ultimate moment capacity at support B:

Ultimate compressive strain in concrete:

$$\varepsilon_{ult} = 0.0035$$

Concrete strain due to prestress at the level of the tendon:

$$\varepsilon_{ce.B} := \frac{1}{E_c}\cdot\left(\frac{P_{supportB}}{A_{gsupport}} + \frac{M_{pB}\cdot e_B}{I_{gsupport}}\right) = 0.000357$$

Total ultimate strain in concrete at the level of the tendons:

$$\varepsilon_{ct.B} = \frac{-\varepsilon_{ult}\cdot\left(d_B - x_B\right)}{x_B}$$

Tendon strain:

$$\varepsilon_{pu.B} = \frac{-P_{supportB}}{A_p\cdot E_p} + \varepsilon_{ct.B} - \varepsilon_{ce.B}$$

Concrete compressive force:

$$F_{c.B} = 0.8\cdot x_B\cdot b_{support}\cdot\frac{\alpha\cdot f_{ck}}{\gamma_c}$$

Total force in tendon:

$$F_{p.B} = A_p\cdot\left(E_p\cdot\varepsilon_{pu.B}\right)$$

Equilibrium of forces:

$$F_{p.B} + F_{c.B} = 0$$

Which leads to:

$x_B := 1\text{mm}$

Given

$$A_p\cdot\left[E_p\cdot\left[\frac{-P_{supportB}}{A_p\cdot E_p} + \frac{-\varepsilon_{ult}\cdot\left(d_B - x_B\right)}{x_B} - \varepsilon_{ce.B}\right]\right] + 0.8\cdot b_{support}\cdot x_B\cdot\frac{\alpha\cdot f_{ck}}{\gamma_c} = 0$$

$x_B := \text{Find}\left(x_B\right) = 1.301\text{ m}$

Check if steel stress is ok:

$$\varepsilon_{ct.B} := \frac{-\varepsilon_{ult}\cdot\left(d_B - x_B\right)}{x_B} = -0.000599$$

$$\varepsilon_{pu.B} := \frac{-P_{supportB}}{A_p\cdot E_p} + \varepsilon_{ct.B} - \varepsilon_{ce.B} = -0.006671$$ Less than f_{pd}/E_p=0.007313

Ultimate moment capacity:

$$z_B := \left(d_B - 0.4 \cdot x_B\right) = 1.003 \cdot m$$

$$F_{cB} := 0.8 \cdot b_{support} \cdot x_B \cdot \frac{\alpha \cdot f_{ck}}{\gamma_c} = 43707 \cdot kN$$

$$M_{ultB} := F_{cB} \cdot z_B = 43846 \cdot kN \cdot m$$

Ultimate moment capacity at span 2:

Ultimate compressive strain in concrete:

$$\varepsilon_{ult} = 0.0035$$

Concrete strain due to prestress at the level of the tendon:

$$\varepsilon_{ce.2} := \frac{1}{E_c}\cdot\left(\frac{P_{span2}}{A_{gspan}} + \frac{M_{p2}\cdot e_2}{I_{gspan}}\right) = 0.000389$$

Total ultimate strain in concrete at the level of the tendons:

$$\varepsilon_{ct.2} = \frac{-\varepsilon_{ult}\cdot\left(d_2 - x_2\right)}{x_2}$$

Tendon strain:

$$\varepsilon_{pu.2} = \frac{-P_{span2}}{A_p\cdot E_p} + \varepsilon_{ct.2} - \varepsilon_{ce.2}$$

Concrete compressive force:

$$F_{c.2} = 0.8\cdot x_2\cdot b_{span}\cdot\frac{\alpha\cdot f_{ck}}{\gamma_c}$$

Total force in tendon:

$$F_{p.2} = A_p\cdot\left(E_p\cdot\varepsilon_{pu.2}\right)$$

Equilibrium of forces:

$$F_{p.2} + F_{c.2} = 0$$

Which leads to:

$x_2 := 1\text{mm}$

Given

$$A_p\cdot\left[E_p\cdot\left[\frac{-P_{span2}}{A_p\cdot E_p} + \frac{-\varepsilon_{ult}\cdot\left(d_2 - x_2\right)}{x_2} - \varepsilon_{ce.2}\right]\right] + 0.8\cdot b_{span}\cdot x_2\cdot\frac{\alpha\cdot f_{ck}}{\gamma_c} = 0$$

$x_2 := \text{Find}\left(x_2\right) = 1.335\,\text{m}$

Check if steel stress is ok:

$$\varepsilon_{ct.2} := \frac{-\varepsilon_{ult}\cdot\left(d_2 - x_2\right)}{x_2} = 0.000424$$

$$\varepsilon_{pu.2} := \frac{-P_{span2}}{A_p\cdot E_p} + \varepsilon_{ct.2} - \varepsilon_{ce.2} = -0.00538$$ Less than f_{pd}/E_p=0.007313

Ultimate moment capacity:

$$z_2 := \left(d_2 - 0.4 \cdot x_2\right) = 0.639 \cdot m$$

$$F_{c2} := 0.8 \cdot b_{span} \cdot x_2 \cdot \frac{\alpha \cdot f_{ck}}{\gamma_c} = 35248 \cdot kN$$

$$M_{ult2} := F_{c2} \cdot z_2 = 22532 \cdot kN \cdot m$$

Ultimate moment capacity at support C:

Ultimate compressive strain in concrete:

$$\varepsilon_{ult} = 0.0035$$

Concrete strain due to prestress at the level of the tendon:

$$\varepsilon_{ce.C} := \frac{1}{E_c}\cdot\left(\frac{P_{supportC}}{A_{gsupport}} + \frac{M_{pC}\cdot e_C}{I_{gsupport}}\right) =$$

Total ultimate strain in concrete at the level of the tendons:

$$\varepsilon_{ct.C} = \frac{-\varepsilon_{ult}\cdot\left(d_C - x_C\right)}{x_C}$$

Tendon strain:

$$\varepsilon_{pu.C} = \frac{-P_{supportC}}{A_p\cdot E_p} + \varepsilon_{ct.C} - \varepsilon_{ce.C}$$

Concrete compressive force:

$$F_{c.C} = 0.8\cdot x_C\cdot b_{support}\cdot\frac{\alpha\cdot f_{ck}}{\gamma_c}$$

Total force in tendon:

$$F_{p.C} = A_p\cdot\left(E_p\cdot\varepsilon_{pu.C}\right)$$

Equilibrium of forces:

$$F_{p.C} + F_{c.C} = 0$$

Which leads to:

$$x_C := 1\text{mm}$$

Given

$$A_p\cdot\left[E_p\cdot\left[\frac{-P_{supportC}}{A_p\cdot E_p} + \frac{-\varepsilon_{ult}\cdot\left(d_C - x_C\right)}{x_C} - \varepsilon_{ce.C}\right]\right] + 0.8\cdot b_{support}\cdot x_C\cdot\frac{\alpha\cdot f_{ck}}{\gamma_c} = 0$$

$$x_C := \text{Find}\left(x_C\right) = 1.25\,\text{m}$$

Check if steel stress is ok:

$$\varepsilon_{ct.C} := \frac{-\varepsilon_{ult}\cdot\left(d_C - x_C\right)}{x_C} = -0.000767$$

$$\varepsilon_{pu.C} := \frac{-P_{supportC}}{A_p\cdot E_p} + \varepsilon_{ct.C} - \varepsilon_{ce.C} = -0.006409$$ Less than f_{pd}/E_p=0.007313

Ultimate moment capacity:

$$z_C := \left(d_C - 0.4 \cdot x_C\right) = 1.024 \cdot m$$

$$F_{cC} := 0.8 \cdot b_{support} \cdot x_C \cdot \frac{\alpha \cdot f_{ck}}{\gamma_c} = 41990 \cdot kN$$

$$M_{ultC} := F_{cC} \cdot z_C = 42982 \cdot kN \cdot m$$